STATENS GEOTEKNISKA INSTITUT
SWEDISH GEOTECHNICAL INSTITUTE

RAPPORT
REPORT No 4

Basic behaviour of Scandinavian soft clays

ROLF LARSSON

LINKÖPING 1977

STATENS GEOTEKNISKA INSTITUT
SWEDISH GEOTECHNICAL INSTITUTE

RAPPORT
REPORT No 4

Serien "Rapport" ersätter våra tidigare serier: "Proceedings" (27 nr), "Särtryck och Preliminära rapporter" (60 nr) samt "Meddelanden" (10 nr).

Our new series "Report" supersedes the previous series: "Proceedings" (27 Nos), "Reprints and Preliminary Reports" (60 Nos) and "Meddelanden" (10 Nos).

Basic behaviour of Scandinavian soft clays

ROLF LARSSON

Denna rapport hänför sig till forskningsanslag 750894-2 från Statens råd för byggnadsforskning.

LINKÖPING 1977

PREFACE

In recent years new aspects of the shear strength and deformation properties of clay have been introduced. At Cambridge University, the Norwegian Geotechnical Institute, Laval University and Queens University in Canada and many other places the "Critical Stresses" at which large plastic deformations occur have been investigated. The role of horizontal stresses in analysing shear strengths and deformations has been recognized and methods for measuring horizontal stresses *in situ* have been developed. New techniques for determination of compression characteristics of clay, such as constant rate of strain oedometer tests and oedo-triaxial testing, have been introduced. A large amount of work has also been done throughout the world to determine creep processes in clay.

In Sweden work on these subjects has mainly been done at Chalmers University and in recent years also at the Swedish Geotechnical Institute.

In this report the influence of deformation characteristics on shear strength is discussed. A simple hypothesis for critical stresses leading to plastic deformations and a generalized model for undrained shear strength and anisotropy in soft clays is presented. Results from a series of creep tests are presented and analysed and current methods of reducing field vane shear strength are discussed.

This report is supported by grants from the Swedish Council for Building Research, the Swedish National Road Administration and internal research funds at the Swedish Geotechnical Institute.

Linköping June 1977

SWEDISH GEOTECHNICAL INSTITUTE

CONTENTS

SUMMARY

The purpose of the present report is to make clear what factors determine strengths and deformations of soft clays. In the report is shown how stress-history and deformation characteristics affect the strengths that can be mobilized. A hypothesis for undrained shear strength and anisotropy is presented and compared with experimental results. Results from a comprehensive series of undrained creep tests are presented and analysed. The reduction of undrained shear strength in long-term conditions is analysed.

A clay at a certain level in the ground has a preconsolidation pressure. The effective vertical stress in the clay can be increased up to the preconsolidation pressure without causing large deformations. If the preconsolidation pressure is exceeded the deformations increase considerably. The preconsolidation pressure primarily depends on the overburden pressure, previous loads and the ground water level and its fluctuations. As the vertical effective stress increases the effective stresses in all other directions simultaneously increase. The lowest effective stress created by a vertical load is the effective horizontal stress. Between the effective vertical and horizontal stresses for which the clay has been prestressed there is a fixed relation.

$$\sigma'_{Hmax} / \sigma'_{Vmax} = K^{o}_{nc}$$

where

σ'_{Hmax} = effective horizontal prestress

σ'_{Vmax} = preconsolidation pressure

A comparison of measurements that have been obtained by a number of investigators shows that K^{o}_{nc} depends on the liquid limit or alternatively the plasticity

of the clay.

$$K_{nc}^{o} = 0,31 + 0,71\ (w_L - 0,2)$$

or

$$K_{nc}^{o} = 0,315 + 0,77\ I_p$$

These formulas are not valid for organic clays.

When K_{nc}^{o} is known the prestress in all other directions can be calculated.

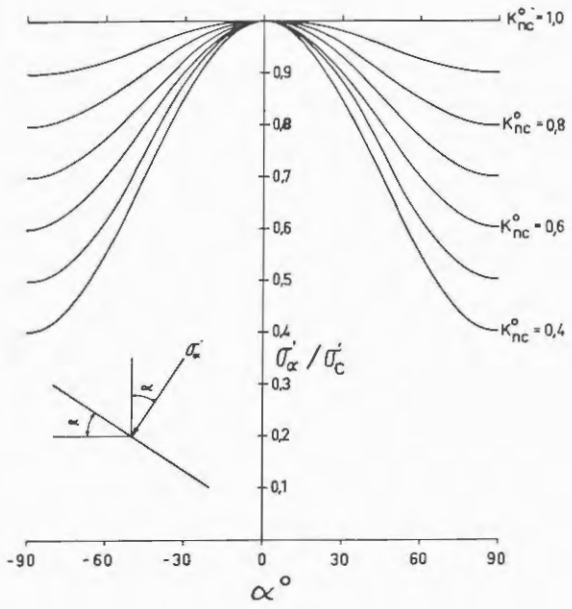

α = angle between the actual plane and the horizontal plane

σ'_α = prestress in the actual plane.

In Scandinavian clays it has empirically been found that an effective angle of friction can be mobilized when the effective stresses are lower than the pre-

stresses. If the prestresses are exceeded large deformations occur and the effective angle of friction that can be mobilized in drained cases will be considerably lower than 30^0.

The prestresses can be considered as critical stresses which cannot be exceeded without causing large deformations. Another critical limitation for the stresses is the mobilization of the effective angle of friction of 30^0 where shear failure will occur.

In undrained cases the pore water pressure is changed. The pore water pressure during shear in soft clay is changed so that the prestresses are not exceeded. In heavily overconsolidated clays the pore water pressure decreases and the stresses increase. The major effective principal stress at failure will be close to the prestress in the same direction.

Using the effective angle of friction $\phi' = 30^0$ the undrained shear strength in different planes can be calculated.

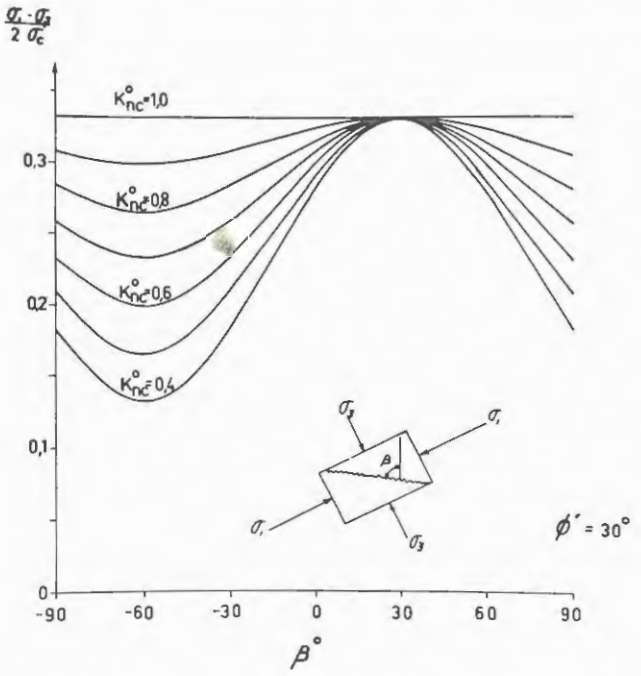

β = angle between the shear plane and the vertical plane

In normally consolidated clays with a brittle structure only a part of this shear strength can be mobilized.

As the effective normal stresses in heavily overconsolidated clays do not quite reach the prestresses the calculated undrained shear stress should be reduced by a factor of 0,8 in these clays.

In undrained creep tests with effective stresses close to the prestresses the pore pressure increases with time. This will cause failure if the effective angle of friction is thereby mobilized.

From the creep tests presented in this report and from other Scandinavian investigations it can be concluded that the undrained shear strength for normally consolidated clays should be reduced by a factor of 0,8 in long-term cases.

NOTATIONS AND SYMBOLS

A_f	Skemptons pore pressure parameter at undrained failure
A	Area
c_v	Coefficient of consolidation
CRS test	Oedometer test, constant rate of strain
e	Void ratio
E	Modulus of elasticity
f	Failure
h	Height of sample
I_p	Plasticity index
k	Permeability
k_1, k_2, k_3	Constants
K_o	Coefficient of effective earth pressure at rest σ'_H/σ'_V
K^o_{nc}	Coefficient of effective earth pressure in normally consolidated stage $\sigma'_v = \sigma'_c$
K^o_{pl}	Coefficient of effective earth pressure at reloading (preloaded)
K^o_{rb}	Coefficient of effective earth pressure at unloading (rebound)
m_c	Slope of logarithm strain rate versus logarithm time straight line
M	Oedometer modulus
OCR	Over consolidation ratio σ'_c/σ'_v
p'	Mean effective stress $(\sigma_1+\sigma_2+\sigma_3)/3$
p'_c	Mean effective normal preconsolidation stress $\sigma'_c(1 + 2\ K^o_{nc})/3$
q	Deviator stress, $(\sigma_1 - \sigma_3)$
S_t	Sensitivity
t, t_1, t_2	Time

t_f	Time to failure
u	Pore pressure
V	Volume
w	Natural water content
w_F	Cone liquid limit
w_L	Percussion liquid limit
w_P	Plasticity limit
α	Angle
β	Angle
ε_f	Deformation at failure, in % of sample height
ε_H	Horizontal deformation in simple shear test, in % of sample height
ε_V	Vertical deformation in % of sample height
ε_{vol}	Volumetric strain
ε_1	"Initial" vertical deformation in creep tests. (ε at t = 1 minute)
$\dot{\varepsilon}$	Vertical creep rate
$\dot{\varepsilon}_1$	"Initial" vertical creep rate ($\dot{\varepsilon}$ at t = 1 minute)
γ	Angular deformation
μ	Reduction factor
ρ	Density
σ	Total pressure
σ'	Effective pressure
σ'_c	Vertical preconsolidation pressure
σ'_H	Effective horizontal pressure
σ'_{HO}	*In situ* effective horizontal pressure
σ'_V	Effective vertical pressure
σ'_{VO}	*In situ* effective vertical pressure

σ_1, σ_2, σ_3	Principal stresses
σ'_α	Effective normal stress in direction α
τ	Shear stress
τ_{fu}	Undrained shear strength
τ_{fd}	Drained shear strength
ϕ'	Effective angle of friction
ϕ_p	Angle of interparticle friction
ϕ'_u	Residual angle of friction
CTH	Chalmers University of Technology
NGI	Norwegian Geotechnical Institute
SGI	Swedish Geotechnical Institute

1 STRESS-STRAIN CHARACTERISTICS OF SOFT CLAYS IN OEDOMETER TEST

The shear strength and deformation characteristics of a clay are highly dependent on the effective stresses, stress history and the rate of deformation.

The effective stress-strain characteristics of a clay are usually determined in oedometer tests. The new CRS test (constant rate of strain) enables the determination of a continuous stress-strain curve and continuous evaluation of compression modulus versus effective stress. Generalized stress-strain and modulus-stress curves for a soft clay are shown in Figs 1 and 2.

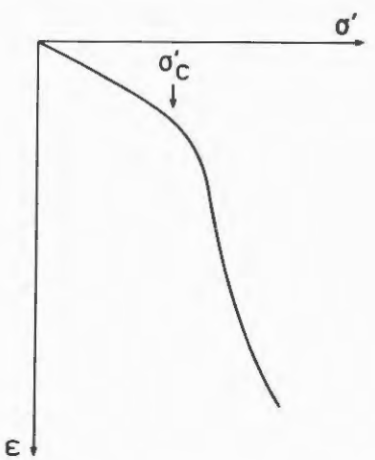

Fig 1 Oedometer test CRS plotted in linear scales. σ_c' evaluated according to Sällfors (1975).

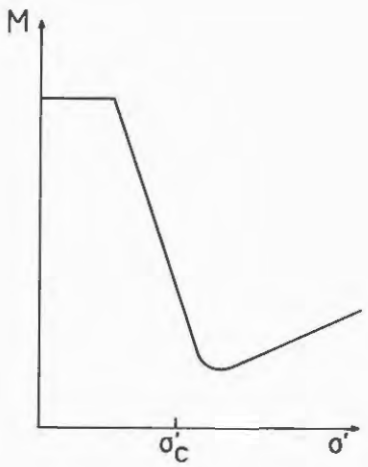

Fig 2 Oedometer modulus M versus effective vertical stress σ'.

In Fig 1 it can be seen that for stresses well below the preconsolidation pressure there is a linear relation between stress and strain. As the stress approaches the preconsolidation pressure the strains start to increase further and after passing the pre-

consolidation pressure the strains become very large. For stresses well above the preconsolidation pressure the strain increment per stress increment slowly decreases as the stress increases. A better picture of the different parts of the stress-strain curve is given in Fig 2 where the compression modulus is plotted against the effective stress. The compression modulus is constant for stresses well below the preconsolidation pressure. As the stress approaches the preconsolidation pressure the clay structure starts to break down, secondary compressions increase and the compression modulus decreases. When the stress exceeds the preconsolidation pressure all the rigidity of the clay due to previous stress history is overcome and further stresses will cause very large deformations. The lowest compression modulus which is obtained at stresses just above the preconsolidation pressure remains constant only in a very small stress interval and increases slowly thereafter with increasing stress.

For some clays, often described as cemented, the breakdown of the structure at the preconsolidation pressure is so great that there will be a peak in the stress-strain curve and the compression modulus becomes negative. This behaviour can only be detected in strain-controlled tests.

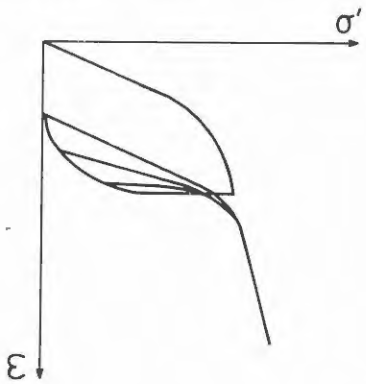

Fig 3 Oedometer tests with loading, unloading and reloading. The figure shows 3 tests on identical material with different degrees of unloading.

In tests with loading and unloading it can be seen that swelling in the interval σ'_c - 0,5 σ'_c is quite small, Fig 3. As the effective stress decreases further there is a significant increase in swelling which becomes larger and larger as the effective stress decreases.

At reloading it is found that the compression modulus at stresses below the preconsolidation pressure depends on the amount of swelling that has occurred. A higher degree of unloading gives more swelling and a lower compression modulus at reloading.

Results from oedometer tests are often plotted in diagrams with stress in logarithmic scale and strain in linear scale. In this case the strain-log stress curve often becomes a straight line for stresses above the preconsolidation pressure. For soft clays with a high swelling capacity and relatively low compression modulus for stresses below the preconsolidation pressure, this plotting is disadvantageous. The logarithmic scale will distort the linear stress-strain curve and give the curve a shape that is classically called disturbed, making the evaluation of the preconsolidation pressure difficult. Most clays brought into the laboratory have undergone some swelling. This is partly due to disturbance during sampling but also because many clays are more or less overconsolidated and have swollen in the ground. Oedometer curves for soft clays therefore ought to be plotted in linear scales.

The total swelling capacity for clays investigated have varied between 2 and 6% of the sample height. Organic clays usually have a higher swelling capacity than organic clays.

Swelling, like consolidation, is a time-dependent process. This time process depends on modulus and

permeability. As the permeability is almost the same in swelling and consolidation for moderate deformations and the swelling modulus for low stresses is very low it is easily understood that times for swelling are of the same order as times for consolidation.

Some oedometer curves from tests with loading and unloading with c_v values for both loading and unloading are given in Appendix 1.

In soft clays the compensated foundation method is often used. During and after excavation the bottom often heaves and continues to do so. This has mainly been attributed to shear stresses and shear creep deformations while swelling has been neglected.

Time-dependent swelling in soft clays is of such a magnitude that it cannot be neglected. It should if possible be prevented as all swelling that occurs will cause settlement when the building is erected.

Oedometer tests are sometimes performed on samples cut in different directions. They give stress-strain curves of the same shape but the "breaking point" varies with the cutting direction.

2 *IN SITU* STRESSES

When soil is consolidated for a uniform load in the field horizontal effective stresses as well as vertical effective stresses increase. It has been established that in the normally consolidated state the ratio $\sigma'_H/\sigma'_c = K^o_{nc}$ is fairly constant. The most widely used expression for calculating K^o_{nc} is Jaky's formula

$$K^o_{nc} = 1 - \sin \phi' \qquad (1)$$

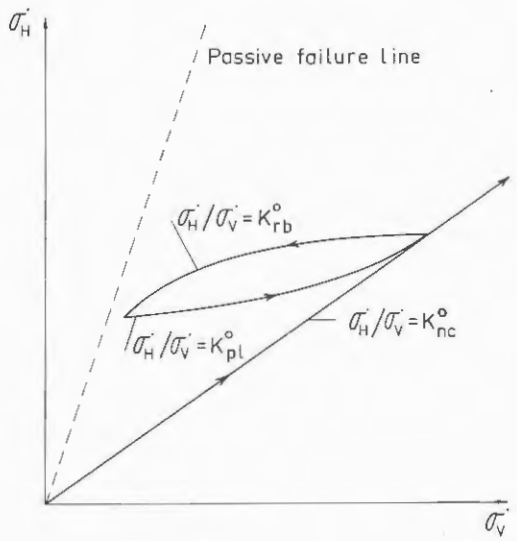

Fig 4 Effective stresses during loading, unloading and reloading.

If the soil is subjected to long-term loading and secondary settlements occur, a quasi-preconsolidation is developed which means that the soil will behave as if it had consolidated for higher vertical stresses than the overburden pressure. Measurements of horizontal stress during secondary consolidation in the oedometer have shown that the horizontal stresses increase as the settlement and quasi-preconsolidation pressure increase. Similar results are obtained at cyclic loading. There is no evidence that the ratio

of maximal "preconsolidation" stresses $\sigma'_H = \sigma'_c K^o_{nc}$ and σ'_c should be seriously affected by the way the preconsolidation effect is created as long as it is obtained from natural uniform processes such as overburden pressure or lowering and seasonal fluctuations of ground water table.

If the soil is unloaded the vertical effective stress will decrease faster than the horizontal and the ratio $\sigma'_H/\sigma'_V = K^o_{rb}$ will be dependent on the overconsolidation ratio.

For clay, Schmidt (1967) has formulated the expression

$$K^o_{rb} = K^o_{nc} \, OCR^{\sin 1{,}2\phi'} \qquad K^o_{rb} = K^o_{nc}(\sigma'_c/\sigma'_v)^{\sin 1{,}2\phi'} \qquad (2)$$

This formula is valid within a limited range of overconsolidation ratios as the maximum value of σ'_H is $\sigma'_v \tan^2(45+\phi'/2)$ where passive failure occurs.

There is no expression formulated for the ratio between effective horizontal and vertical stress during reloading K^o_{pl}, but the value when unloading ends and reloading starts is equal to K^o_{rb} and it will be equal to K^o_{nc} as the vertical stress reaches the preconsolidation pressure.

In recent years a number of measurements of horizontal stresses have been carried out in field and laboratory in Scandinavia.

From these tests K^o_{nc} has been calculated using OCR and Schmidt's formula with ϕ' estimated as 30^0. The K^o_{nc} values are plotted against plasticity index and liquid limit in Figs 5 and 6. As a comparison the values presented by Brooker and Ireland from remoulded laboratory-consolidated samples are also plotted in the figures.

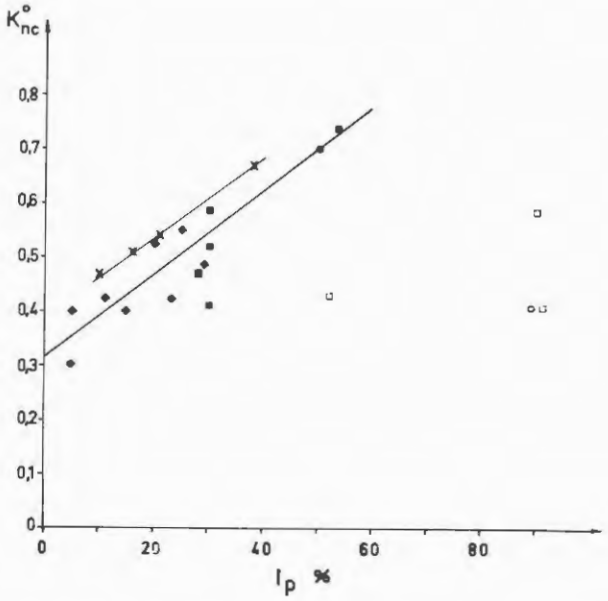

Fig 5 K^o_{nc} *versus plasticity. Open symbols represent organic clay.*

◆ Bjerrum and Andersen (1972)
x Brooker and Ireland (1965)
■ Massarsch et al (1975)
● Author's measurements

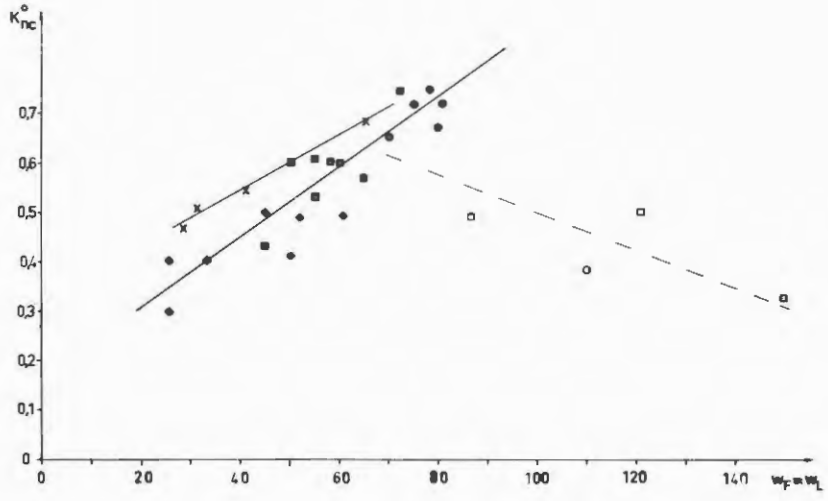

Fig 6 K^o_{nc} *versus liquid limit. Open symbols represent organic clay.*

From the Scandinavian measurements it is found that K^o_{nc} for inorganic clays can roughly be expressed as

$$K^o_{nc} = 0,315 + 0,77\ I_p \qquad (3)$$

or

$$K^o_{nc} = 0,31 + 0,71\ (w_F - 0,2) \qquad (4)$$

As can be seen in Figs 5 and 6 these formulas cannot be used for organic clays. The reason for this probably lies in the different nature of organic and inorganic clays. Micrographs of typical clays show that inorganic clays can be considered as granular materials while organic clays are of more fibrous nature, Appendix 3.

Wroth (1975) has found that K_o during unloading K^o_{rb} can be evaluated from

$$m\left[\frac{3(1-K^o_{nc})}{1+K^o_{nc}} - \frac{3(1-K_o)}{1+2K_o}\right] = \ln\left[\frac{OCR(1+K^o_{nc})}{1+2K_o}\right] \qquad (5)$$

where $m = 1,2 + 2,3\ I_p$

3 SHEAR STRENGTH IN DIRECT SHEAR TESTS

In Sweden the shear strength is often determined by direct shear tests in the SGI apparatus. The apparatus is a modified SGI oedometer with facilities to shear the soil sample after consolidation. The soil sample has a diameter of 50 mm and in drained tests a height of 10 mm. In undrained tests the sample has a height of 20 mm. The sample is surrounded by a rubber membrane.

Outside the rubber membrane thin metal rings are threaded to keep the sample diameter constant during the test. There are small clearances between the rings to prevent transmission of vertical forces by the rings. The rubber membrane is sealed and drainage of the sample is provided by filter stones below and above the sample. The drainage channels from the filter stones can be closed. The apparatus is shown in Fig 7.

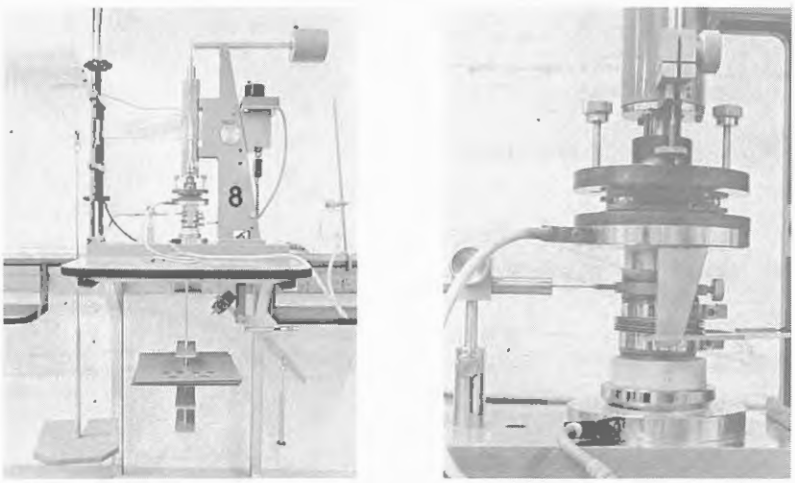

Fig 7 The SGI shear apparatus.

The test is performed so that first the vertical stress is applied to the sample and the sample is allowed to consolidate. After consolidation the sample is sheared to failure. This is made by moving the upper filter stone horizontally while the lower filter stone is in a fixed position. The sample thereby gets a uniform angular distortion up to failure and there is no forced shear surface. In the tests horizontal stress, horizontal deformation and vertical deformation are measured. The vertical stress remains constant. Tests can be made drained or undrained and are nowadays usually sheared with constant rate of horizontal deformation.

Typical results from direct shear tests are shown in Figs 8a and 8b. The tested material is a grey clay from Linköping with natural water content w = 90%, liquid limit w_L = 80% and plasticity limit w_p = 28%. The undrained shear strength measured by fall cone test is 11 kPa and the preconsolidation pressure determined by CRS test is 47 kPa.

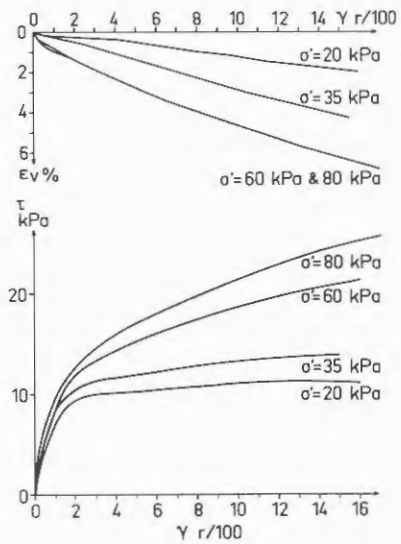

Fig 8a Shear stress, angular distortion and vertical deformation in consolidated drained direct shear tests.

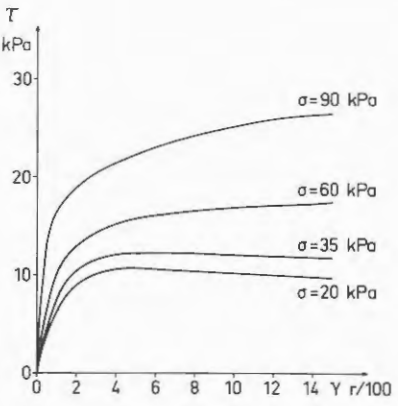

Fig 8b Shear stress versus angular distortion in consolidated undrained direct shear tests.

Failure in direct shear test is in accordance with Swedish practice evaluated as peak shear stress or the shear stress at an angular distortion of 0,15 radians if no peak is obtained.

The shear strength obtained from the test on Linköping clay are plotted in Fig 9.

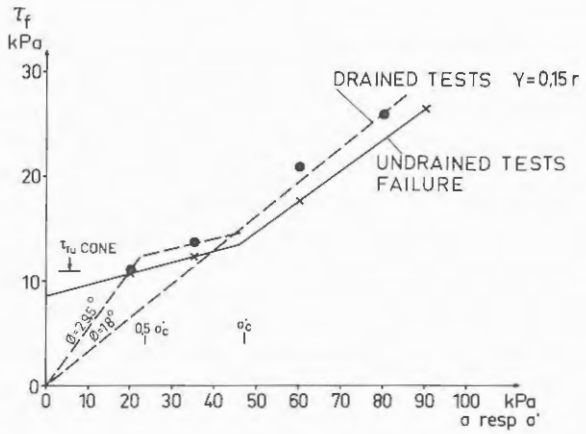

Fig 9 Shear stress at failure versus vertical stress in direct shear tests.

That the relation between shear strength and normal stress changes at the preconsolidation pressure is generally accepted. In drained shear strength of soft clays there is a second breaking point in the $\tau_{fd} - \sigma'$ curve. When the effective vertical stress decreases beyond a certain stress the undrained shear strength rapidly decreases. This has been established in numerous tests and empirically the breaking point has been found to be at a vertical effective stress of about half the preconsolidation pressure. That is why the drained failure line is drawn as a straight line through origo in the stress interval $0 < \sigma' < 0{,}5\ \sigma'_c$. This will be discussed further in Part 7.

In Fig 8a it can be seen that all the shear stress - angular distortion curves in drained test can be simplified by two straight lines, Fig 10.

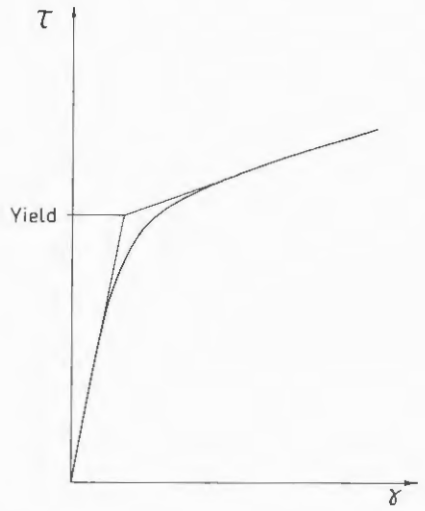

Fig 10 Evaluation of yield in drained direct shear tests.

The intersection between these two lines is called critical shear stress or yield stress. This yield stress can be regarded as the maximum shear stress the soil can take without undergoing large plastic deformations. At vertical stresses well below the preconsolidation pressure yield is equal to failure as the failure in this stress region is brittle.

4 FRICTION DILATANCY AND YIELD IN DIRECT SHEAR TESTS

To show the mechanics of drained strength the mobilized angle of internal friction ϕ' for each per cent of horizontal deformation has been evaluated from $\tau = \sigma' \tan\phi'$ in a number of tests. The horizontal deformation is expressed in per cent of sample height and one per cent horizontal deformation corresponds to 0,01 radians angular distortion. Simultaneously the direction of average particle displacement has been evaluated. The sample diameter is kept constant during the test and the only deformations are horizontal displacement in the shear direction and vertical compression. Thus the average particle displacement will be in a direction deviating an angle from the horizontal plane of $\alpha^{\circ} = \text{arc tan } d\varepsilon_V/d\varepsilon_H$.

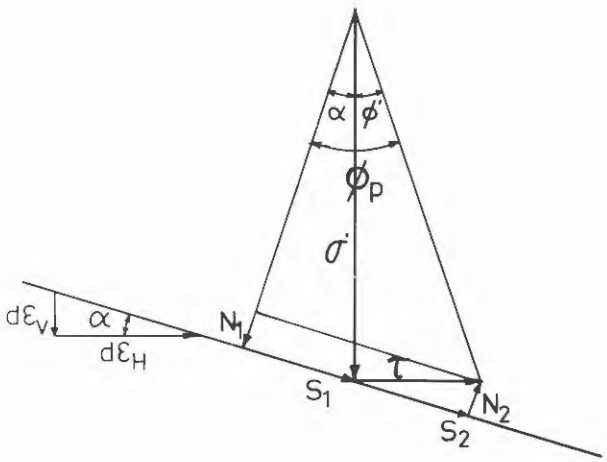

Fig 11 Stresses in drained direct shear tests.

If the stresses acting in the plane of average displacement are analysed and the angle of interparticle friction is assumed to be ϕ_p it is found that τ can be written as $\sigma'\tan(\phi_p-\alpha)$, Fig 11.

In Fig 12 the results from this type of evaluation on the drained tests on Linköping clay are plotted.

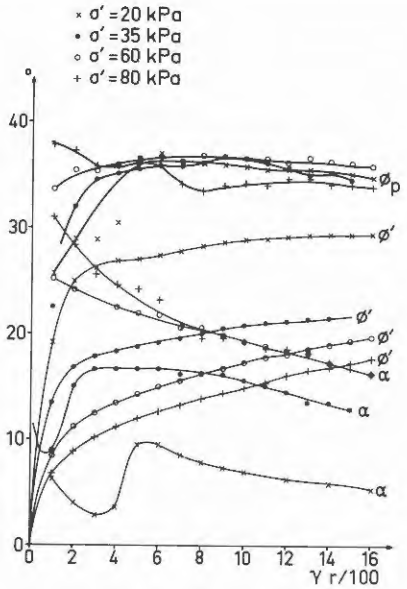

Fig 12 ϕ', α *and* ϕ_p *in drained direct shear tests on Linköping clay.*

It is found that in the tested stress region $\phi_p = 36^0$ can be considered as a constant for the clay and depends on the compression modulus at the stress level in the test. Oedometer curves for Linköping clay are given in Figs 13 and 14. The shear strength for this clay is thus a function of interparticle friction and compression characteristics only. A similar interpretation was suggested by Bjerrum (1961).

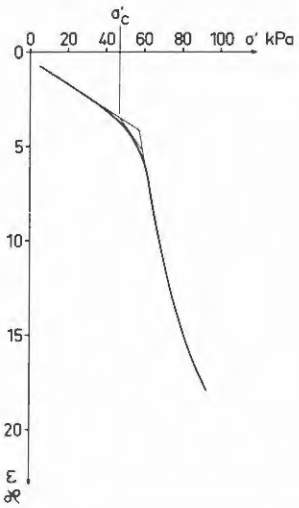

Fig 13 Stress-strain curve from CRS test on Linköping clay.

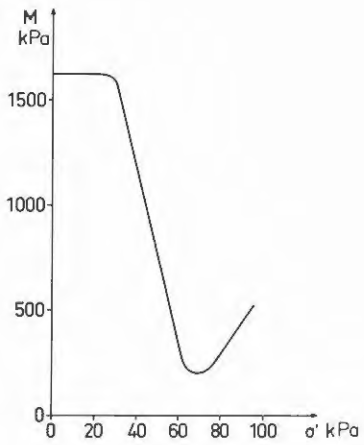

Fig 14 Oedometer modulus versus vertical effective stress in Linköping clay.

In connection with the creep tests described in Part 11 a large series of direct shear tests were performed on clay from Lilla Mellösa. The results from the drained tests are plotted in Fig 15.

The failure line in the upper diagram clearly shows the two breaking points at σ'_c and ~ 0,5 σ'_c. At stresses higher than σ'_c both the failure line and the yield line are straight lines with extensions going through origo.

The angle of interparticle friction, shown in Fig 15 lower diagram (upper curve), remains constant for stresses below the preconsolidation pressure. When the effective stress exceeds the preconsolidation pressure the angle of interparticle friction starts to decrease. The slope of the curve decreases as the stress increases and at high stresses the angle of interparticle friction asymptotically approaches an end value.

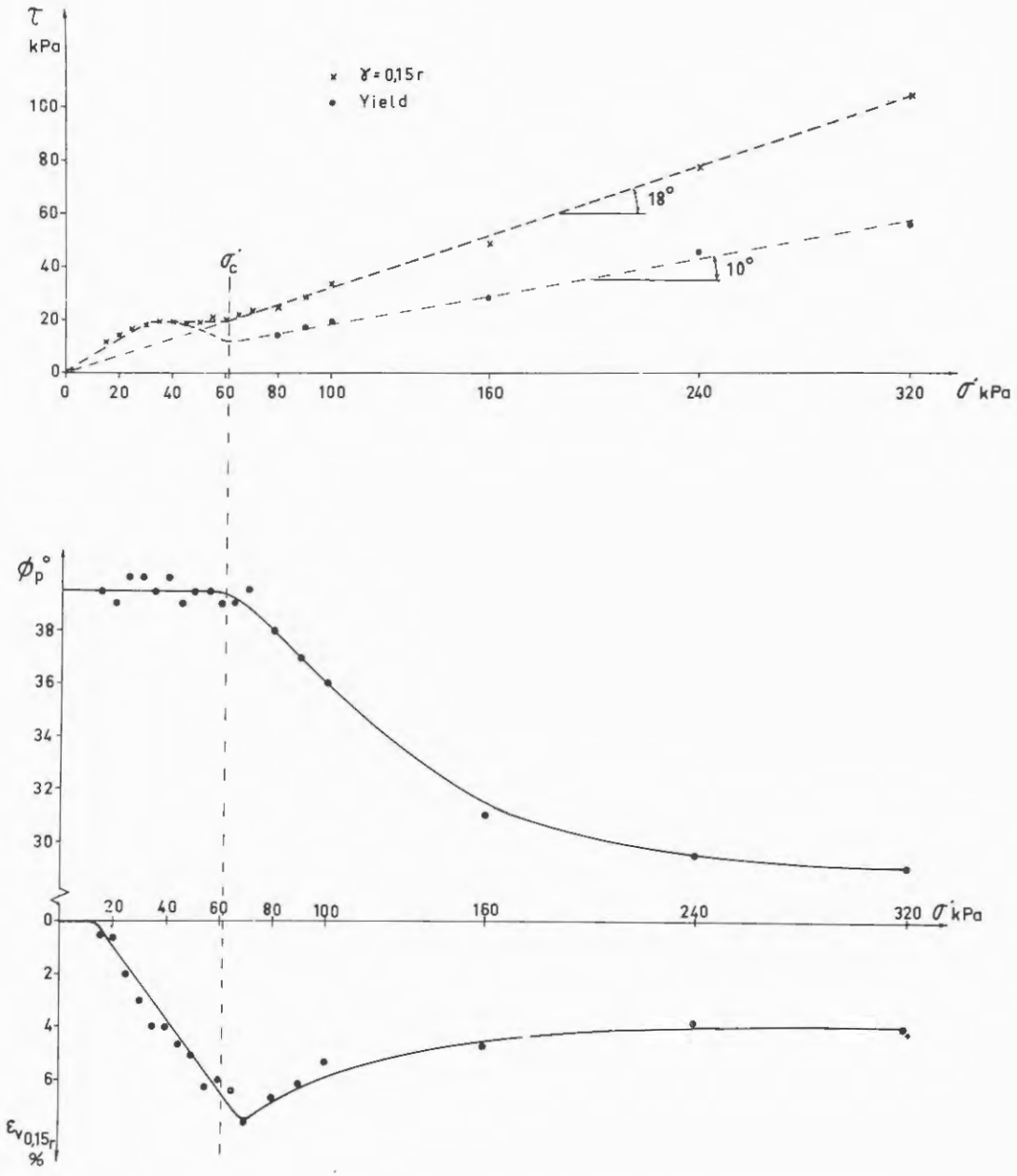

Fig 15 Results from drained direct shear tests on Lilla Mellösa clay.

The lowest curve shows the total vertical compression during the shear tests. The shape of this curve is very close to that of the M-σ' curve from oedometer tests. As ε_v is a function of α the two lower curves explain the shape of the failure line in the upper diagram. In the stress region 0 ~ 0,5 σ'_c the angle of interparticle friction is a constant and the vertical compression small. In the stress region 0,5 σ'_c - σ'_c the angle of interparticle friction still remains constant but the vertical compression and thereby α increase and the angle of friction that can be mobilized $\phi' = \phi_p - \alpha$ decreases. When the preconsolidation pressure has been exceeded ϕ_p decreases while the vertical compression also decreases. These two effects seem to equalize each other and as a result of this ϕ' becomes a constant.

The angle of interparticle friction of $39,5^0$ for low stresses might seem high but if the very irregular shape of particles and particle aggregates, which can be seen in micrographs of the clay is considered, it is reasonable (Appendix 3). When the stress level exceeds the preconsolidation pressure aggregates in the clay will be subjected to higher stresses than they can take and they will start to break and crush until, at high stresses, all the part of the interparticle friction that is due to aggregate shape is eliminated.

The reason why the vertical deformations start to increase at such a low stress as 0,5 σ'_c is that in the direct shear test the major and minor stresses are rotated $(45 + \phi'/2)^0$. This means that the major normal stress at failure is higher than the vertical pressure and this major normal stress acts on a plane that, due to the anisotropy of the effective stresses during natural consolidation, has a lower maximum prestress than the preconsolidation pressure σ'_c.

Another way to investigate the angle of interparticle friction is to run drained direct shear tests with constant sample height. There are no possibilities of doing this in the SGI apparatus but Kamenov (1976) has run a number of direct shear tests on sand with constant sample height. These tests show that although the normal stress and shear stress vary, the mobilized angle of friction remains constant throughout the test and this angle is the same as the angle obtained in tests with constant vertical load at critical density.

The evaluation of ϕ_p is now a standard procedure at SGI and normal values of ϕ_p for clay are 34^0-40^0 in the low stress region decreasing to about 30^0 at high stresses. The lowest value of ϕ_p measured so far is $27,8^0$ which was obtained in a sandy silt with rounded grains.

Fig 16 shows the results from a series of seven tests on an organic silt from Umeå with vertical stresses below the preconsolidation pressure.

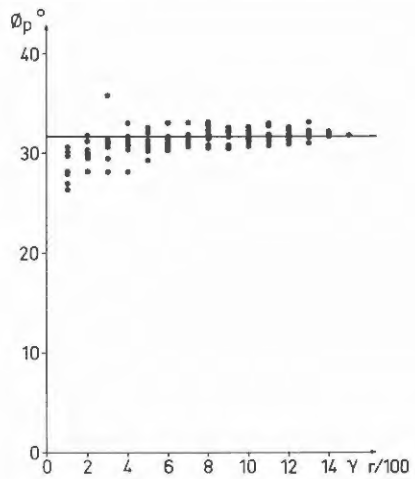

Fig 16 Interparticle friction ϕ_p from drained direct shear tests on organic silt.

Results from the series of drained direct shear tests on Lilla Mellösa clay in the lower stress region are plotted in Fig 17.

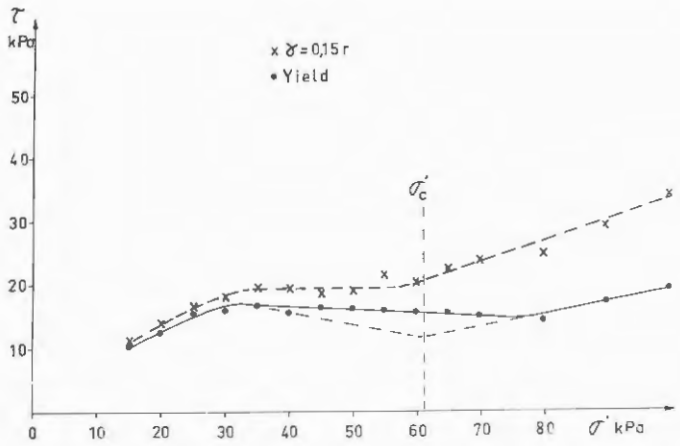

Fig 17 Undrained shear strength and yield in drained direct shear tests on Lilla Mellösa clay.

The figure shows the relation between yield stress and evaluated failure stress. When the vertical stress is lower than 0,5 σ'_c yield and failure almost coincide as the failure is brittle. As the vertical stress approaches the preconsolidation pressure the ratio $\tau_{yield}/\tau_{failure}$ decreases and when the vertical stress is well above the preconsolidation pressure the ratio becomes a constant. Due to an error in the testing technique the yield values close to the preconsolidation pressure have to be corrected.

The error is that when the sample is consolidated in the shear apparatus the horizontal stresses will not be *at rest* pressures but active earth pressures and thus too low. This means that when shear starts and the principal stresses are rotated it is possible to increase the horizontal stress component before yield starts more in the apparatus than in the field.

The correction is made by extending the straight yield line for high stresses to the preconsolidation pressure and connecting this intersection with the yield point at $\sigma' = 0{,}5\ \sigma_c'$ as the lower broken line in Fig 17 shows.

5 DILATANCY EFFECTS IN TRIAXIAL TESTS

The importance of dilatancy for the angle of effective friction that can be mobilized in triaxial tests has been extensively investigated for sands. The most widely used correction for dilatancy is derived by Rowe (1962) from energy relations

$$\sigma_1' = \sigma_3' \left[1 - \left(\frac{d\varepsilon_{vol}}{d\varepsilon_1} \right)_f \right] \tan^2 \left(45 + \frac{\phi_p}{2} \right) \qquad (6)$$

Feda (1971) has compared triaxial tests and direct shear tests and found that to get similar results the correction for triaxial tests should rather be

$$\sin \phi_p = \frac{\sigma_{1f}' - \sigma_{3f}' \left[1 - \left(\frac{d\varepsilon_{vol}}{d\varepsilon_1} \right)_f \right]}{\sigma_{1f}' + \sigma_{3f}'} \qquad (7)$$

Feda denotes that this correction was probably used by Bishop and Eldin (1953).

It is also possible to use the correction $\phi_p = \phi' + \alpha$ in triaxial tests.

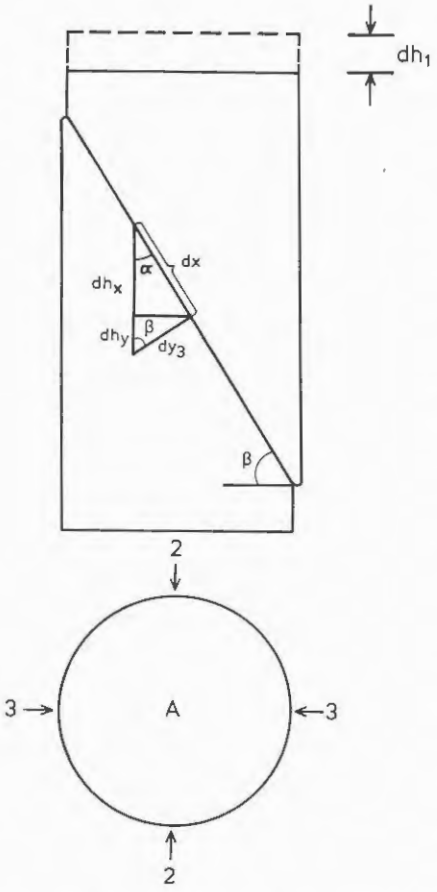

Fig 18 Evaluation of the angle α in triaxial tests.

In the standard triaxial test the cell pressure $\sigma_2' = \sigma_3'$ is kept constant and the axial stress σ_1' is increased. In tests with low or medium relative density shear will occur along a number of shear planes simultaneously and the sample will become barrel shaped. If the projections of the shear planes in 3 directions are put together in one shear plane α can be evaluated according to Fig 18.

$$dh_1 = dh_x + dh_y$$

$$dh_x = dx \sin\beta$$

$$dh_y = dy_3 \cos\beta$$

and assuming that $dy_3 = dy_2$

$$dy_3 = \frac{dV \cdot \cos\beta}{2\ A}$$

where V is the sample volume

$$dx \sin\beta = dh_1 - \frac{dV \cos^2\beta}{2\ A}$$

$$\tan\alpha = \frac{dy_3}{dx}$$

$$\tan\alpha = \frac{\frac{dV \cos\beta}{2\ A}}{\frac{dh_1}{\sin\beta} - \frac{dV \cos^2\beta}{2\ A \sin\beta}} = \frac{dV \tan\beta}{\frac{2\ A\ dh_1}{\cos^2\beta} - dV}$$

$$\alpha = \arctan \frac{dV \tan\beta}{\frac{2\ A dh_1}{\cos^2\beta} - dV} \qquad (8)$$

In this formula all values are in absolute numbers and if α is expressed in relative deformations it will be

$$\alpha = \arctan \frac{d\varepsilon_{vol} \tan\beta}{\frac{2\ \varepsilon_1}{\cos^2\beta} - d\varepsilon_{vol}} \qquad (9)$$

In soils with a very high relative density a single shear plane will develop and after formation of this plane

$$\alpha = \arctan \frac{d\varepsilon_{vol} \tan\beta}{\frac{\varepsilon_1}{\cos^2\beta} - d\varepsilon_{vol}} \qquad (10)$$

ϕ' is evaluated from

$$\phi' = \arcsin \frac{\sigma_1' - \sigma_3'}{\sigma_1' + \sigma_3'} \qquad (11)$$

and β is assumed to be $(45 + \phi'/2)^0$

In Figs 19a, b, c and d stress, strain and volume change for four tests on a sand from Luleå are shown.

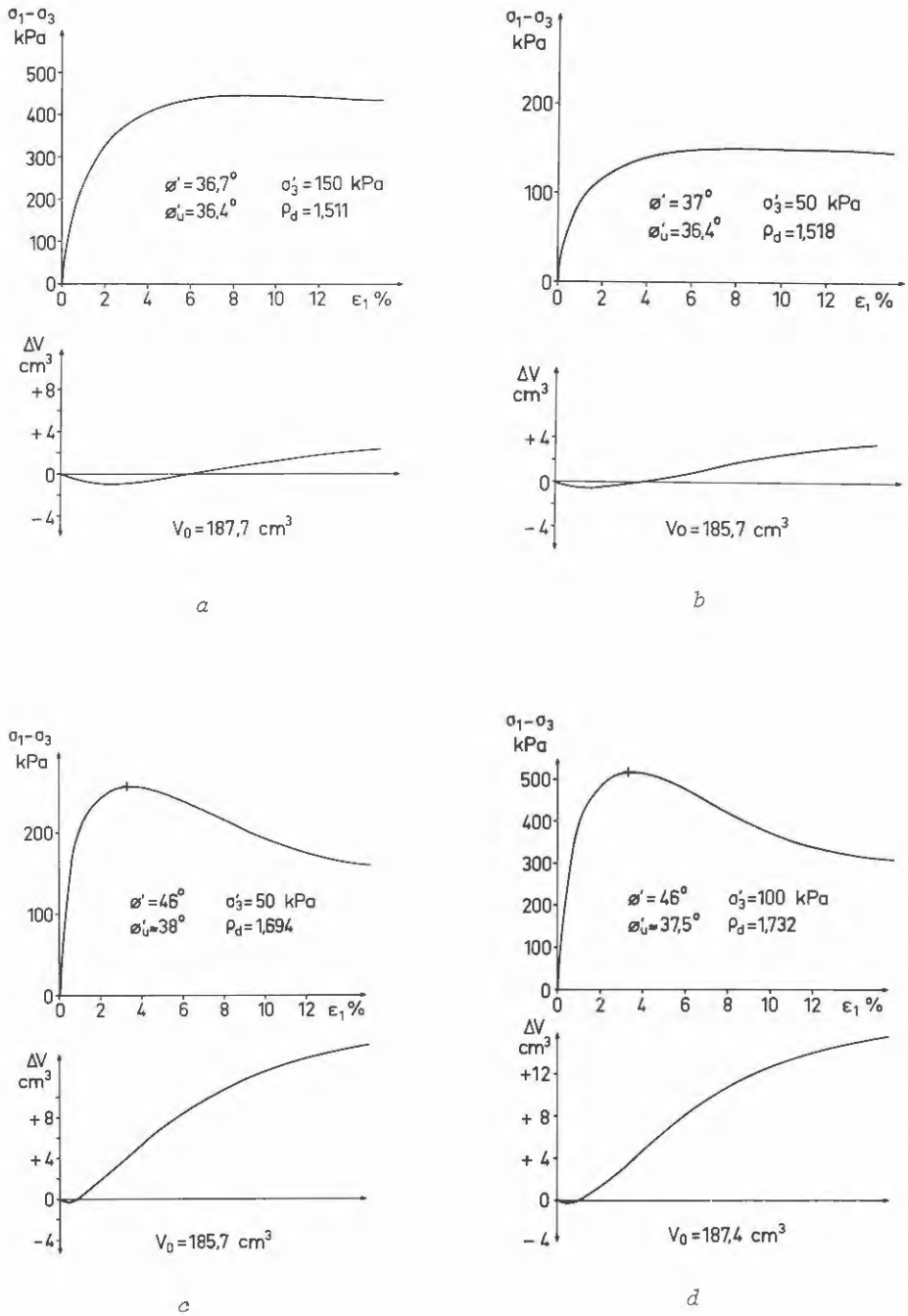

Fig 19 Stress, strain and volume change in drained triaxial tests on sand from Luleå.

The interparticle friction has been evaluated according to $\phi_p = \phi' + \alpha$ and the results are shown in Fig 20.

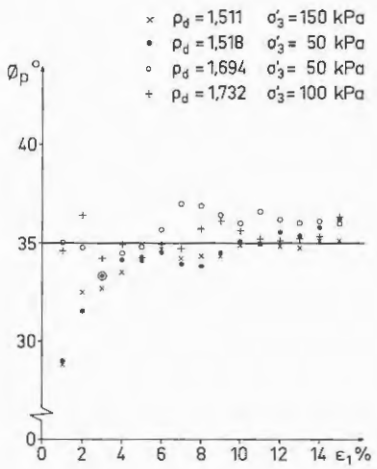

Fig 20 Interparticle friction in triaxial tests on Luleå sand.

The interparticle friction evaluated from triaxial tests with correction for dilatancy has been shown to be slightly dependent on the initial porosity, Feda (1971). This is probably due to change in modulus of elasticity with porosity. In triaxial tests corrections are made for volume change only but no correction is made for the elastic change of sample shape. This is of minor importance in stiff soils but will cause errors in soils with low modulus of elasticity such as soft clays. In direct shear tests where the diameter of the sample is kept constant these errors will not occur.

6 TIME EFFECTS ON SHEAR STRENGTH OF SOFT CLAYS

The rate of strain in shear testing has an influence on the measured shear strength. This influence can be divided into two parts, one pure rate effect and one effect that is due to secondary compression in drained tests or secondary pore pressure increase in undrained tests.

The pure rate effect might be considered mainly as an effect of the energy required to pump water between pores during shear. In sands this effect is very small and is negligible at normal testing rates. In clay this effect remains down to very slow testing rates. To ensure complete pore pressure dissipation drained tests on clay are run at so low strain rates that the rate effect will be very small. In undrained tests which are run at higher strain rates it will be of some importance.

Several series of undrained tests on a clay have been run on samples consolidated for different stresses and at different strain rates. All consolidation pressures were lower than the maximum *in situ* stresses and pore pressures were measured. If the effective stress paths from tests with the same strain rate are plotted in a Mohr-Coulomb diagram the effective failure line will become a straight line with an intercept at the axis of deviator stress, Fig 21.

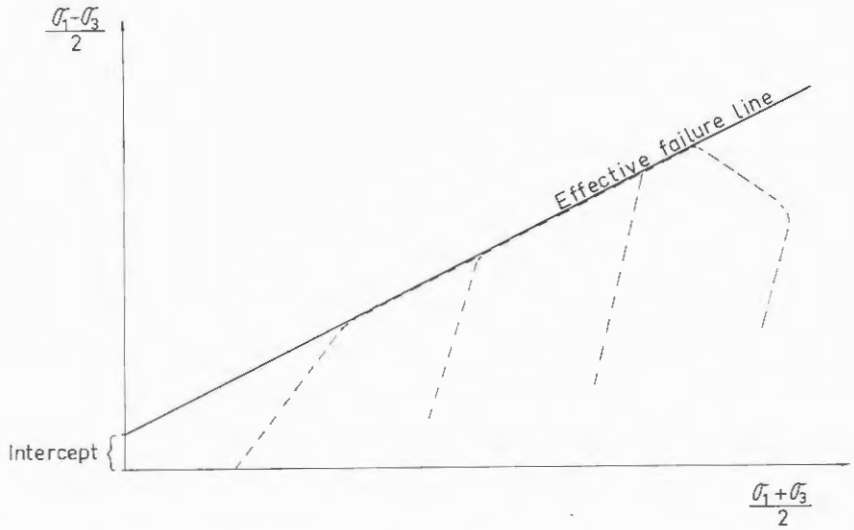

Fig 21 Effective stress paths from undrained tests with equal strain rate.

This intercept increases with strain rate and disappears in very slow tests. (Larsson, 1975 b).

In Scandinavia undrained triaxial tests on soft clays are normally run at a strain rate of 0,6% of the sample height per hour. At this rate the intercept will usually be in the order of 1-2 kPa.

The effect of secondary compression in drained tests on clay will appear as a greater volume decrease during slow tests than in tests at higher speed. As a greater volume decrease means a lower angle of friction that can be mobilized, the mobilized shear stress at equal shear deformations decreases with decreasing rate of strain. Secondary compression is dependent on overconsolidation ratio. When the effective stresses are low in relation to the preconsolidation pressure the secondary compression is very small. As the effective stresses increase, the secondary compression increases and becomes maximal when the stress reaches the preconsolidation pressure.

The effect of secondary compression on the drained shear strength is thus dependent on the overconsolidation ratio.

In undrained tests there is no volume change but instead secondary pore pressures will build up in slow tests. As the pore pressure increases the effective stresses and thereby the shear strength decrease. The secondary pore pressure increase is dependent on the overconsolidation ratio in the same way as secondary compression. The effect of secondary pore pressure increase on undrained shear strength is therefore also dependent on the overconsolidation ratio.

The pure rate effect is independent of overconsolidation ratio but dependent on permeability.

In soft, normally consolidated clays with low permeability, the combined time effects are very important.

7 GENERALIZED MODEL FOR DRAINED SHEAR STRENGTH OF SOFT CLAY IN DIRECT SHEAR

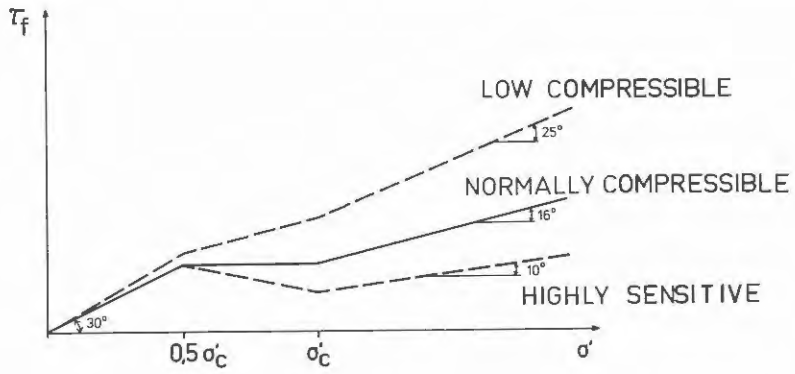

Fig 22 Generalized drained shear strength in direct shear.

The drained shear strength that can be mobilized in a clay is directly dependent on the compressibility of the clay and the stress level. If the shear strength in direct shear is plotted versus the effective vertical pressure, a failure line, which can be divided into three parts, is obtained, Fig 22. In Fig 22 three types of clay are represented. The solid line represents a normally compressible soft clay ($w \approx w_L \approx 70\%$ St ≈ 15) and a clay content of about 60%. At effective stresses higher than the preconsolidation pressure, the drained shear strength can be written $\tau_{fd} = \sigma' \text{ tg } \phi'$ where ϕ' will be of the order of 16-18°. If the effective vertical stress is within the stress interval 0,5 σ'_c - σ'_c the shear strength is practically independent of the vertical stress. As shown before, this is because the increasing compressions during shear compensate the increasing effective stress when the vertical stress approaches the preconsolidation pressure. That the shear strength decreases when the effective stress is lower than

0,5 σ'_c has been found empirically.

The upper broken failure line represents a clay with low compressibility, sensitivity and rapidity. (Low rapidity means that the structure of the clay is insensitive to deformations and vibrations and a lot of work is required to break it down, Söderblom 1974). The failure line has the same breaking points as the failure line for the normally compressible clay but the difference between the three parts is not as pronounced. The mobilized angle of friction in the stress interval 0-0,5 σ'_c is usually one or two degrees higher than that for normally compressible clay as the modulus of compression is higher. In the stress interval 0,5 σ'_c - σ'_c there is an increase in shear strength when the vertical stress increases as the compression is too small to fully compensate for the stress increase. The angle of friction that can be mobilized at vertical stresses higher than σ'_c is considerably higher than the corresponding angle for normally compressible clays.

The lower broken line represents a highly sensitive clay with high rapidity. Such clays often have a water content higher than the liquid limit and the compression modulus at the preconsolidation pressure is very low or even negative. In these clays the structural breakdown in direct shear tests is so great that the shear strength decreases with increasing vertical stress in the stress interval 0,5 σ'_c - σ'_c. The angle of friction that can be mobilized at vertical stresses above the preconsolidation pressure will be of the order of 10^0. If the failure line is compared with the yield curve in Fig 15 it is found that in these highly sensitive clays failure will occur when the yield stress is reached. Failure lines like these have mainly been reported for Canadian clays, Lo & Morin (1972) and Lefebvre & La Rochelle (1975). Bjerrum (1961) has measured friction angles between

9 and 13° for highly sensitive Scandinavian clays. Bjerrum also reported a number of slides in Scandinavia which occurred at a mobilized effective angle of friction of about 10°. The analysis of the well-known slide at Stigbergskajen in Gothenburg showed that the mobilized effective angle of friction at failure vas 9°40' (Pettersson & Hultin 1916).

There are a number of reasons why the failure lines for vertical stresses below 0,5 σ'_c are drawn as straight lines through origo although there are no test results from the lowest stresses. The SGI direct shear apparatus has a lower limit for vertical stress of 15 kPa and the soft Swedish clays have normally preconsolidation pressures lower than 100 kPa, but empirically it has been possible to establish that the failure line has a breaking point at vertical stresses of about 0,5 σ'_c and that its extension will intersect the τ-axis close to origo at zero vertical stress.

At NGI a large series of drained triaxial tests has been run on Drammen clay at very low stresses, Ramanatha Iyer (1975). The results are plotted in Fig 23.

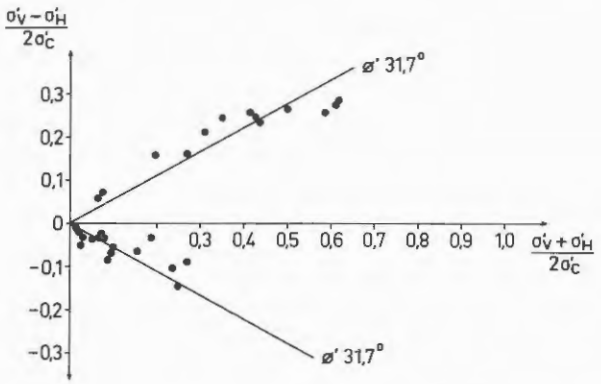

Fig 23 Failure in drained triaxial tests on plastic Drammen clay. Values from Ramanatha Iyer (1975) and Berre (1975).

This investigation shows that the failure line for low stresses can be drawn as a straight line through origo without greater errors.

This means that in soft clays there will be no volume increase during shear even if the overconsolidation ratio is high.

In fact it is not even possible to mobilize an effective angle of friction corresponding to the interparticle friction. As shown in Fig 3 a considerable swelling will occur in a clay at effective stresses below 0,5 σ'_c and the modulus of compression at reloading decreases. The elastic compression during shear at low stresses means that although the interparticle friction is of the order of 34-40^0 it is only possible to mobilize an effective angle of about 30^0 in soft clays. A number of Scandinavian soft clays have been investigated and the value of ϕ' at low stresses of 30^0 seems fairly constant.

Bäckebol	30^0
Drammen Lean[1]	30^0
Drammen Plastic[1]	31,7^0
Fävren	32^0
Lilla Mellösa	30^0
Linköping	29,5^0
Studenterlunden[1]	30^0
Vaterland[1]	30^0

[1)] Berre and Bjerrum 1973

In laboratory test on stiffer clays the measured shear strength at low stresses is often higher due to volume increase. As these clays are normally more inhomogenous it might be hazardous to use these values unless large-scale tests are used. Drained failures at low stresses are brittle and once the weakest zone has yielded there is no possiblity for strength increase due to consolidation.

In coarse friction materials the natural density normally corresponds to a very high preconsolidation pressure. These materials are very stiff and will show a considerable amount of volume increase during shear at low stresses which it would be very uneconomic to disregard.

8 GENERALIZED MODEL FOR UNDRAINED SHEAR STRENGTH OF SOFT CLAY IN DIRECT SHEAR

In undrained shear the effective stresses are dependent on the changes in pore pressure during the test. In the early stage of the test the pore pressure will strive to keep the mean effective stress p' constant. When yield occurs the pore pressure development will change so that the effective material will have no tendency to change its volume during shear.

In direct shear tests this means that the effective vertical stress at failure will be slightly lower than $0,5\ \sigma'_c$. If the sample is consolidated for a vertical stress lower than about $0,45\ \sigma'_c$ the pore pressure will decrease during shear and if the sample is consolidated for a higher vertical stress the pore pressure will increase.

Combined with the empirical value $\phi' = 30^0$ this gives the relation $\tau_{fu} \approx 0,45\ \sigma'_c \tan 30^0 \approx 0,26\ \sigma'_c$.

A comparison between undrained shear strength and the empirical relation for Lilla Mellösa clay is shown in Figs 24 and 25. As a further comparison the drained shear strength, the yield curve and the undrained shear strength measured by fall cone and field vane tests are shown.

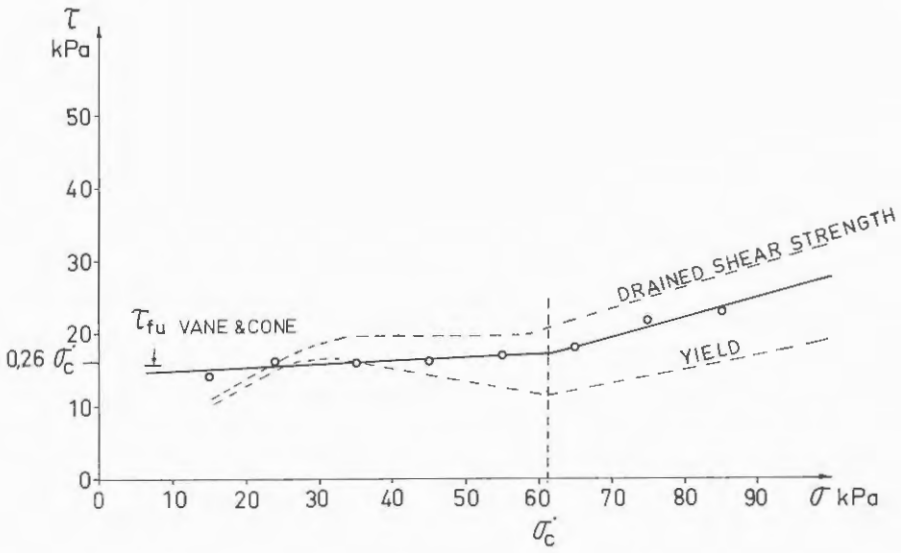

Fig 24 Undrained strength in direct shear tests on Lilla Mellösa clay.

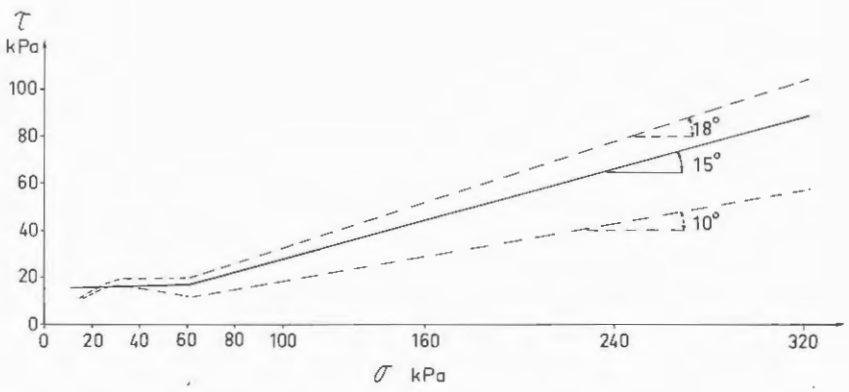

Fig 25 Undrained strength in direct shear tests on Lilla Mellösa clay.

The undrained shear strength of clay in direct shear will later be discussed theoretically and is shown to vary with plasticity. (Part II)

There are other similar empirical expressions for the undrained shear strength of soft clay. Karlsson & Viberg (1967) proposed the formula $\tau_{fu} = 0,3\ \sigma'_c$ from field vane tests.

For undrained triaxial active tests Bishop & Henkel have suggested the typical pore pressure parameter at failure A_f for normally consolidated clay of 1,0. The corresponding value for marine clays is 1,3. The tests have been isotropically consolidated and this leads to the formula

$$\frac{\tau_{fu}}{\sigma'_c - A_f\ \tau_{fu}} = \sin \phi' \qquad (12)$$

If $\phi' = 30^0$ is used the empirical expression will be $\tau_{fu} = 0,33\ \sigma'_c$ or $\tau_{fu} = 0,30\ \sigma'_c$ for active triaxial tests.

These expressions are empirical and there are exceptions. The most serious exceptions are clays with high sensitivity and rapidity. In these materials stresses to which the material responds elastically can safely be applied but when yield occurs the structure of the materials will break down and very high pore pressures will develop. This phenomenon is similar to liquefaction in sands with low relative density.

In these brittle clays the undrained shear strength will coincide with yield. Test results from brittle clays where the undrained shear strength decreases with increasing vertical stress in the stress interval $0,5\ \sigma'_c - \sigma'_c$ have mainly been reported for Canadian clays, Lo & Morin (1972), Lefebvre & La Rochelle (1975).

The parameters of sensitivity and rapidity are not quite suited for judgement of brittleness. Sensitivity is determined from the lowest possible strength after much remoulding and rapidity is determined by means of a number of blows. Massarsch (1976) has suggested a new sensitivity parameter based on the reduction in strength after a limited amount of remoulding and this or a similar method would probably give a much better measure of the brittleness of the clay.

9 CRITICAL STRESSES

Critical stresses or yield stresses are the combinations of principal effective stresses at which the deformations of a soil change from being elastic to become elastic-plastic. In soft clays this is a very drastic change. In drained cases the exceeding of yield stresses means failure or very large deformations. These deformations are so large that in many engineering cases they cannot be accepted and it is of vital importance to keep the stresses below the yield stresses. In undrained cases reaching the yield stresses will mean a change in deformations and pore water pressure that may lead to failure.

The first advanced model of soil behaviour that includes the strength and deformation properties of the soil is the concept of "Critical State Soil Mechanics" developed at Cambridge University, Scofield & Wroth (1968). This model does not account for anisotropy and is derived from much stiffer soils than Scandinavian soft clays.

Wong & Mitchell (1975) have proposed a new model derived from tests on cemented Canadian clays. This model includes the effect of anisotropy and as it is derived from tests on a material more similar to the Scandinavian soft clays it might be modified and used

for them.

Both models include formulas for prediction of yield stresses and stress-strain relationships after yield.

At NGI investigations have been made to determine the yield curve for Norwegian clays, Berre (1975). Most of the tests have been performed on Plastic Drammen clay, w = 52% w_L = 61% w_P = 32%.

Berre presents values related to the effective overburden pressure *in situ*. The overconsolidation ratio is given to be 1,5. The yield values have been recalculated in relation to the preconsolidation pressure and are plotted together with the values from Ramanatha Iyers tests in Fig 26.

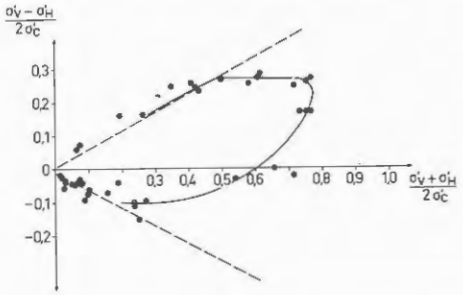

Fig 26 Yield stresses for plastic Drammen clay.

In Drammen clay measurements of the effective horizontal stress have been made in field and laboratory. From these measurements K_{nc}^{o} can be evaluated to 0,5.

Using this value the yield stresses have been plotted versus the mean effective stress p', Fig 27.

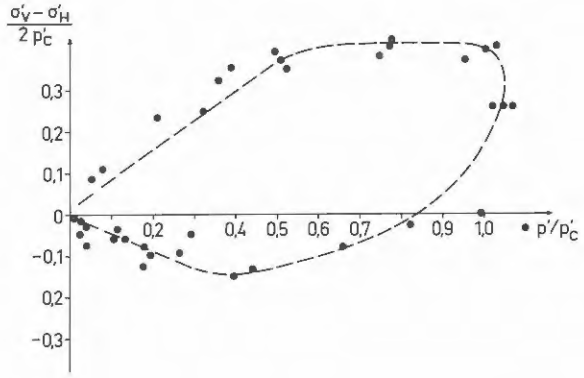

Fig 27 Yield stresses for plastic Drammen clay.

This type of diagram is being used more often and the two models for yield stresses mentioned both use the relation between deviator stress and mean effective stress.

10 CRITICAL STRESSES IN SOFT CLAYS

Today there are methods for accurate determination of the maximum stresses for which a clay has consolidated in a vertical as well as in a horizontal direction.

Various types of compression tests have shown that a soft clay cannot be submitted to stresses in any direction higher than the previous stresses in that direction without yielding.

Shear failure in a clay will occur when the effective angle of friction is mobilized.

Provided that the maximum previous effective horizontal stresses have been the yield criteria will be

$$\left|\sigma'_v=\sigma'_c\right| \quad \left|\sigma'_H=K^o_{nc}\ \sigma'_c\right| \quad \left|\frac{\sigma'_v-\sigma'_H}{\sigma'_v+\sigma'_H}=\sin\phi'\right| \quad \left|\frac{\sigma'_H-\sigma'_v}{\sigma'_v+\sigma'_H}=\sin\phi'\right| \qquad (13)$$

The yield stresses are shown in single dimension projection in Fig 28 and in stress space in Fig 29.

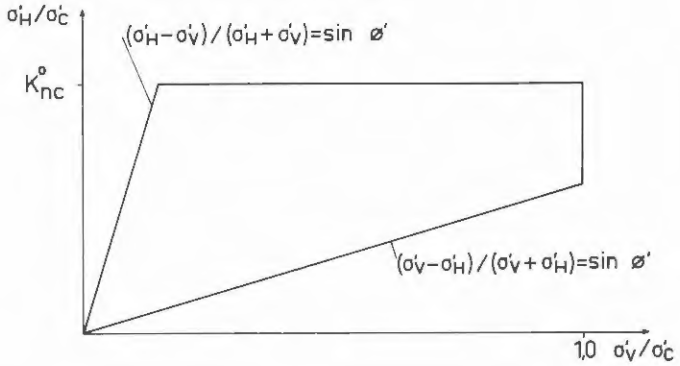

Fig 28 Yield stresses.

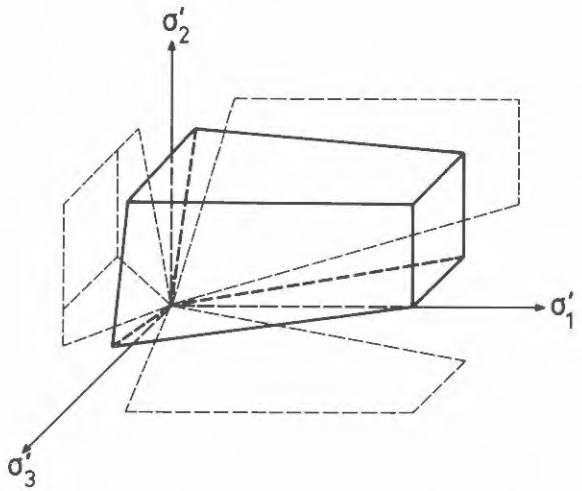

Fig 29 Yield stresses in stress space.

This yield criteria is partly of an early date. Rendulic (1937) and Henkel (1950) consolidated clays for isotropic stresses in triaxial apparatus, unloaded them and tried different stress paths to investigate what stress combinations led to large changes in water content. This was almost the same as defining

the yield stresses. Hvorslev (1960) recalculated Rendulic's results and plotted them together with Henkel's, Fig 30.

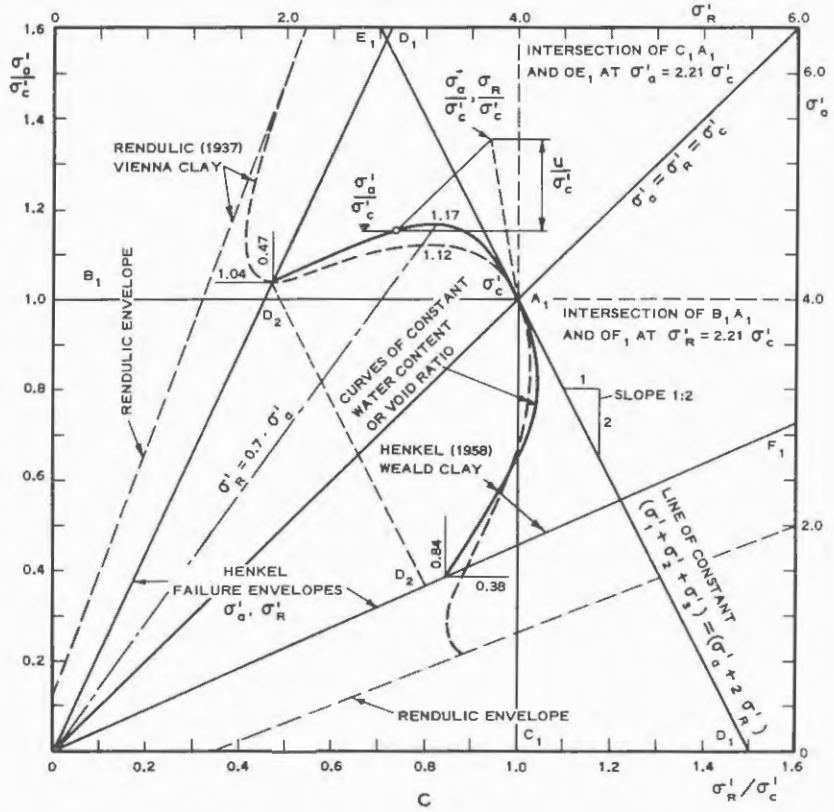

Fig 30 Curves for constant water content. From Hvorslev 1960.

The yield points from Berre's tests on Drammen clay are plotted in the same way in Fig 31. They show a good agreement with theory apart from the points for yield at isotropic pressure. Berre has indicated the difficulty in determining yield as some stress strain curves have distinct breaking points while others are evenly rounded.

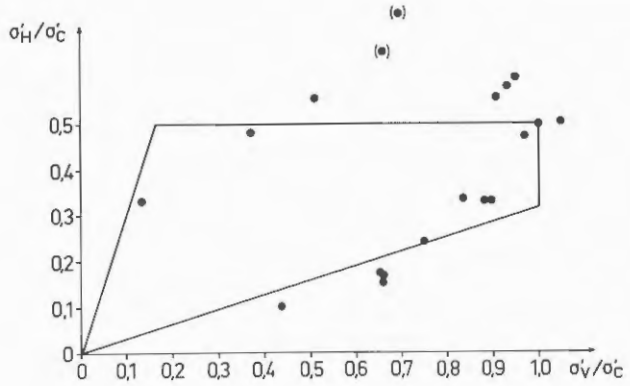

Fig 31 Yield stresses for Drammen clay.

A series of triaxial tests on a quick clay from Fävren has been run at SGI. (w = 60% w_L = 50% St = 50 σ'_c = 70 kPa) The series comprises two active undrained tests, two passive undrained tests, two drained active tests and three drained tests with isotropic pressure.

Stress-strain curves from the undrained tests are shown in Figs 32a and b. The deformation is fairly elastic up to yield and in this clay a well-defined failure is obtained also in the passive tests. This behaviour is common among Swedish clays but contrary to what is reported for Norwegian clays where no peak failure is obtained in undrained passive tests. Norwegian clays are generally siltier and have lower plasticity than Swedish clays. This may make them more sensitive to small deformations. The Fävren clay can obviously take the deformations to passive failure with the structure intact although it is a quick clay. The relation between undisturbed shear strength and ultimate shear strength after complete remoulding is therefore not a good measure of how the clay will behave during small shear deformations.

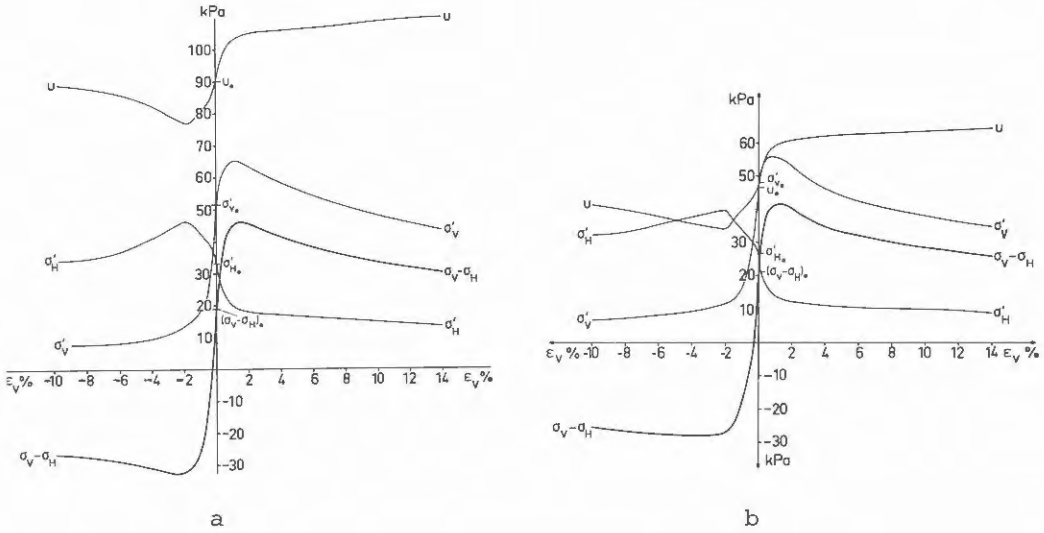

Fig 32 a & b *Stress-strain curves from undrained active and passive triaxial tests on Fävren clay.*

In Fig 33 the stress paths from these tests are shown. The sudden increase in effective stresses at a certain stress level in undrained passive tests run with constant rate of deformation is typical. In tests with constant rate of shear stress increase and free strain development there will be an increase in deformation at the same stress level.

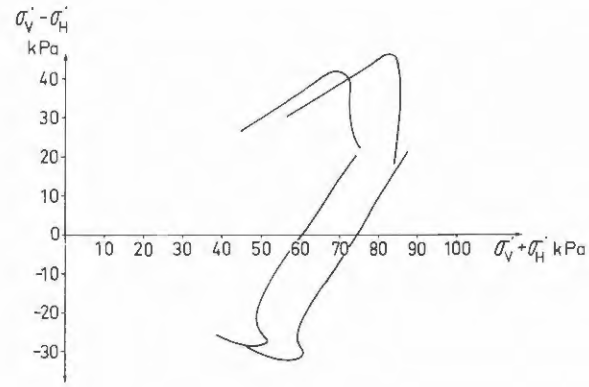

Fig 33 *Stress paths from undrained triaxial tests on Fävren clay.*

The drained active tests were run with constant rate of deformation and were stopped directly after yield.

The drained tests with isotropic pressure were performed with stress increments of 5 kPa with a consolidation time of 24 hours between the increments. In all tests the initial part of the stress-volume change curve plotted in linear scales was a straight line and yield showed as a distinct breaking point. The samples in the tests came from three different levels and yield was obtained at an effective pressure of 0,54 σ_c', 0,56 σ_c' and 0,64 σ_c' respectively. The average K_{nc}^{o} is approximated to 0,6.

The yield stresses for Fävren clay are plotted in Fig 34.

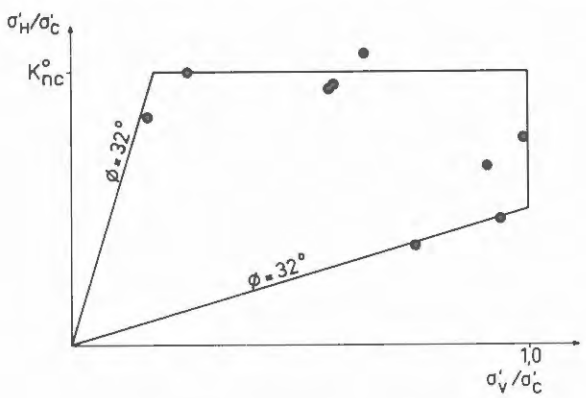

Fig 34 Yield stresses for Fävren clay.

Stresses are usually plotted as shear stress versus normal stress and the theoretical yield stresses are plotted as shear stress versus mean effective stress in Fig 35 and in Mohr-Coulomb, diagram in Fig 36.

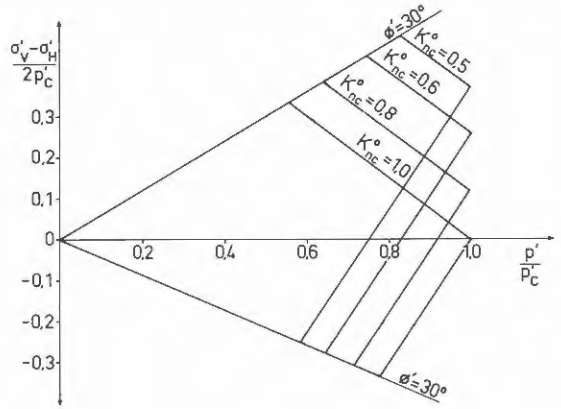

Fig 35 Theoretical yield curves drawn as shear stress versus mean effective stress.

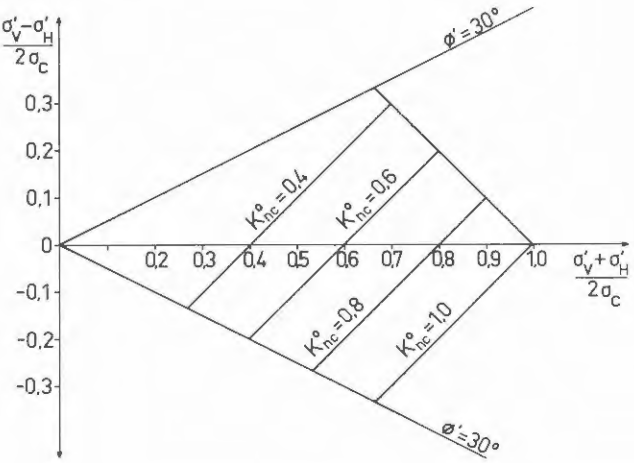

Fig 36 Theoretical yield curves in Mohr-Coulomb diagram.

The yield points from tests on Drammen clay and Fävren clay are plotted in these two types of diagrams in Figs 37a-b and 38a-b respectively. For comparison the theoretical yield curves are drawn in the figures.

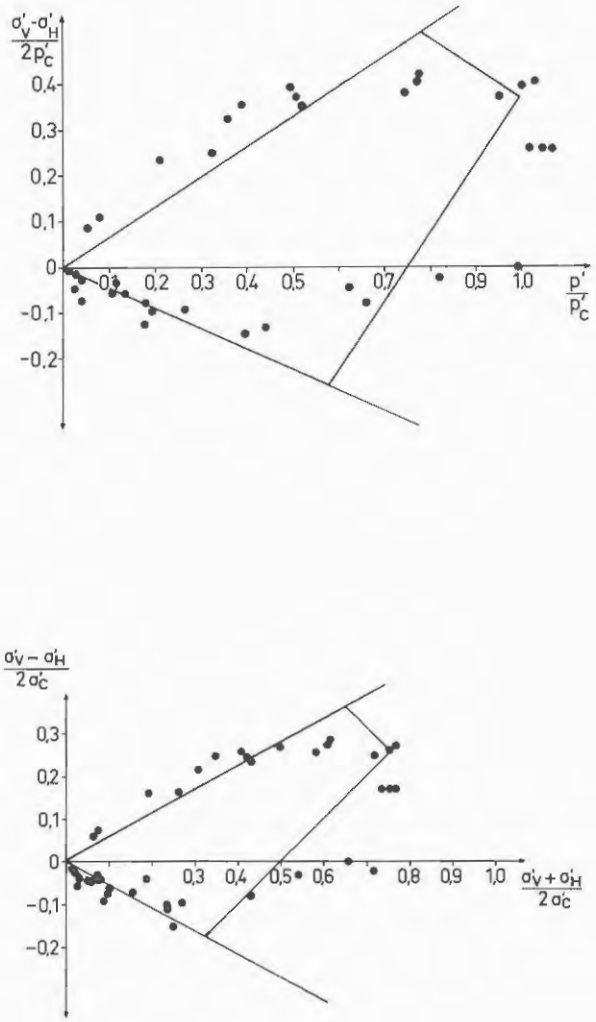

Fig 37 Yield stresses and theoretical yield curve for Drammen a & b clay.

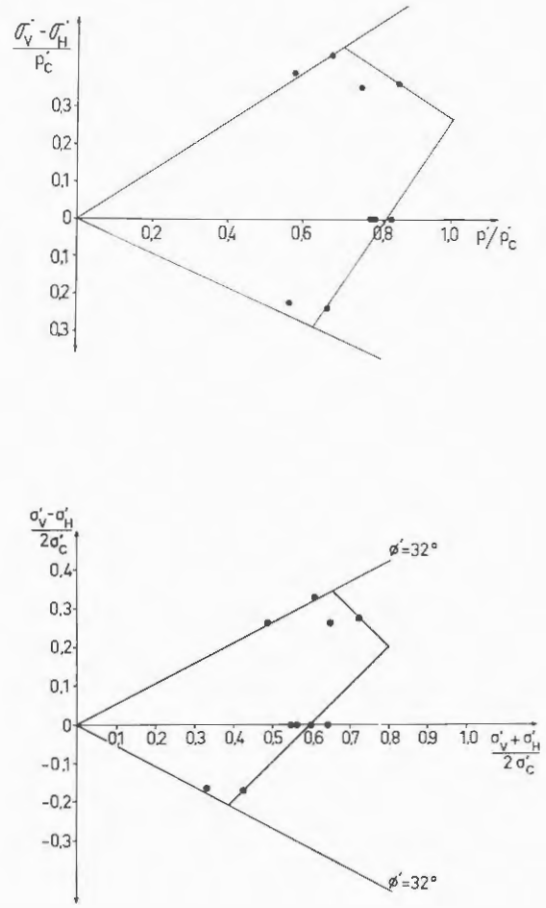

Fig 38 Yield stresses and theoretical yield curve for Fävren a & b clay.

In Fig 39 the yield points obtained by Wong & Mitchell in cemented Champlain clay are shown. The value of K_{nc}^{o} is not given and the diagram has the axes q and p which means that the vertical axis is $\sigma_v - \sigma_H$ instead of $\frac{\sigma_v - \sigma_H}{2}$ as in Fig 35 but the shape of the yield curve is clearly similar to the yield curves for Scandinavian clays.

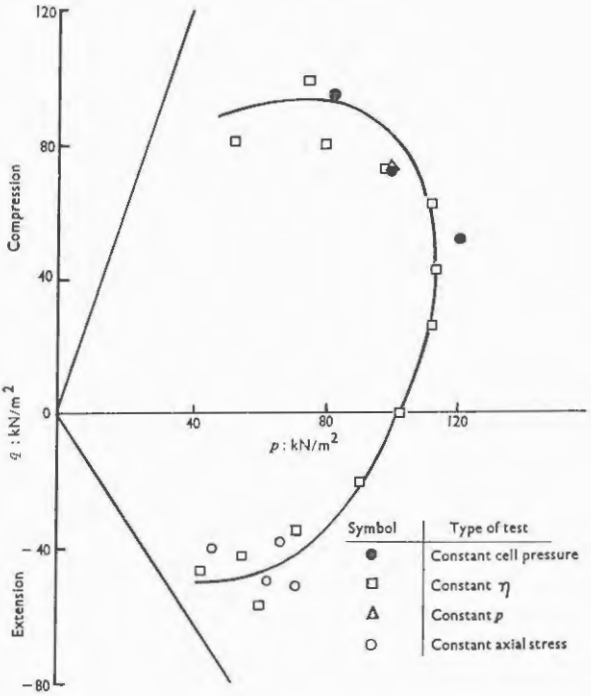

Fig 39 Yield stresses in a cemented Champlain clay. From Wong and Mitchell 1975.

Further test results will be given in Part 12.

11 ANISOTROPY OF UNDRAINED SHEAR STRENGTH

The structure of a naturally consolidated clay has been prestressed for normal stresses that vary in magnitude depending on the orientation of the plane considered. A horizontal plane has been prestressed for the preconsolidation pressure σ_c' and a vertical plane for a stress of $K_{nc}^{o}\ \sigma_c'$. A plane with an orientation such that the angle between the plane and the horizontal plane is α will be prestressed for the normal stress,

$$\sigma_\alpha' = \sigma_c'(\cos^2 \alpha + K_{nc}^{o} \sin^2 \alpha) \qquad (14)$$

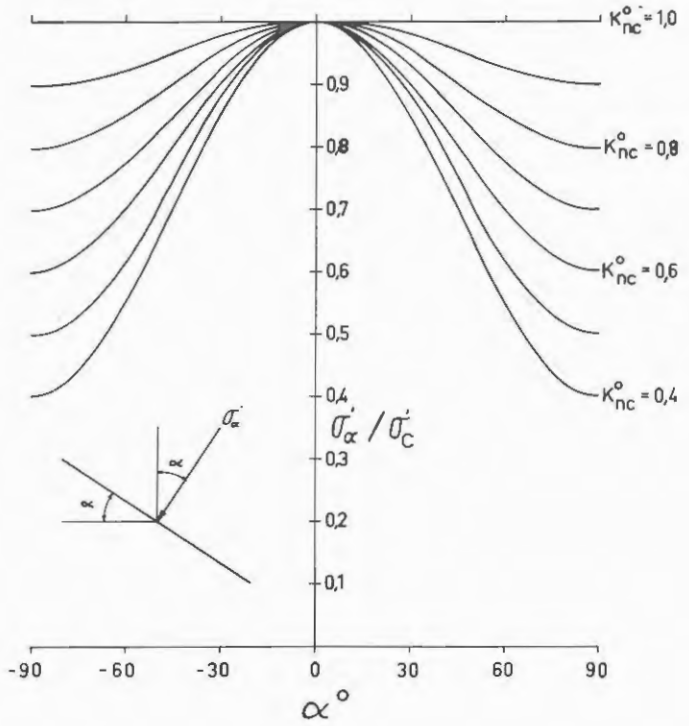

Fig 40 Effective prestress in planes with different orientation.

This prestress is a yield stress and in undrained shear of soft clay the pore pressure development will be such that σ'_α is not exceeded. If σ'_α is the major stress in a shear test, failure will occur along a plane with the angle $(45 - \phi'/2)$ between the plane and the direction of σ'_α. Using the empirical value $\phi' = 30^0$ the maximum undrained shear stress in any plane can be calculated from $\frac{\sigma'_1 - \sigma'_3}{\sigma'_1 + \sigma'_3} = \sin\phi'$ which for $\phi' = 30^0$ gives

$$\tau_{fu} = \frac{\sigma_1 - \sigma_3}{2} = \sigma'_\alpha/3 \qquad (15)$$

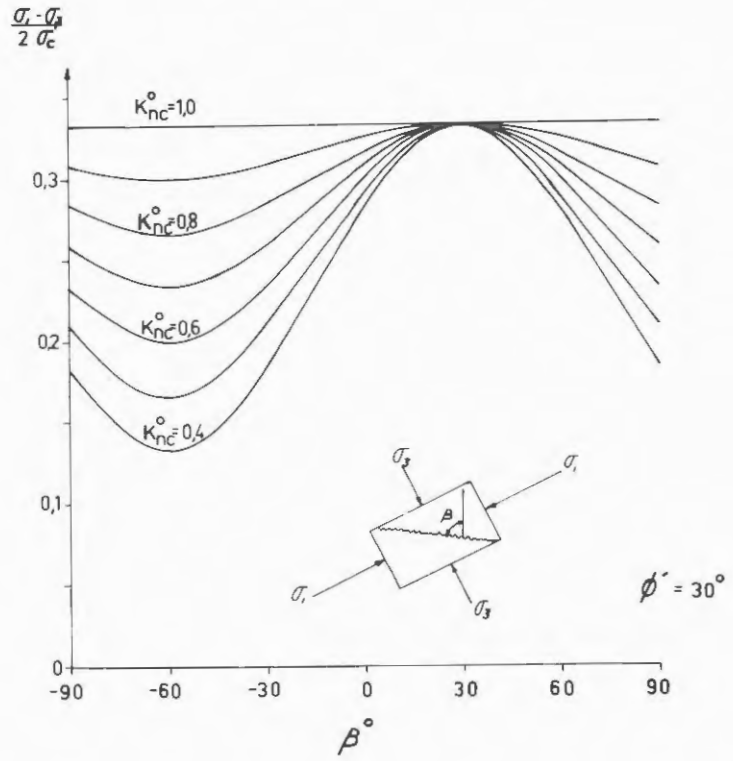

Fig 41 Undrained shear strength in planes with different orientation.

In Fig 41 β is the angle between the failure plane and the vertical. The angle is positive in compression tests and negative in extension tests so that $\beta = 30^0$ corresponds to an active triaxial compression test, $\beta = -60^0$ corresponds to a passive triaxial extension test and $\beta = \pm 90^0$ corresponds to a direct shear test. All values are for vertical samples. These values for undrained shear stress are maximum values that will be obtained provided that the structure of the clay is flexible enough to let the effective stress path follow the yield curve until ϕ' is mobilized. In brittle clays only a part of this shear strength will be obtained and it will depend on the effective stress path.

In heavily overconsolidated clays the theoretical undrained shear strength should be reduced by a factor of about 0,8 as the effective normal stresses will not quite reach the critical stresses.

There will also be anisotropy in the vertical shear plane depending on the orientation of the principal stresses. In vane tests and pressiometer tests one horizontal stress will be the major stress and a horizontal stress perpendicular to the major stress will be the minor stress. The shear plane will be vertical. In pile tests or tests with a pulled auger the shear plane will also be vertical but the direction of the major stress will have an angle of $(45 + \phi'/2)^0$ to the horizontal plane and the shear strength will be different from that measured by the vane.

11.1 Reduction of vane strength for anisotropy

The most common way of measuring undrained shear strength in Sweden is to use the field vane or fall cone.

As the fall cone is calibrated against the field vane the results should be the same.

There are two empirical relations for the undrained shear strength measured by the field vane.

1 SGI relation $\tau_{vane} = 0,30\ \sigma'_c$ (16)

2 Hansbo's relation $\tau_{vane} = \sigma'_c \cdot 0,45\ w_L$ (Hansbo 1957) (17)

Hansbo's relation is in much better agreement with the relations between τ_{fu} and σ'_c measured in the low-plastic Norwegian clays than the SGI relation and many Swedish clays fit well into it. It should be emphasized, though, that far from all clays fit into this relation and the scatter in measured data is wide.

The theoretical shear strengths based on the yield criteria are dependent on K^o_{nc} which in turn is a function of the liquid limit. To correlate theoretical shear strength and strength measured by the field vane the Hansbo relation which is also based on liquid limit must be used.

If the empirical relations

$$\tau_{vane} = \sigma'_c \cdot 0,45\ w_L \qquad (17)$$

$$K^o_{nc} = 0,31 + (w_L - 0,2) \cdot 0,71 \qquad (4)$$

and

$$\tau_{fu} = \sigma'_c(\cos^2\alpha + K^o_{nc} \sin^2\alpha)/3 \qquad (14,15)$$

are combined, correction factors for the undrained shear strength with respect to anisotropy and pure rate effect are obtained, Fig 42.

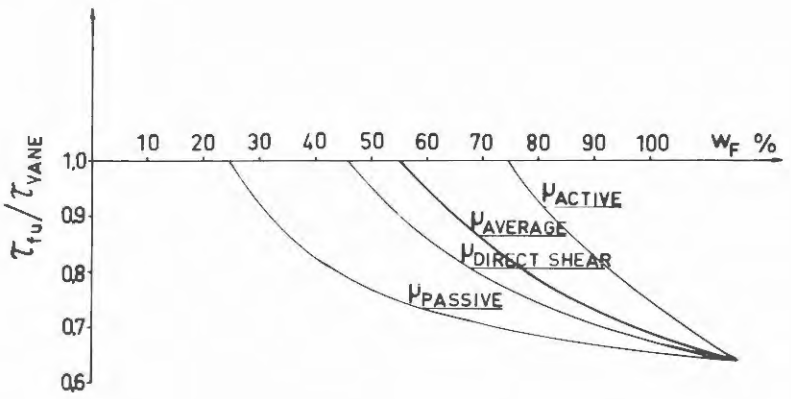

Fig 42 Reduction of field vane strength for anisotropy.

The undrained shear strength from field vane tests may have to be reduced further with respect to secondary time effects, see Part 14. As mentioned earlier the empirical relation for K_{nc}^{o} is not valid for organic clays and triaxial tests have shown that the shear strength in these clays cannot be explained by friction alone.

This difference in behaviour may be explained by the high fibre content in organic clays. In the micrographs in Appendix 3 it can be seen that while the Lilla Mellösa clay which has a low organic content can be considered as a granular material the organic Välen clay is a fibrous-granular material.

The reduction factors are derived from two empirical relations which both show a wide scatter in measured data. Therefore Fig 42 should serve only as an explanation of the nature of the reduction factors that are in use at present.

The best method of reducing the shear strength measured by field vane seems to be to make oedometer

tests in addition to the vane tests and evaluate the relation τ_{vane}/σ'_c. From this relation it can be judged whether the material behaves in a brittle manner or not and by comparison with the theoretical strengths in Fig 41 the actual reduction factors can be chosen.

12 UNDRAINED CREEP TESTS

In 1975 SGI obtained research grants to investigate undrained creep in different test conditions. It was decided that the tests should be made on natural undisturbed samples as some of the natural characteristics are lost in remoulded laboratory consolidated samples. The Lilla Mellösa clay was selected since many previous investigations had been made on it (e.g. Chang 1969) and its characteristics are typical for many Swedish clays. A layer of grey clay between 7,5 and 10,5 metres below the ground surface can be considered as very homogenous with regard to the type of clay and it was expected that fairly uniform samples could be taken from adjacent boreholes.

Sampling was performed with the Swedish piston sampler and samples were taken from 18 boreholes with a spacing of 2 metres between adjacent holes. In one boring samples were taken from every metre of depth down to 11 metres below the ground surface and in the other holes samples were taken from 8, 9 and 10 metres of depth.

An extensive program to determine the undrained shear strength in this clay by field vane tests has previously been carried out by Wiesel.

The samples from the borehole with sampling at every metre have been investigated for water content and density and the shear strength and sensitivity have been determined by fall cone tests. Duplicated oedometer tests with constant rate of strain have been

run on clay from each depth. The results from these investigations are shown in Fig 43.

A large number of direct shear tests have been run on clay from 9 metres depth and the results have been shown in Parts 3 and 8. K_{nc}^{o} has been determined by drained triaxial tests with isotropic pressure on samples from 8, 9 and 10 metres depth.

The samples yielded at stresses of 0,73 σ_c', 0,78 σ_c' and 0,72 σ_c' respectively and a value of K_{nc}^{o} = 0,74 has been used as an average.

A later investigation of the clay has been made on freeze-dried samples in an electron microscope and the photographs are shown in Appendix 3.

The creep tests were performed in four different ways

1. active tests with σ_v increasing and σ_H constant
2. active tests with σ_v constant and σ_H decreasing
3. passive tests with σ_v decreasing and σ_H constant
4. passive tests with σ_v constant and σ_H increasing.

Special creep cells were designed with loading pistons of the same diameter as the sample, i.e. 50 mm. This was to enable change of the vertical stress without affecting the horizontal stress or vice versa. [1)]

[1)] As the sample will deform and change its area when the horizontal stress is changed the vertical stress will change if the vertical load is constant. In creep tests with constant load the vertical stress and the shear stress will change when the area of the sample is changed. When the failure deformation of the sample is small this is not a serious objection especially as it is only the difference between the cell pressure and the stress applied by the vertical load that is affected. In previous creep tests in Sweden (Hansbo 1973) it has been evident that small disturbances during undrained creep such as small load increments during the creep process have serious effects on the creep rates.

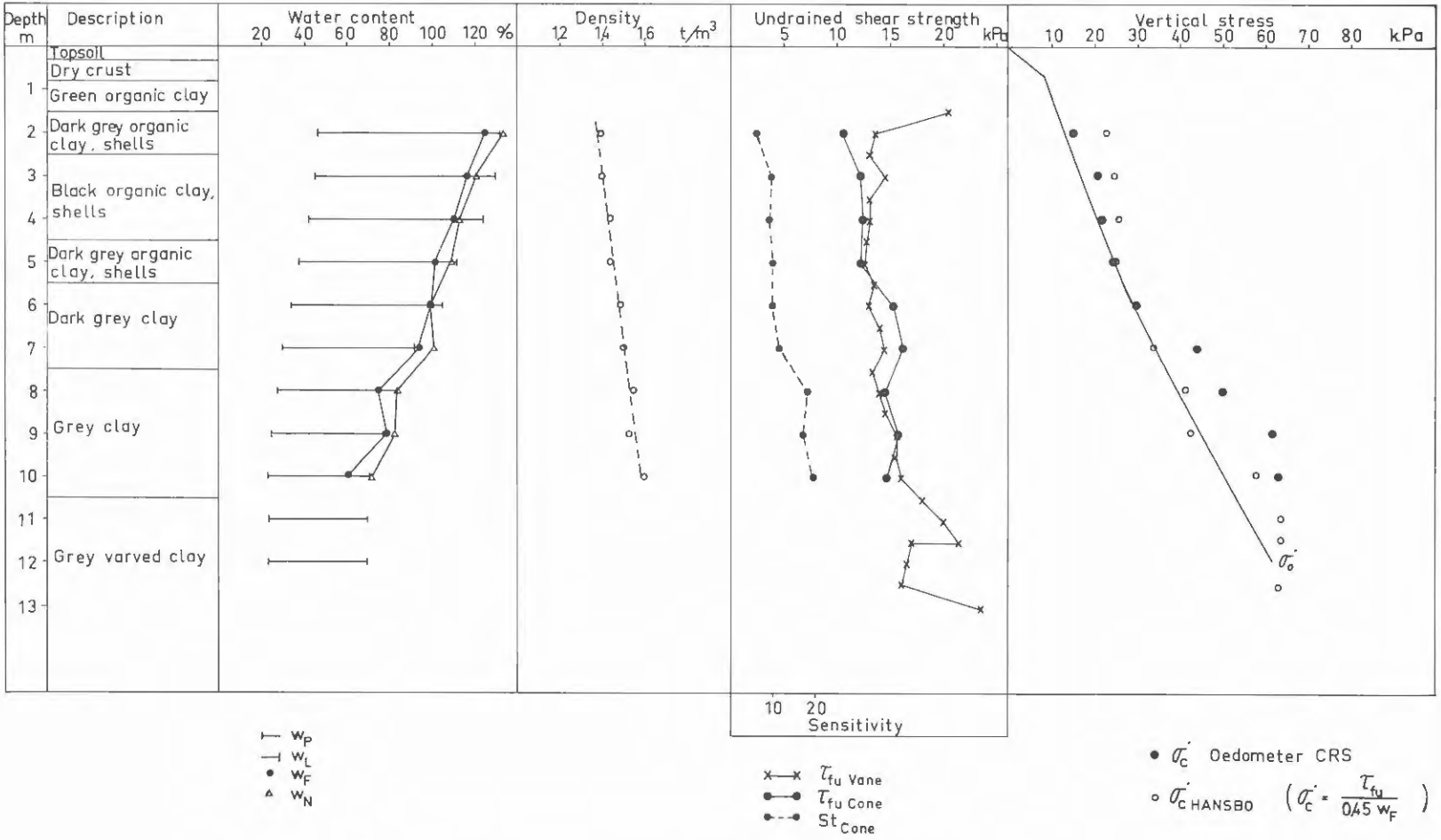

Fig 43 Summary of the properties of Lilla Mellösa clay.

Vertical load was applied by weights on a hanger. Piston friction was reduced by extra long casings and the pistons were rotated with a slow oscillating movement.

To prevent torque being applied to the samples the loads were transmitted by small steel balls in the active tests and by small swivel heads in the passive tests. Cell pressures were regulated by compressed air regulators and paraffin oil was used as chamber fluid. All tests were performed on samples with a height of 100 mm and a diameter of 50 mm. The samples had filter strips on the surface and were enclosed in rubber membranes. Top caps were of perspex with a thin layer of silicone grease on the contact surface. Drainage during consolidation was allowed through filter stones at the base and pore pressures during the tests were measured with electronic pressure transducers in contact with the filter stones. The changes in sample height were measured with electronic displacement transducers.

To avoid temperature effects all tests were run in a climate room where the temperature was kept constant at 7^{0}C which is the average temperature in soil a few metres below the ground surface in Sweden.

12.1 Pilot tests

Before the creep tests were started a series of undrained tests was run to determine the shear strength at normal test rates. The tests were run on samples from 8, 9 and 10 metres and the four types of creep tests were simulated.

The tests with constant horizontal pressure were run with constant rate of strain 0,6%/hour and cells with internal load tranducers were used. The tests with constant vertical load were run in creep cells and

the horizontal pressure was changed by a motor-driven compressed air regulator at a rate of 4 kPa/hour. The cell pressure was measured by pressure transducers. The first fourteen tests, of which two were doubled due to leakage during the tests, were consolidated for the *in situ* stresses. The back pressure in the pore water was equal to the pore water pressure *in situ* so that total stresses as well as effective stresses were simulated.

Consolidation was allowed for 24 hours before the drainage lines were closed and the tests started. The last two tests were run to investigate the effect of overconsolidation ratio and were first consolidated for in situ stresses for 24 hours. Cell pressure and vertical load were then lowered until the effective stresses corresponded to an overconsolidation ratio of 2,5 and the samples were allowed to swell for 24 hours before drainage was closed and the tests started.

The test results are listed in Table 1.

It can be noted that the failure deformations are quite small in this clay. The ratios τ_{fu}/σ'_c seem rather high but a closer examination shows that the undrained shear strength is about 2 kPa higher than the shear stress calculated by $\frac{\sigma_1 - \sigma_3}{\sigma'_1 + \sigma'_3} = \sin 30^0$ which is quite normal for this testing rate.

The effective stress paths in the pilot tests are plotted together with the theoretical yield curve in Figs 44, 45 and 46. It can be seen how the effective stresses are steered by the pore pressure towards the intersection between the yield line for effective prestress and the line for effective shear failure. The stress paths for the overconsolidated samples also strive towards this point even if they cannot quite reach it. The pore pressures also keep the effective stresses at or within the yield curve.

Pilot tests

Type of test	Depth m	σ'_c kPa	σ'_{VO} kPa	σ'_{HO} kPa	$\frac{(\sigma_V-\sigma_H)_f}{2}$ kPa	$\frac{(\sigma'_V+\sigma'_H)_f}{2}$ kPa	ε_f %	$\frac{(\sigma'_V-\sigma'_H)_f}{2\,\sigma'_c}$
Active σ_V increasing	8	50,5	40,0	32,2	18,5	32,6	2,3	0,368
Active σ_H decreasing	8	50,5	40,0	32,2	20,2		~2,7	0,396
Active σ_H decreasing	8	50,5	40,0	32,2	20,0	32,7	~2,7	0,396
Active σ_V increasing	9	61,5	45,5	38,3	23,5	41,8	1,7	0,382
Active σ_H decreasing	9	61,5	45,5	38,3	24,0	41,5	~1,6	0,390
Active σ_V increasing	10	64,0	51,0	43,6	26,2	42,5	2,1	0,410
Active σ_H decreasing	10	64,0	51,0	43,6	28,0	46,7	~2,0	0,436
Passive σ_V decreasing	8	50,5	40,0	32,2	-13,2	20,6	-4,4	-0,262
Passive σ_H increasing	8	50,5	40,0	32,2	-13,0		~-4,0	-0,258
Passive σ_H increasing	8	50,5	40,0	32,2	-13,5	20,7	~-3,2	-0,268
Passive σ_V decreasing	9	61,5	45,5	38,3	-16,2	28,7	-2,4	-0,264
Passive σ_H increasing	9	61,5	45,5	38,3	-15,2	27,4	~-2,1	-0,248
Passive σ_V decreasing	10	64,0	51,0	43,6	-15,9	28,5	-4,6	-0,248
Passive σ_H increasing	10	64,0	51,0	43,6	-15,5	28,0	~-3,4	-0,242
Active σ_V increasing	8	50,5	20,0	20,0	14,25	26,0	7,5	0,282
Passive σ_V decreasing	8	50,5	20,0	20,0	-13,0	19,7	-6,4	-0,258

TABLE 1

In addition, the sudden increases in effective stresses in the undrained passive tests with constant rate of deformation should be noted. They occur when the vertical effective stresses are about 0,4 σ'_c.

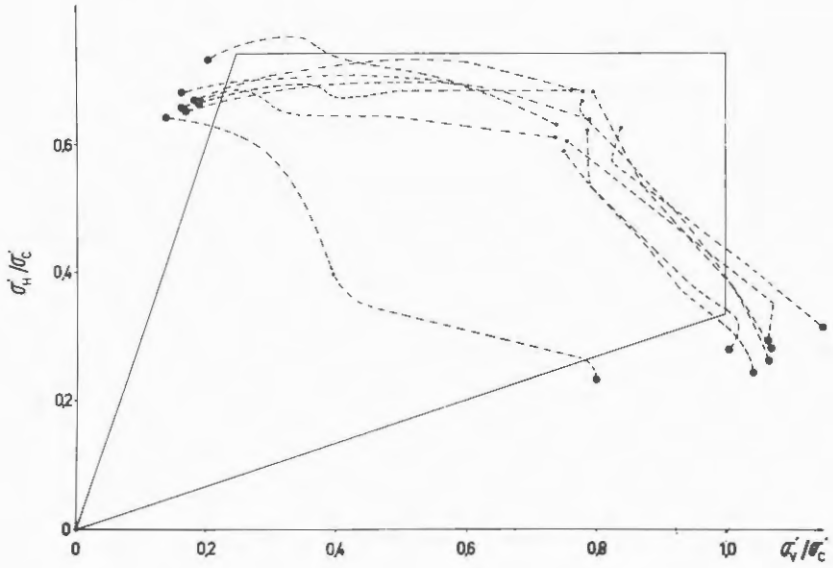

Fig 44 Effective stress paths and theoretical yield curves for pilot tests on Lilla Mellösa clay. Filled circles denote failure.

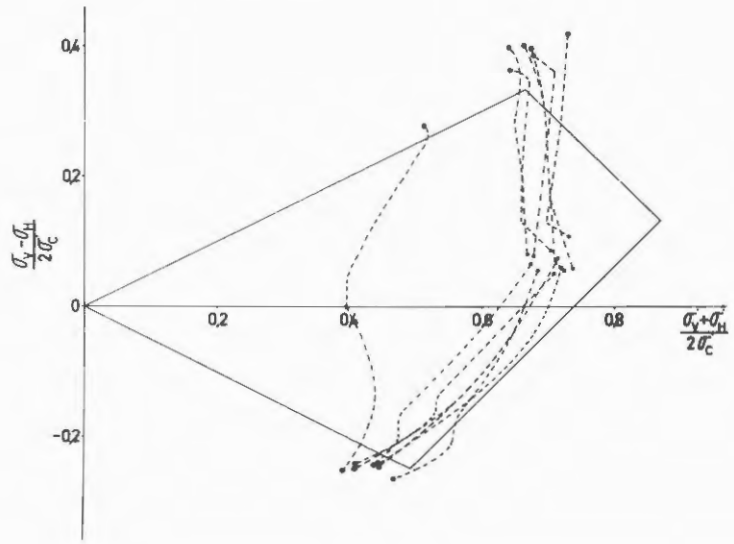

Fig 45 Effective stress paths and theoretical yield curves for pilot tests on Lilla Mellösa clay. Filled circles denote failure.

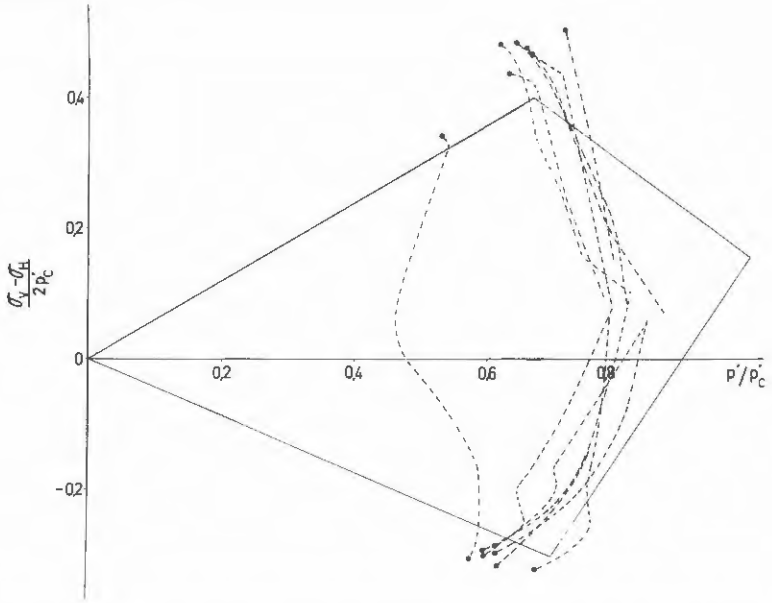

Fig 46 Effective stress paths and theoretical yield curves for pilot tests on Lilla Mellösa clay. Filled circles denote failure.

12.2 Creep series

Five creep series were run. Each series comprised ten tests. The first four series were run on samples that were reconsolidated for the *in situ* stresses for 24 hours. In the last series on overconsolidated clay the samples were first consolidated for *in situ* stresses during 24 hours and then allowed to swell for stresses corresponding to an overconsolidation ratio of 2,5 for 24 hours. After consolidation the drainage was closed and the ten tests in each series were submitted to individual stress changes chosen so that the series should represent the whole region of stresses from consolidation stresses to failure stresses. Vertical stress changes were introduced by a rapid but smooth change of the weights on the hangers and horizontal stress changes were made by changing the adjustment of the compressed air regulators in one step. Readings of deformation and pore pressure were taken continuously by a data logger.

Data from the test series are listed in Tables 2-6.

Creep series K1

9 m

σ_{VO} = 128,0 kPa σ_{HO} = 120,8 kPa u_o = 82,5 kPa σ'_{VO} =45,5 kPa σ'_{HO} = 38,3 kPa σ'_c = 61,5 kPa

σ_V = increasing σ_H = constant

Test No	$\Delta\sigma_V$ kPa	$\sigma_V-\sigma_H$ kPa	ε_1 %	$\dot{\varepsilon}_1$ %/h	m_c	$\frac{(\sigma_V-\sigma_H)_f}{2}$ kPa	$\frac{(\sigma'_V+\sigma'_H)_f}{2}$ kPa	ε_f %	t_f min	Remarks
1	2,5	9,7	0,0209	0,34	0,79					
2	7,5	14,7	0,068	0,40	0,80					
3	12,5	19,7	0,157	1,67	0,80					
4	17,5	24,7	0,275	2,40	0,81					
5	22,5	29,7	(0,49)							Friction
6	27,5	34,7	(0,30)							leak
7	30,0	37,2	0,36	2,90	0,85	18,3	38,3	2,0	$1,3\cdot10^4$	
8	32,5	39,7	0,57	4,19	0,86	19,3	37,5	2,1	$1,7\cdot10^7$	
9	35,0	42,2	0,56			20,4	41,4			leak
10	37,5	44,7	0,78	6,96	0,84	21,8	39,2	2,0	$1,5\cdot10^2$	

TABLE 2

Creep series K 2

8 m

σ_{VO} = 112,5 kPa σ_{HO} = 104,7 kPa u_o = 72,5 kPa σ'_{VO} = 40,0 kPa σ'_{HO} = 32,2 kPa σ'_c = 50,5 kPa

σ_V = decreasing σ_H = constant

Test No.	$\Delta\sigma_V$ kPa	$\sigma_V - \sigma_H$ kPa	ε_1 %	$\dot{\varepsilon}$ %/h	m_c	$\frac{(\sigma_V-\sigma_H)_f}{2}$ kPa	$\frac{(\sigma'_V+\sigma'_H)_f}{2}$ kPa	ε_f %	t_f min	Remark
1	- 7,8	0	-0,08	-1,5	1,40					Samples in tests 4 and 10 came from the same bore-hole and appeared to have a higher pre-consolida-tion press-ure than the rest.
2	-11,8	- 4	-0,28	-3,3	0,92					
3	-15,8	- 8	-0,34	5,0	0,92					
4	-19,8	-12	-0,45		0,92					
5	-23,8	-16	-0,58	-8,6	0,90					
6	-25,8	-18	-0,77	-11,3	0,89	- 9,3	19,8	-2,9	10^3	
7	-27,8	-20	-1,00	-14,0	0,805	-10,3	20,3	-3,0	130	
8	-29,8	-22	-1,07	-18,0	0,745	-11,3	20,5	-3,6	80	
9	-31,8	-24	-1,50	-22,0	0,69	-12,5	21,0	-4,1	40	
10	-33,8	-26	(-1,0)			-13,2	21,0	(-2,0)	(40)	

TABLE 3

Creep series K 3

10 m

σ_{VO} = 143,5 kPa σ_{HO} = 136,1 kPa u_o = 92,5 kPa σ'_{VO} = 51,0 kPa σ'_{HO} = 43,6 kPa σ'_c = 64,0 kPa

σ_V = constant σ_H = decreasing

Test No.	$\Delta\sigma_H$ kPa	$\sigma_V-\sigma_H$ kPa	ε_i %	$\dot{\varepsilon}_i$ %/h	m_c	$\frac{(\sigma_V-\sigma_H)_f}{2}$ kPa	$\frac{(\sigma_V+\sigma_H)_f}{2}$ kPa	ε_f %	t_f min	Remarks
1	- 4,1	11,5	0,024	0,16	0,72					Various loading rates
2	-15,6	23,0	0,11	0,9	0,68					
3	-22,6	30,0	0,32	1,4	0,70					
4	-27,6	35,0	0,55	2,2	0,71					
5	-32,6	40,0	0,53	5,5	0,75	19,6	40,4	2,2	800	
6	-35,1	42,5	0,45	3,6	0,80	20,8	41,8	1,5	900	
7	-37,6	45,0	0,58	5,5	0,75	22,1	40,2	2,2	400	
8	-40,1	47,5	0,46	(2,2)	0,71	23,5	45,9	1,2	600	Valve leak (tightened)
9	-42,6	50,0	0,60	4,1	0,73	24,6	43,8	1,4	160	
10	-45,1	52,5	0,61	6,1	0,73	25,9	45,3	1,06	18	

TABLE 4

Creep series K 4

9 m

σ_{VO} = 128,0 kPa σ_{HO} = 120,8 kPa u_o = 82,5 kPa σ'_{VO} = 45,5 kPa σ'_{HO} = 38,3 kPa σ'_c = 61,3 kPa

σ_V = constant σ_H = increasing

Test No.	$\Delta\sigma_H$ kPa	$\sigma_V-\sigma_H$ kPa	ε_1 %	ε'_1 %	m_c	$\frac{(\sigma_V-\sigma_H)_f}{2}$ kPa	$\frac{(\sigma'_V+\sigma'_H)_f}{2}$ kPa	ε_f %	t_f min	Remarks
1	7,2	0	0,10	0,85	1,10					
2	17,2	-10	0,275	2,1	0,94					
3	22,2	-15	0,30	3,2	0,89					
4	27,2	-20	0,45	5,2	0,79					
5	29,7	-22,5	0,630							Leak
6	32,3	-25	0,655	7,8	0,80	-12,6	25,2	-1,6	100	
7	34,7	-27,5	0,85	12,0	0,64	-14,0	23,1	-2,7	47	
8	37,2	-30	1,09	16,5	0,66	-15,0	26,1	-2,1	10	
9	39,7	-32,5	1,28	26,0	0,61	-16,6	29,5	-2,3	6	
10	42,2	-35	1,70	43,0	0,60	-18,0	29,0	-3,3	4,5	

TABLE 5

Creep series K 5

8 m

σ_{VO} = 92,5 kPa σ_{HO} = 92,5 kPa u_o = 72,5 kPa σ'_{VO} = 20,0 kPa σ'_{HO} = 20,0 kPa σ'_c = 50,5 kPa

σ_V = increasing σ_H = constant

Test No	$\Delta\sigma_V$ kPa	$\sigma_V - \sigma_H$ kPa	ε_1 %	$\dot{\varepsilon}_1$ %/h	m_c	$\frac{(\sigma_V - \sigma_H)_f}{2}$ kPa	$\frac{(\sigma'_V + \sigma'_H)_f}{2}$ kPa	ε_f %	t_f min	Remarks
1	4,0	4,0	0,054	1,55	1,20					
2	8,0	8,0	0,255	2,55	1,20					
3	12,0	12,0	0,335	(2,65)	(0,89)					
4	16,0	16,0	0,270	2,70	1,08					
5	20,0	20,0	0,340	3,2	1,06					
6	22,0	22,0	1,1	13,8	0,90					Shock loading
7	24,0	24,0	0,640	6,5	0,96					
8	26,0	26,0	0,70	(5,6)	(0,98)					Leak
9	28,0	28,0	1,05	16,0	0,85	13,5	22,5	4,1	800	
10	30,0	30,0	1,35	23,5	0,85	14,3	24,4	4,9	250	

TABLE 6

12.3 Technical notes on the creep tests

A total of fifty creep tests have been run and of these nine were partly or totally unsuccessful due to technical faults or inhomogenity. In creep series K1 test number 5 fell out due to piston friction and test number 4 due to a leak in the pore water system. In test number 9 there was an initial leak in the drainage valve which was tightened after a few seconds. From this test only the initial deformation and the failure stresses have been considered fit for use.

In creep series K2 the samples in tests 4 and 10 showed much lower creep rates than the rest of the samples. The samples in these two tests came from the same boring and behaved as if they had a higher pre-consolidation pressure than the rest.

In creep series K3, which was the first series where the horizontal stress was changed, it appeared that some of the pressure supply tubing was too long and had too small dimensions. As a result of this the time for stress change varied. Later this turned out to be fortunate as it showed the influence of time for stress application on the creep rate. In test number 8 the drainage valve started to leak when drainage was closed. The leak was tightened but a certain amount of consolidation seems to have occurred in the sample due to the leak.

In creep series K4 there was a leak in the rubber membrane in test number 5. As this was a passive test paraffin oil soon penetrated between the top cap and the sample and the shear stresses disappeared.

In creep series K5 the final consolidation stresses were isotropic. In test number 6 a small gap appeared between the piston and the top cap and when the vertical stress increase was applied there was a small

free fall before the piston hit the top cap and the sample became shock-loaded. In test number 8 there was a leak in the pore pressure system.

When creep series K5 had been running for two days large areas in Linköping were flooded by melting snow causing failure of the electrical power and compressed-air supply and the series was stopped. When the results were plotted it was seen that the samples which eventually would fail had already failed. The further development of strains and stresses was quite predictable and so the damage was limited.

12.4 Effective stresses and failure in creep tests

The effective stress paths during the creep tests are shown in Figs 47-49. More detailed information is given in Appendix 2.

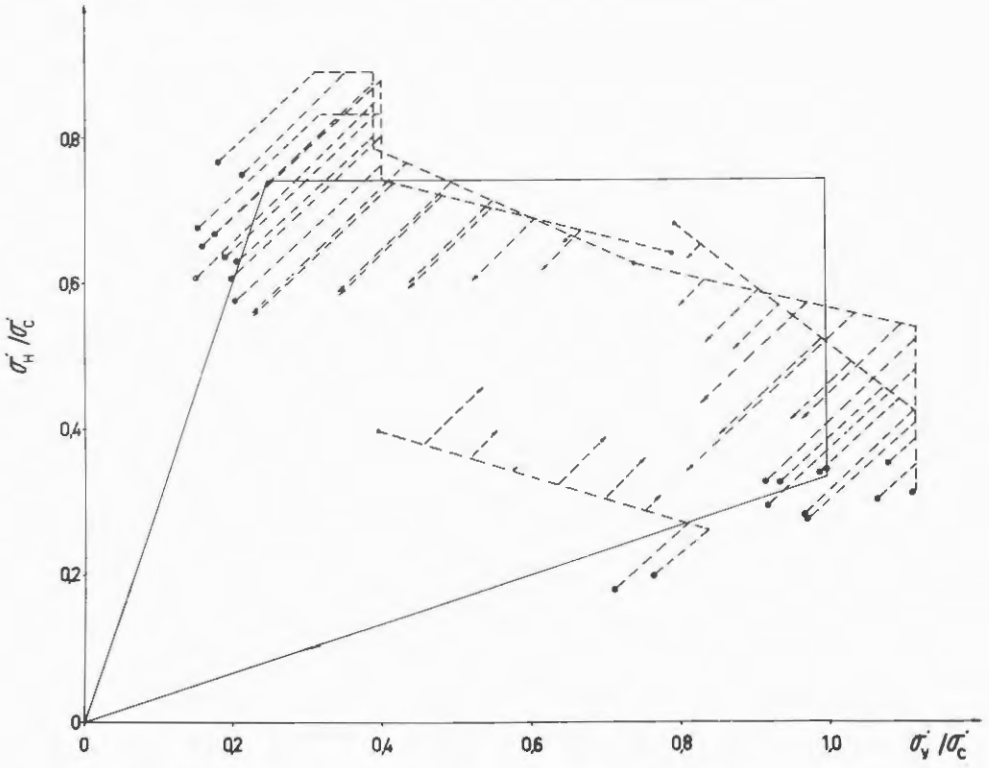

Fig 47 Effective stress paths and theoretical yield curves for creep tests on Lilla Mellösa clay. Filled circles denote failure.

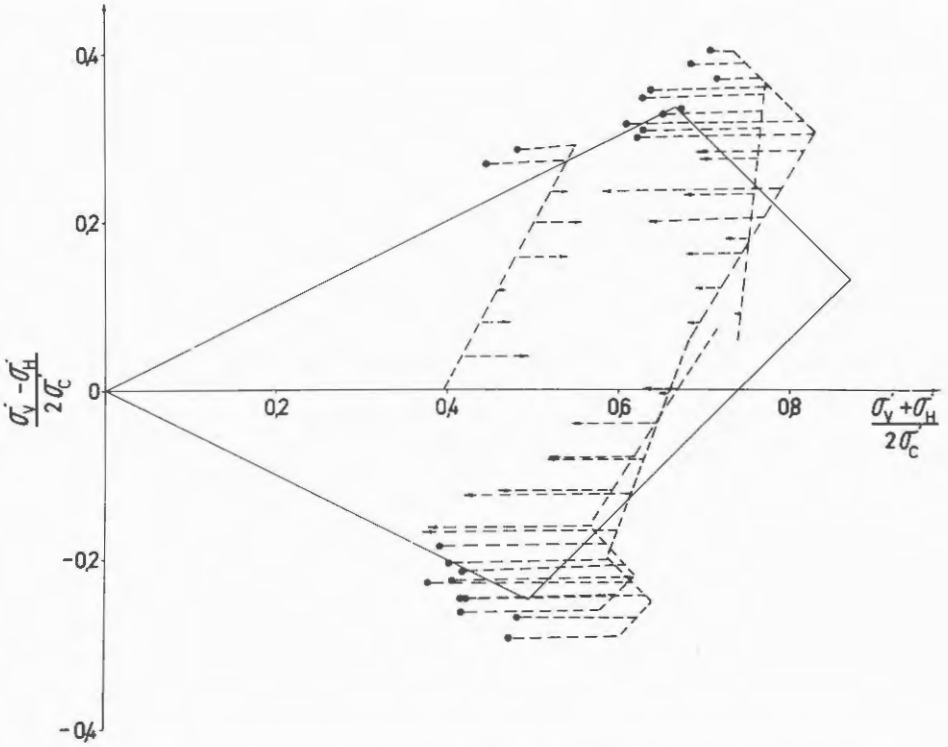

Fig 48 Effective stress paths and theoretical yield curves for creep tests on Lilla Mellösa clay. Filled circles denote failure.

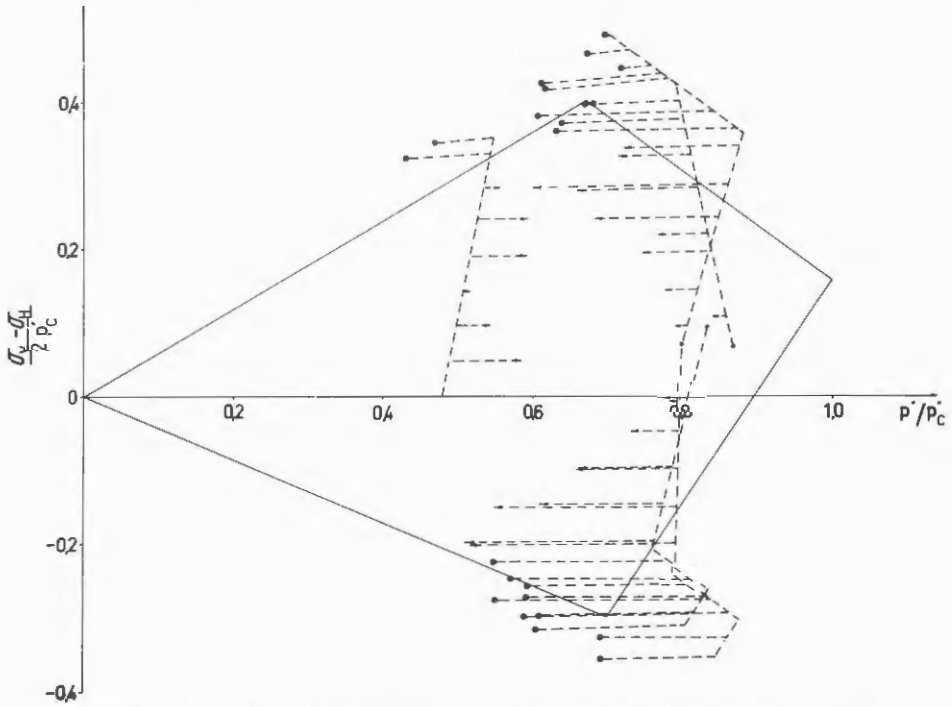

Fig 49 Effective stress paths and theoretical yield curves for creep tests on Lilla Mellösa clay. Filled circles denote failure.

The initial stress paths are not exact as pore pressures during the tests were measured at the base of the sample and although there were filter strips on the sample surfaces the time for pore pressure equalization is too long to allow exact measurement of the initial pore pressures. The initial effective stresses are taken as the stresses one minute after stress application and even they are not exact the trend is quite clear. The initial stress paths in active tests follow straight lines. When the effective vertical stress reaches a critical stress it cannot increase any more and the stress path breaks off. This critical stress is about ten per cent higher than the preconsolidation pressure. This can be expected as the preconsolidation pressure is time dependent and is evaluated from relatively slow tests while the loading in the creep tests was almost instantaneous.

The initial stress paths in passive tests also follow straight lines but when the effective vertical stress comes down to a stress of about 0,4 σ'_c it suddenly stops decreasing. This is exactly the same behaviour as in passive tests with constant rate of strain. The vertical stress level 0,4 σ'_c is slightly lower than the vertical stress at which clay in oedometer tests starts to swell. It is believed that it is the swelling capacity of the clay that is released at the vertical stress 0,4 σ'_c and causes the break in the initial effective stress path. When the horizontal effective stress reaches a stress level about ten per cent higher than $K^o_{nc}\ \sigma'_c$ it cannot increase further and there is a new break in the initial stress path.

When the pore pressure changes during the creep process the changes in effective vertical and horizontal stress will be about the same and the shear stress remains fairly constant (see note, page 67). If the effective stress path passes the line for effective shear failure the sample will fail. It can be seen

that samples with high shear stresses which failed after a short time had failure stresses slightly exceeding the effective failure line while samples which failed after a long time failed at stresses coinciding with the effective failure line. In Fig 47 it can be seen that the stress paths for all tests that did not fail approached the effective stresses $\sigma'_v = 0,8\ \sigma'_c$ or $\sigma'_H = 0,8\ K^o_{nc}\ \sigma'_c$. The stress paths for overconsolidated samples also approached these values as the pore pressures in these tests decreased during the creep process.

12.5 Pore pressures in creep tests

As earlier pointed out the exact magnitudes of initial pore pressures cannot be measured but the trend can be observed. In Fig 49 it can be seen that the initial pore pressures before yield can roughly be said to be adjusted to keep the mean effective stress constant. At yield the pore pressures are adjusted to prevent the effective stresses from exceeding the critical stresses and in passive tests the pore pressure at a vertical effective stress of about $0,4\ \sigma'_c$ is adjusted to momentarily prevent this stress from further decrease.

The pore pressures measured one minute after stress application are shown in Fig 50.

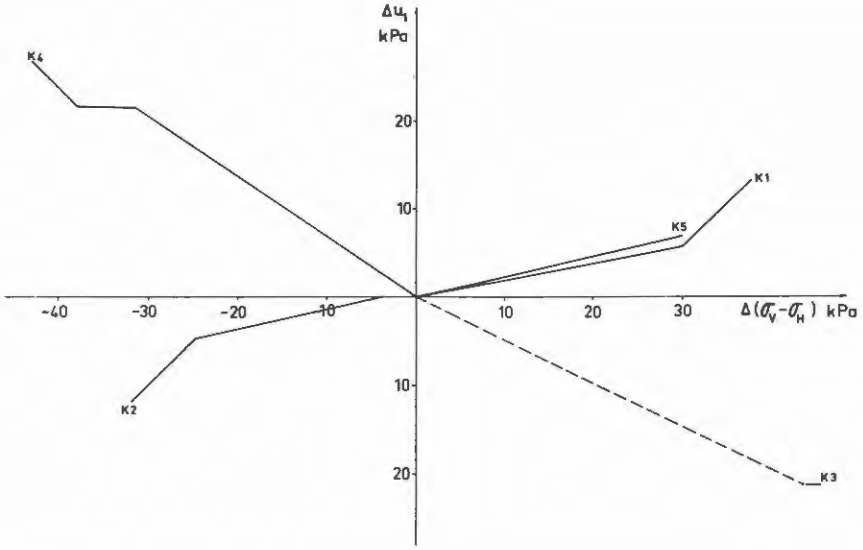

Fig 50 Initial pore pressure change versus stress change.

Some of the initial pore pressures from creep series K3 had to be estimated by extrapolation as some of the times for load application were long. The samples in creep series K2 did not seem to have been fully consolidated at the start of the tests.

The pore pressure development during the creep process was found to be a function of deformation.

In Figs 51 and 52 the pore pressure changes versus deformation in the creep series K1 and K4 are shown.

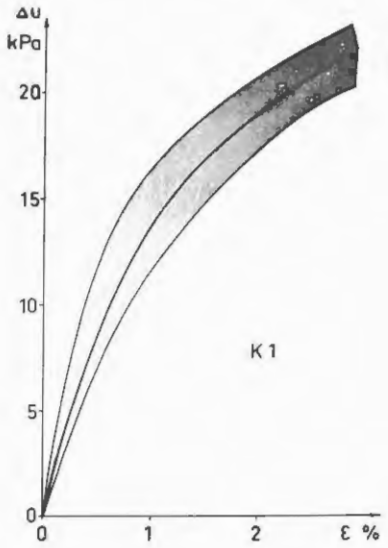

Fig 51 Pore pressure change versus deformation in creep series K1.

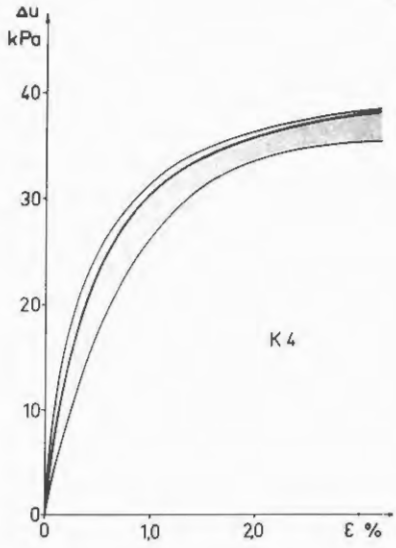

Fig 52 Pore pressure change versus deformation in creep series K4.

In Figs 51 and 52 lower and upper limits of pore pressure and the average pore pressure versus deformation are shown. Similar curves have been reported by Holtzer et al (1973).

In Fig 53 the pore pressure changes in creep series K2 are shown. During the initial deformation the pore pressure changes were negative but they became positive during the creep process.

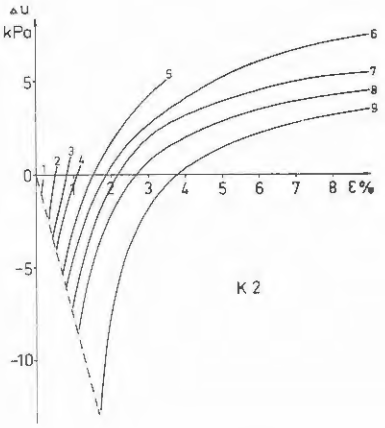

Fig 53 Pore pressure change versus deformation in creep series K2.

The pore pressure changes in creep series K5 on over-consolidated samples were positive in the initial stage but became negative during the creep process.

Holtzer et al (1973) suggested that shear strains during undrained creep were due to increase in pore water pressure and reduction in effective stresses. This is directly contradicted by the results from creep series K5 where the creep strains developed in the same way as in the other creep series although the effective stresses increased.

A summary of the pore pressure developments in creep series K1-K5 would be that initially the pore pressures are adjusted to keep the mean effective stresses constant. At yield the pore pressures prevent the effective stresses from exceeding the critical stresses and in passive tests the pore pressures will momentarily prevent the vertical effective stress from decreasing further at the stress level where the swelling capacity is released. A similar stress level probably exists for horizontal effective stresses

although it has not been found in this investigation. During the creep process the pore pressure changes will be a function of the creep deformation and become positive or negative depending on the overconsolidation ratio. In this particular clay the pore pressure will increase during creep if the horizontal effective stress after the initial deformation is higher than $0,8\ K_{nc}^{o}\ \sigma_c'$ or the effective vertical stress at the same stage is higher than $0,8\ \sigma_c'$. If both principal stresses at this stage are lower than the mentioned limits the pore pressure will decrease during creep provided that the effective stresses have not exceeded the effective failure line.

Holtzer et al have reported that pore pressures in undrained creep tests will increase due to secondary effects and this becomes disturbing after about a week. The same process was found in the tests on Lilla Mellösa clay. In the creep series samples were subjected to very low stress changes and these were used as dummies to compensate for these secondary pore pressure changes. The secondary pore pressure change might have affected the strain rate of test number 5 in creep series K2 but no sample failed due to this effect.

12.6 Initial deformations in creep tests

The initial deformations are evaluated as the deformations measured one minute after stress application, Fig 54. The initial deformations for some of the tests in creep series 3 have been evaluated by extrapolation.

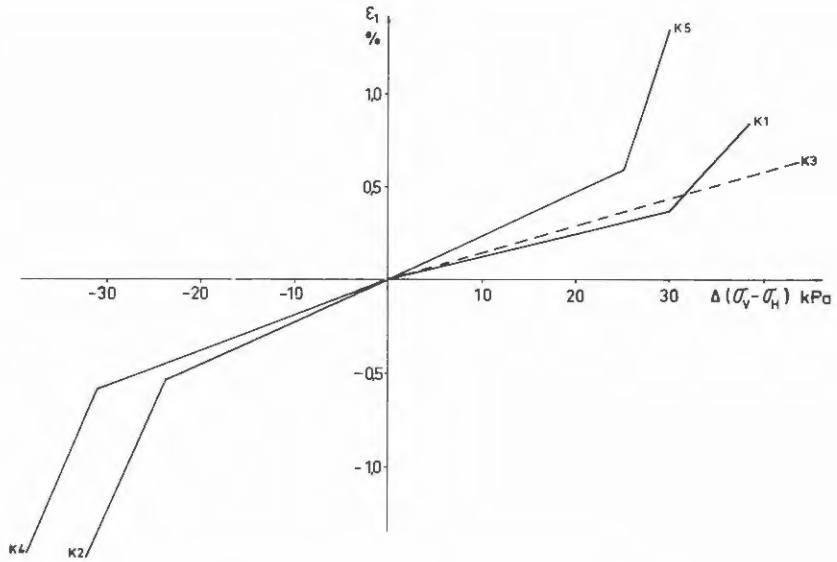

Fig 54 Initial deformation versus stress change.

The initial deformations for stress changes not leading to yield are elastic but the modulus of elasticity varies with the type of test. It can be noted how the modulus of elasticity has decreased due to swelling in creep series K5. When the stress change causes yield the initial deformations become elasto-plastic and rapidly increase.

12.7 Creep rates

The initial creep rates evaluated as the rates of strain one minute after application of stress change depend on the applied stress change in almost exactly the same way as the initial deformations, Fig 55.

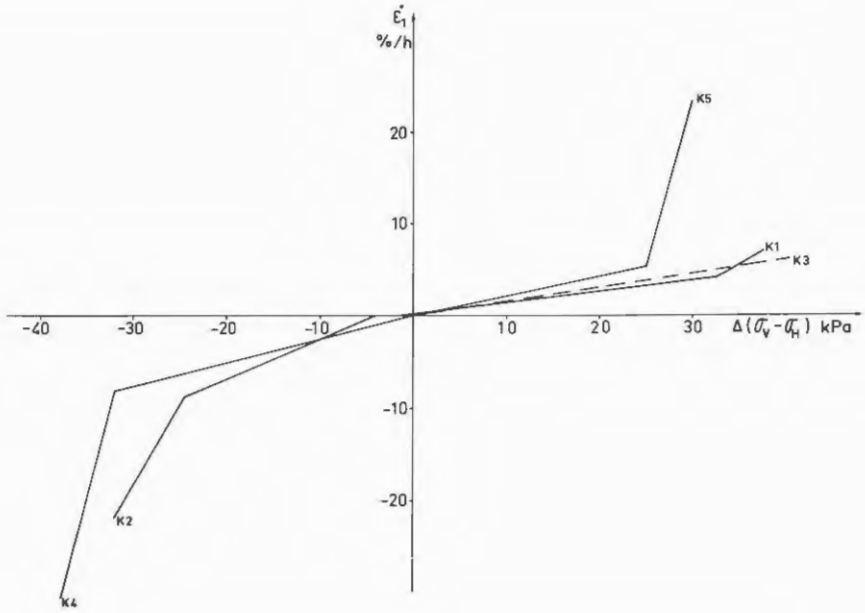

Fig 55 Initial rate of deformation versus stress change.

The initial rates of strain are a linear function of the applied stress changes if the stress changes do not lead to yield. If the initial rate of strain is plotted versus the initial deformation it is found that the initial strain rate is a linear function of initial deformation regardless of whether the sample has yielded or not, Fig 56.

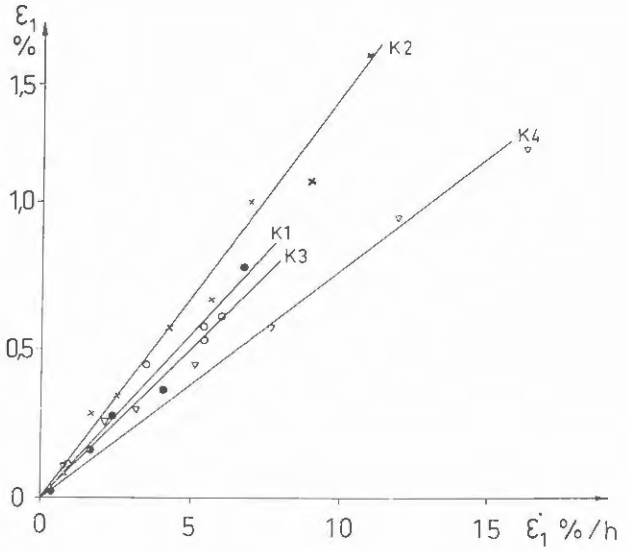

Fig 56 Initial rate of deformation versus initial deformation in creep series K1-K4.

The only exception from this rule is if the stresses during the initial stage as in creep series K5 have exceeded the effective failure line, Fig 57.

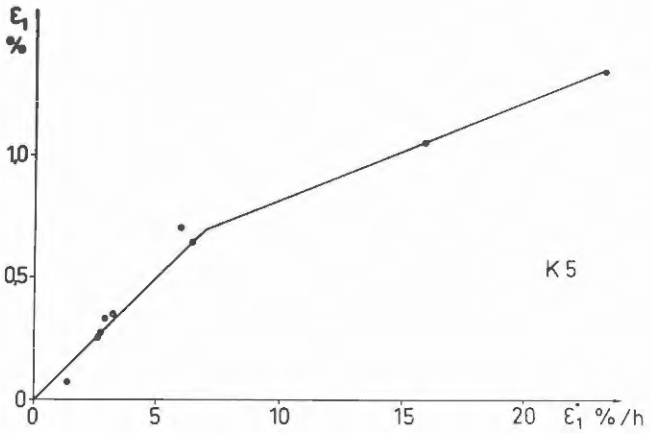

Fig 57 Initial rate of deformation versus initial deformation in creep series K5.

In creep series K3 the time for application of stress change varied. It was found that the slower the loading was the lower the initial creep rate became and the sample in creep series K5 which was shock loaded gave a very high initial creep rate. These effects did not even out in the long run but persisted throughout the whole creep process.

The intial creep rate is thus dependent on the degree of stress change, whether the sample yields or not, the mode of stress change and the time for application of the stress change.

During the creep process the logarithm of creep rate decreases linearly with the logarithm of time, $d \log \dot{\varepsilon}/d \log t = m_c$. This has been found in all previously reported creep tests and is also valid for all the creep tests in this investigation, Figs 58-62.

The creep rate decreases until the effective stress path reaches the effective failure line. The creep rate then becomes constant or increases and the sample fails. The values of m_c for each test are given in Tables 2-6. The scatter in m_c values from each creep series is limited which means that the lines for creep rate in the log $\dot{\varepsilon}$ - log t diagram for each creep series are fairly parallel and an average value can be used in calculations.

Singh & Mitchell (1968) have formulated the expression for creep rate

$$\dot{\varepsilon} = Ae^{\alpha(\sigma_1-\sigma_3)} \left(\frac{t_1}{t}\right)^{m_c} \qquad (18)$$

where $$\alpha = d(\ln \dot{\varepsilon}_1)/d(\sigma_1-\sigma_3) \qquad (19)$$

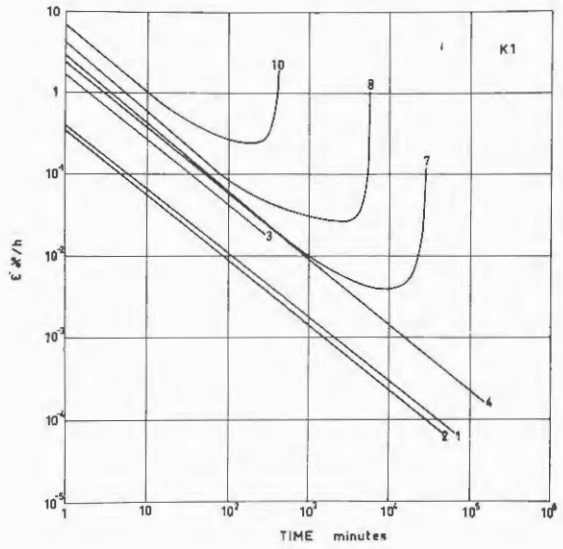

Fig 58 Rate of deformation versus time in creep series K1.

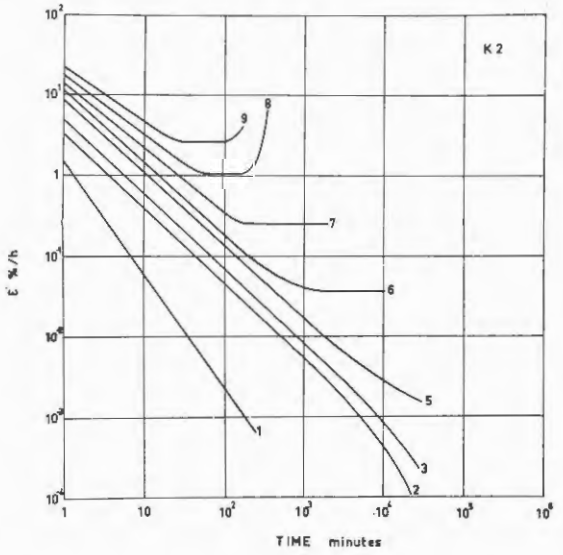

Fig 59 Rate of deformation versus time in creep series K2.

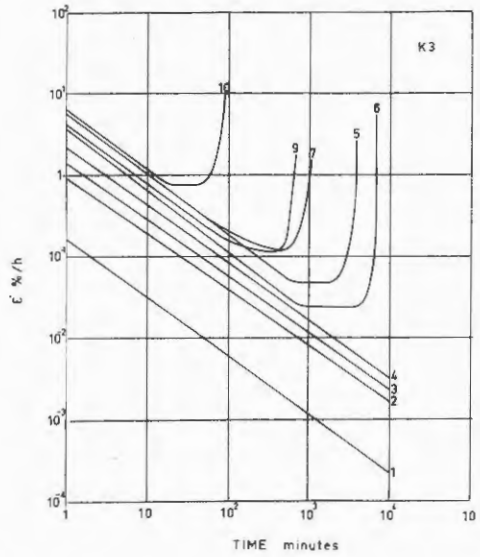

Fig 60 Rate of deformation versus time in creep series K3.

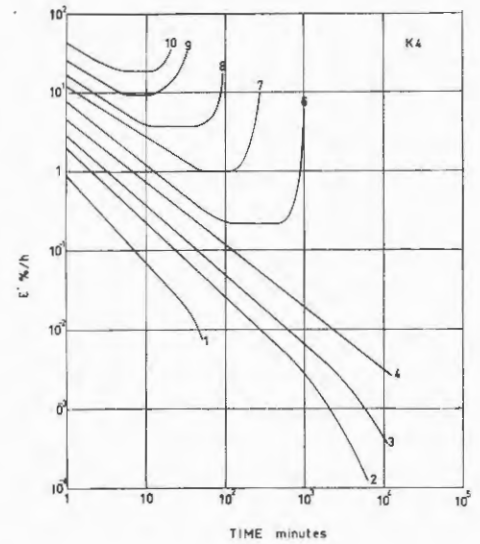

Fig 61 Rate of deformation versus time in creep series K4.

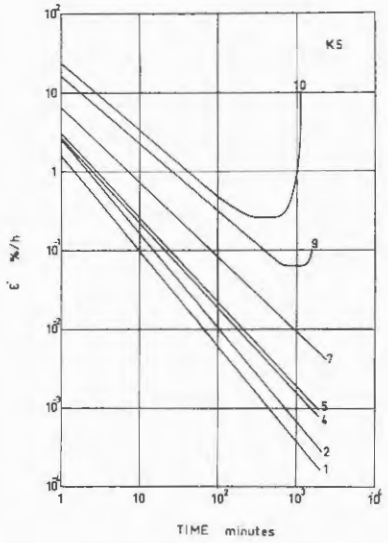

Fig 62 Rate of deformation versus time in creep series K5.

This formula has been used by a number of investigators and has fitted their tests. Most creep tests reported have been run on remoulded laboratory-consolidated samples or natural samples consolidated isotropically for stresses higher than the previous maximum stresses so that ansiotropy effects have disappeared. These tests have also normally started with the initial stresses equal to the preconsolidation stresses. Such tests do not simulate the *in situ* conditions where there is always anisotropy, usually an initial shear stress and usually some degree of overconsolidation. In normally consolidated tests with isotropic consolidation stresses the samples will yield when the applied shear stress is only about 30% of the undrained shear strength while in nature most of the undrained shear strength can be applied without yield. Initial deformations for stress changes not leading to yield and with the same time for load application are linear elastic and deformations and creep rates before failure can be calculated by the following formulas.

σ'_v after the initial deformation can be calculated from

$$\sigma'_v = \sigma'_{vo} + A\,\Delta(\sigma_1-\sigma_3) \tag{20}$$

and provided that

$$\frac{\sigma_1 - \sigma_3}{\sigma'_1 + \sigma'_3} < \sin\phi'$$

and

$$1{,}1\,\sigma'_c > \sigma'_v > 0{,}4\,\sigma'_c$$

the initial deformation will be

$$\varepsilon_1 = \Delta(\sigma_1 - \sigma_3)/E \tag{21}$$

the creep rate at time t will be

$$\dot{\varepsilon}_t = k_1 \cdot \Delta(\sigma_1-\sigma_3)/t^{m_c} \tag{22}$$

and the total deformation at time t will be

$$\varepsilon_t = \varepsilon_1 + \frac{k_1 \cdot \Delta(\sigma_1-\sigma_3)}{1 - m_c} \cdot (t^{m_c} - 1) \quad \text{if } m_c \neq 1 \tag{23}$$

$$\varepsilon_t = \varepsilon_1 + k_1 \cdot \Delta(\sigma_1-\sigma_3) \ln t \quad \text{if } m_c = 1 \tag{24}$$

In the creep series the following values for the constants were obtained.

Creep series	E kPa	A	k_1 %/min·kPa	m_c
K1	8330	0,81	$1,97 \cdot 10^{-3}$	0,82
K2	4165	0,81	$7,27 \cdot 10^{-3}$	0,91
K3	6680	0,56	$2,5 \cdot 10^{-3}$	0,73
K4	5450	0,69	$4,23 \cdot 10^{-3}$	0,90
K5	4280	0,75	$3,62 \cdot 10^{-3}$	1,0

The constants vary with the mode of stress change and as hardly any field case corresponds to the triaxial test they would have to be modified before use. The value of k_1 is valid for instantaneous loading only. This is rarely the field case and so it would have to be modified for the time for stress change.

12.8 Creep shear strength

As mentioned earlier failure occurs in creep tests when the effective stress path reaches the effective failure line. If the effective stresses become lower than $\sigma_v' = 0,8\ \sigma_c'$ and $\sigma_H' = 0,8\ K_{nc}^{o}\ \sigma_c'$ before the stress path reaches the effective failure line failure will probably not occur. The value 0,8 is valid for the Lilla Mellösa clay but test series on Bäckebol clay and Drammen clay with different rates of deformation have given values of the same order.

Liam Finn & Shead (1973) have suggested that the minimum undrained shear strength can be evaluated from the rate of strain at failure in creep tests. This is made by plotting the cubic root of the minimum strain rate against deviator stress and extrapolating the connecting lines to zero strain rate. Creep series K1-K4 are evaluated in this way and the results are good, Fig 63.

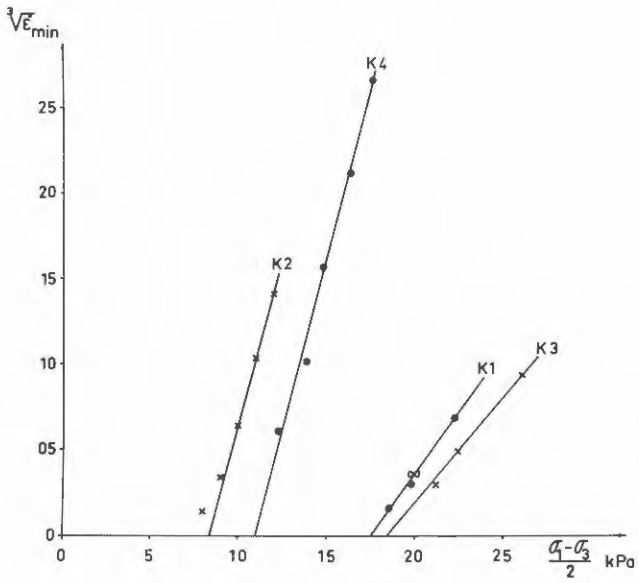

Fig 63 Evaluation of minimum shear strength.

13 CREEP IN FIELD CASES

A number of deformations in field cases are called creep. The most common type of creep is drained secondary consolidation which causes settlements but improves the shear strength.

Bottom-heave in excavations is often attributed to shear creep but depends to a large extent on time-bound swelling unless the shear stresses are close to failure.

The settlements of a small loaded area are often to a large part due to horizontal deformations in the soil. The horizontal deformations are often attributed to shear strains and shear creep. From compression tests with measurements of horizontal stress it is known that the effective horizontal stress will be equal to the maximum horizontal prestress when the

vertical effective stress amounts to the preconsolidation pressure unless the sample is allowed to deform horizontally. In the field the soil just outside the edge of a loaded area will thus be subjected to a horizontal stress greater than the prestress when the effective vertical stress under the loaded area exceeds the preconsolidation pressure. This will result in large horizontal deformations regardless of the shear stress. Shear strains will become really important first when the shear stress is close to failure. Deformations in different stress stages are illustrated in Fig 64.

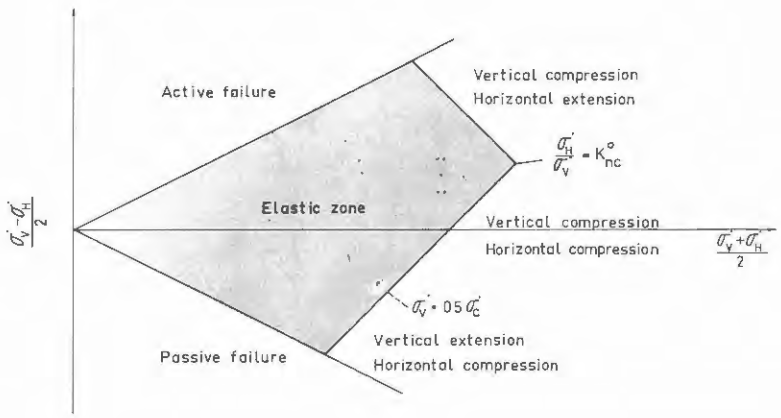

Fig 64 Drained deformations in different stress regions.

Shear creep in slopes often causes serious problems. In soft clays the failure deformations and the strain rates in continuous undrained creep are very low. An analysis of reported cases of serious creep problems in slopes shows that the creep is usually due to seasonal variation in ground water level. In steep slopes a rise in the ground water level will bring the effective stresses close to failure and movements occur in the slope. After a number of seasonal rises in the pore water pressure the accumulated movements

have broken the soil structure and the slope fails. An exceptional high rise in ground water level will also cause failure in steep slopes.

The continuous long-term undrained shear creep in soft clays thus has limited importance unless it causes enough rise in pore water pressure to cause failure.

14 REDUCTION OF UNDRAINED SHEAR STRENGTH FOR TIME EFFECTS

In the creep tests on Lilla Mellösa clay it has been found that the effective stresses in undrained conditions will stabilize when the major effective normal stress is about 80% of the prestress in the same direction. This results in a correction for time on the strength values given in Section 11 of 0,8. This correction factor is in agreement with findings from tests on Drammen clay (Berre & Bjerrum 1973) and Bäckebol clay (Larsson 1975 b).

The creep tests also show that the undrained shear strength measured in overconsolidated clays with standard rate of strain in triaxial tests should not be corrected for secondary time effects and this is in agreement with the test results from Bäckebol clay. As the undrained shear strength in overconsolidated clay is partly due to low pore pressures the risk of water absorption with time should be considered and corrections may have to be made.

The undrained shear strength in soft clays corrected for combined time effects can be expressed

$$\tau_{\text{undrained creep}} = 0{,}8\ \sigma'_c\ (\cos^2 \alpha + K^o_{nc} \sin^2 \alpha)/3 \qquad (25)$$

and the effect of anisotropy is shown in Fig 65.

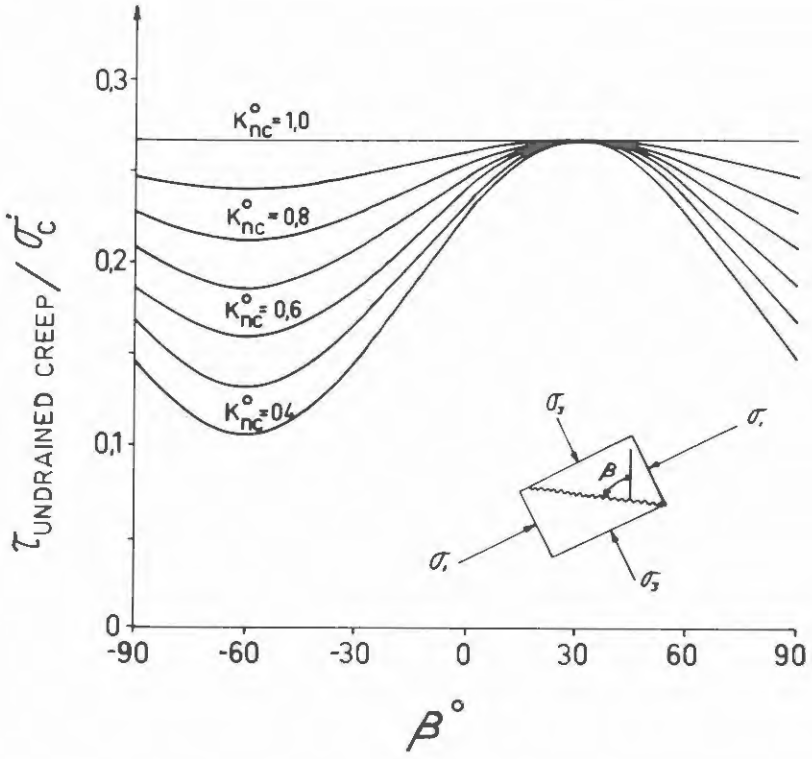

Fig 65 Shear strength of soft clays in long-term undrained shear.

The shear strength measured by field vane can be corrected for anisotropy and pure rate effect according to Section 11 and can in normally consolidated clays be further corrected for secondary time effects by a factor of 0,8, Fig 66.

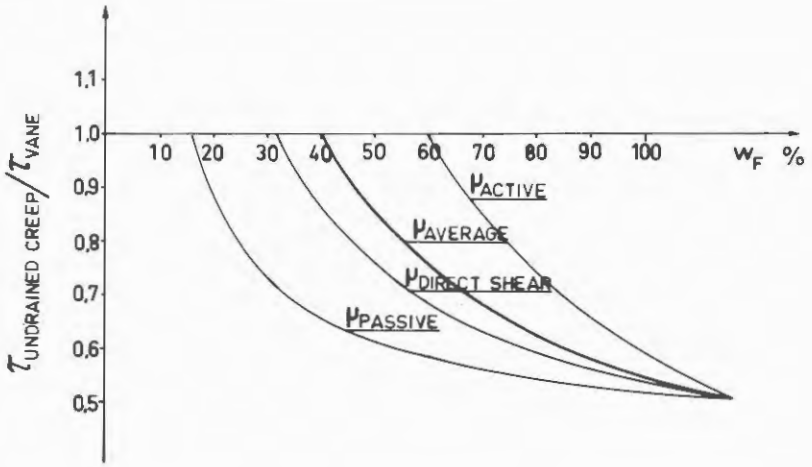

Fig 66 Reduction of field vane strength for anisotropy and time effects.

This reduction is in good agreement with the reduction proposed by Bjerrum (1973) on the basis of natural slides. Bjerrum proposed a reduction for plasticity and Andréasson (1974) has recalculated the reduction for liquid limit to be in accordance with Swedish practice.

Whether the correction for secondary time effects should be applied or not depends on the duration of the shear stress and the drainage conditions *in situ*.

As pointed out in Section 11 it is not recommended to use these reduction factors but a combination of field vane tests and oedometer tests.

REFERENCES

Arulanandan K, Shen C K and Young R B (1971), Undrained creep behaviour of a coastal organic silty clay. Géotechnique, Vol 24, No 4 1971, p 359-375.

Andréasson L (1974), Förslag till ändrade reduktionsfaktorer vid reduktion av vingborrbestämd skjuvhållfasthet med ledning av flytgränsvärdet. Internal report. Chalmers University of Technology, Gothenburg 1974 (not published).

Berre T and Bjerrum L (1973), Shear Strength of Normally Consolidated Clays. International Conference on Soil Mechanics and Foundation Engineering 8, Moscow 1973, Proceedings Vol 1.1, p 39-49.

Berre T (1975), Bruk av triaxial- og direkte skjaerforsök till lösning av geotekniske problemer. Nordiska Geoteknikermötet i Köpenhamn 1975.

Bishop A W and Eldin A K G (1953), The effect of stress history on the relation between ϕ and porosity in sand. International Conference on Soil Mechanics and Foundation Engineering 3, Zürich 1953, Proceedings Vol 1, p 100-105.

Bishop A W and Henkel D J (1962), The Triaxial Test. London Arnold 1962.

Bishop A W (1966), The strength of soils as engineering materials. Sixth Rankine lecture, Géotechnique, Vol 16, No 2, p 89-130.

Bjerrum L, Simons N and Torblaa I (1958), The effect of time on the shear strength of a soft marine clay. Brussels Conference on Earth Pressure Problems, 1958, Proceedings Vol 1, p 148-158.

Bjerrum L (1961), The effective shear strength parameters of sensitive clays. International Conference on Soil Mechanics and Foundation Engineering 5, Paris 1961, Proceedings Vol 1, p 23-28.

Bjerrum L and Andersen K (1972), In situ measurement of lateral pressures in clay. European Conference on Soil Mechanics and Foundation Engineering 5, Madrid 1972, Proceedings Vol 1, p 11-20.

Bjerrum L (1973), Problems of Soil Mechanics and Construction on Soft Clays on Structurally Unstable Soils. General Report. International Conference on Soil Mechanics and Foundation Engineering 8, Moscow 1973, Proceedings Vol 3.

Bozozuk M (1976), Mud Creek Bridge Foundation Movements. Canadian Geotechnical Journal, Vol 13, No 1, p 21-26.

Brink R (1967), Effective Angle of Friction for a Normally Consolidated Clay. Geotechnical Conference on Shear Strength Properties of Natural Soils and Rocks, Oslo 1967, Proceedings Vol 1.

Brooker E and Ireland H (1965), Earth pressures at rest related to stress history. Canadian Geotechnical Journal, Vol 2, No 1, 1965.

Calabresi G (1970), Creep behaviour of undisturbed clays in shear box tests of long duration. Rivista Italiana di Geotecnica 1970, No 1, p 7-16.

Campanella R G and Vaid Y P (1974), Triaxial and Plane Strain Creep Rupture of an Undisturbed Clay. Canadian Geotechnical Journal, Vol 11, No 1, p 1-10.

Chang V C E (1969), Long-term consolidation beneath the test fills at Väsby, Sweden. Thesis, University of Illinois, Urbana, Illinois 1969.

Feda J (1971), Constant Volume Shear Tests of Saturated Sand. Archiwum Hydrotechniki, Warzaw 1971, No 3, p 349-367.

Hansbo S (1957), A new approach to the determination of the shear strength of clay by the fall cone test. Swedish Geotechnical Institute, Proceedings No 14.

Hansbo S (1972), Bestämning av tillåten grundpåkänning med hänsyn till viskösa elasto-plastiska egenskaper hos lera. Nordiska Geoteknikermötet i Trondheim 1972, Oslo.

Helenelund K V (1977), Methods for reducing undrained shear strength of soft clay. Swedish Geotechnical Institute, Report No 3, 1977.

Henkel D J (1958), The Correlation between Deformation, Pore Water Pressure and Strength Characteristics of Saturated Clays. Thesis. University of London, April 1958.

Holtzer T L, Höeg K and Arulanandan K (1973), Excess pore pressures during undrained clay creep. Canadian Geotechnical Journal, Vol 10, No 1, p 12-24.

Hvorslev M J (1960), Physical Components of the Shear Strength of Saturated Clays. ASCE Research Conference on Shear Strength of Cohesive Soils. University of Colorado 1960.

Janbu N (1975), Skjaerstyrken av granulaere materialer. Nordiska Geoteknikermötet i Köpenhamn 1975.

Kamenov B (1976), The constant volume shear box tests of sand. Conference on Soil Mechanics and Foundation Engineering 5, Budapest 1976, Proceedings Vol 1, p 75-81.

Karlsson R and Viberg L (1967), Ratio c/p' in Relation to Liquid Limit and Plasticity Index, with Special Reference to Swedish Clays. Geotechnical Conference, Oslo 1967, Proceedings p 43-47.

Ladd C C and Lambe T W (1963), The strength of undisturbed clay determined from undrained tests. Special Technical Publication 361 NRC-ASTM Symposium on Laboratory Shear Testing of Soils.

Larsson R (1975a), Measurement and Calculation of Horizontal Stresses in Clay. Chalmers University of Technology, Gothenburg 1975.

Larsson R (1975b), The effect of rate of loading on the shear strength parameters of a high-plastic marine clay. Chalmers University of Technology, Gothenburg 1975.

Lefebvre G and La Rochelle R (1974), The Analyses of Two Slope Failures in Cemented Champlain Clays. Canadian Geotechnical Journal, Vol 11, No 1 1974.

Liam Finn W D and Shead D (1973), Creep and creep rupture of undisturbed sensitive clay. International Conference on Soil Mechanics and Foundation Engineering, Moscow 1973, Proceedings Vol 1.1, p 135-142.

Lo K Y and Morin J P (1972), Strength Anisotropy and Time Effects of Two Sensitive Clays. Canadian Geotechnical Journal Vol 9, No 3, 1972.

Magnusson O (1975), Deformations of the bottom of an excavation in clay. National Swedish Building Research, Report R21:1975.

Massarsch R, Holtz R D, Holm D G and Fredriksson A (1975), Measurement of horizontal in situ stresses. ASCE Specialty Conference on In Situ Measurements of Soil Properties, Raleigh North Carolina, June 1-4 1975.

Massarsch R (1976), Soil movements caused by pile driving in clay. Thesis. Royal Institute of Technology, Stockholm 1976.

Mitchell J K, Campanella R G and Singh A (1968), Soil creep as a rate process. American Society of Civil Engineers, Proceedings Vol 94, No SM 1, p 231-253.

Mitchell R J and Eden W J (1972), Measured Movements of Clay Slopes in the Ottawa Area. Canadian Journal of Earth Sciences, Vol 9, No 8, p 1001-1013.

Noble C A and Demirel T (1969), Effect of Temperature on Strength Behaviour of Cohesive Soil. Highway Research Board, Special Report 103, p 204-219, Washington 1969.

Pettersson K E and Hultin S (1916), Kajraset i Göteborg den 5 mars 1916. Teknisk tidskrift. Årgång 46, häfte 31, 29 juli 1916.

Ramanatha Iyer T S (1975), The Behaviour of Drammen Plastic Clay under Low Effective Stresses. Canadian Geotechnical Journal, Vol 12, No 1, Febr 1975.

Rendulic L (1938), Ein Grundgesetz der Tonmechanik und sein experimenteller Beweiss. Der Bauingenieur, Vol 18, p 459-467, 1937.

Rowe P W (1962), The stress-dilatancy relation for static equilibrium of an assembly of particles in contact. Roy. Soc. Academy, Proceedings 269:500-527.

Schmertmann J H and Osterberg J O (1961), An experimental Study of the Development of Cohesion and Friction with Axial Strain in Saturated Cohesive Soils. ASCE Research Conference on Shear Strength of Cohesive Soils, Boulder Colorado 1960, p 643-694.

Schmidt B (1967), Lateral stresses in uniaxial strain. Danish Geotechnical Institute. Bulletin No 23, 1967.

Schofield A and Wroth P (1968), Critical State Soil Mechanics, Mc Graw-Hill, London 1968.

Sekiguchi H (1973), Flow Characteristics of Clays. Soils and Foundations Vol 13, No 1, 1973.

Shibata I and Karube D (1969), Creep rate and creep strength of clays. International Conference on Soil Mechanics and Foundation Engineering Mexico 1969, Proceedings Vol 1, p 361-367.

Singh A and Mitchell J K (1968), General stress-strain-time function for soils. American Society of Civil Engineers, Proceedings, Vol 94, No SM 1, p 21-46.

Skempton A W (1954), Discussion of the structure of inorganic soil. American Society of Civil Engineers, Proceedings Vol 80, Sept 1954, No 478, p 19-22.

Sällfors G (1975), Preconsolidation Pressure of Soft, High-Plastic Clays. Thesis. Chalmers University of Technology, Gothenburg 1975.

Söderblom R (1974), New Lines in Quick Clay Research. Swedish Geotechnical Institute, Reprints and Preliminary Reports No 55, 1974.

Ter-Stepanian G (1975), Creep of a clay during shear and its rheological model. Géotechnique, Vol 25, No 2, p 299-320.

Wiesel C E, Swedish Geotechnical Institute (Personal communication).

Wong P K K and Mitchell R J (1975), Yielding and plastic flow of sensitive cemented clay. Géotechnique, Vol 25, No 4, p 763-782.

Wroth P (1975), In situ measurement of initial stresses and deformation characteristics. Specialty Conference on In Situ Measurement of Soil Properties. State-of-the-Art Paper, Session 4, North Carolina State University, Raleigh, North Carolina, June 1-4 1975.

APPENDIX 1

Oedometer curves from tests with unloading.

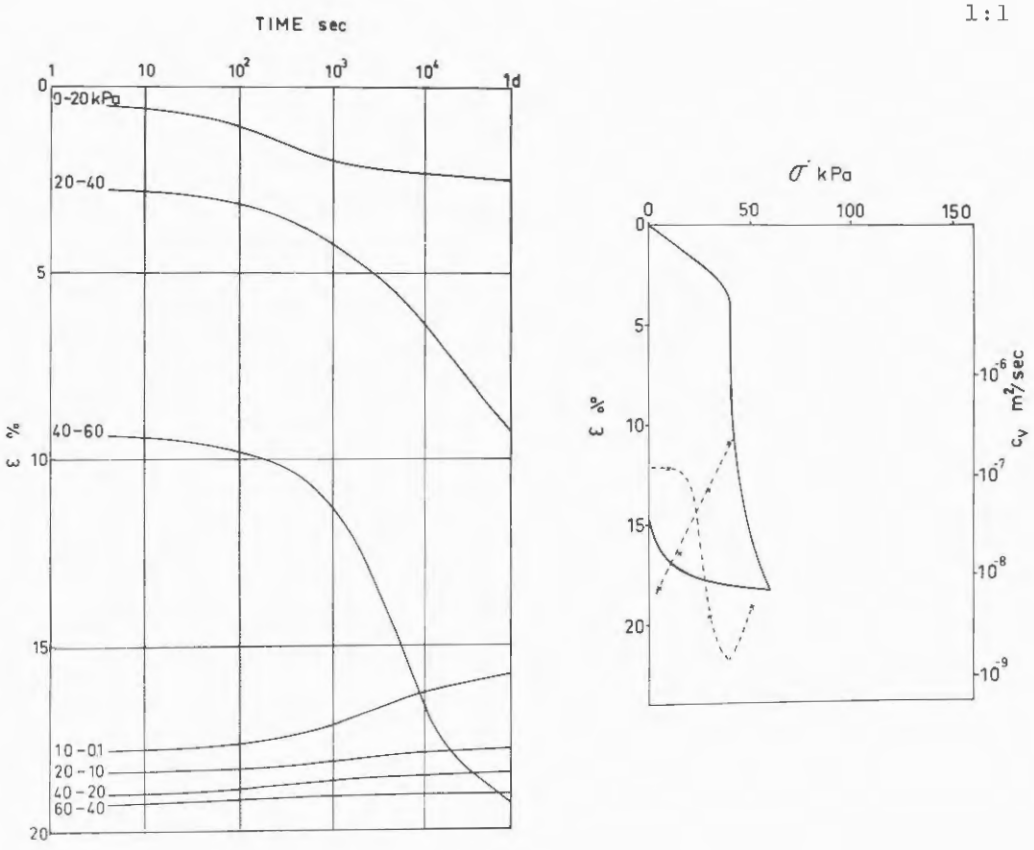

Oedometer test with stepwise loading and unloading

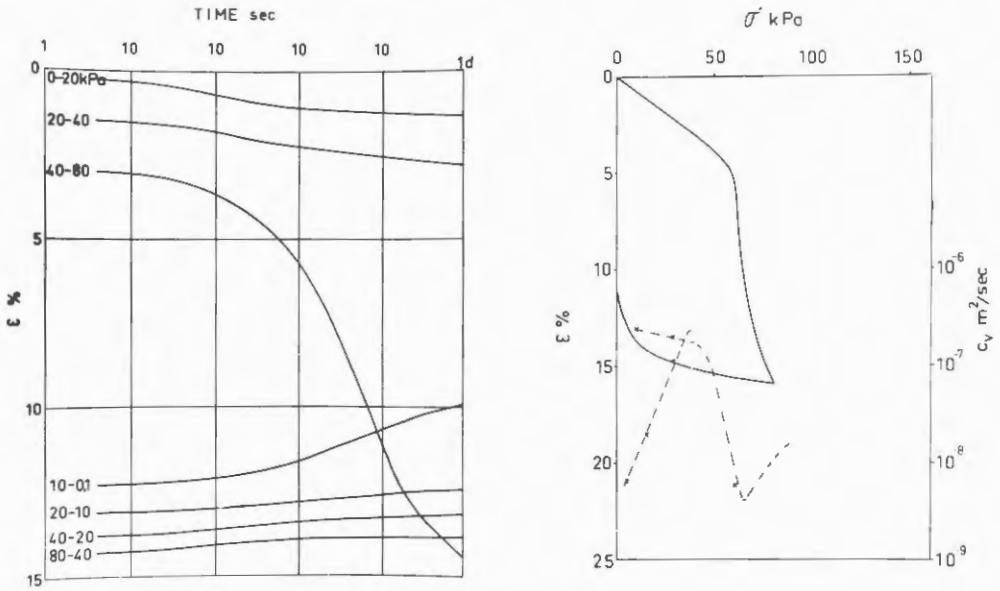

Oedometer test with stepwise loading and unloading.

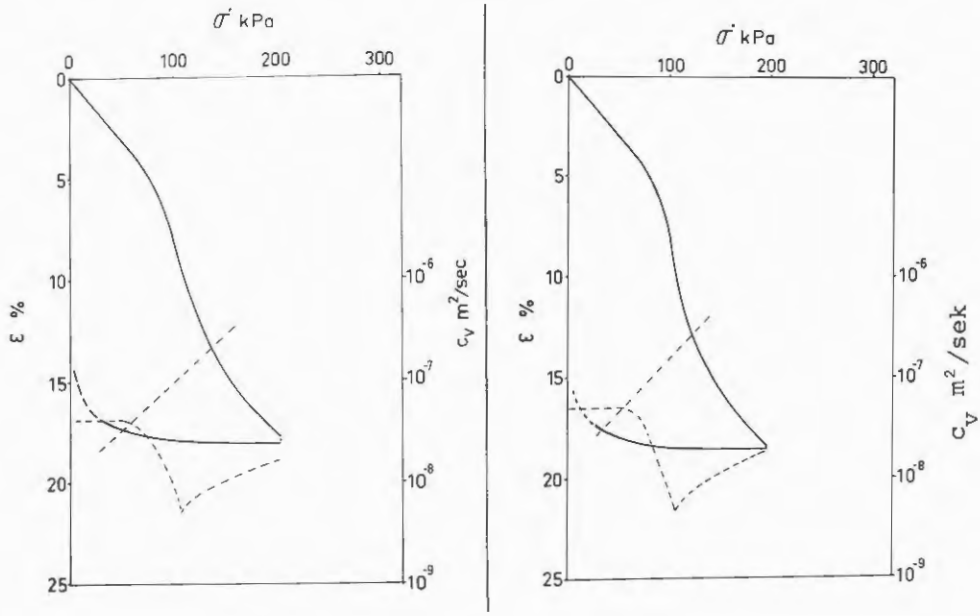

CRS tests with loading and unloading.

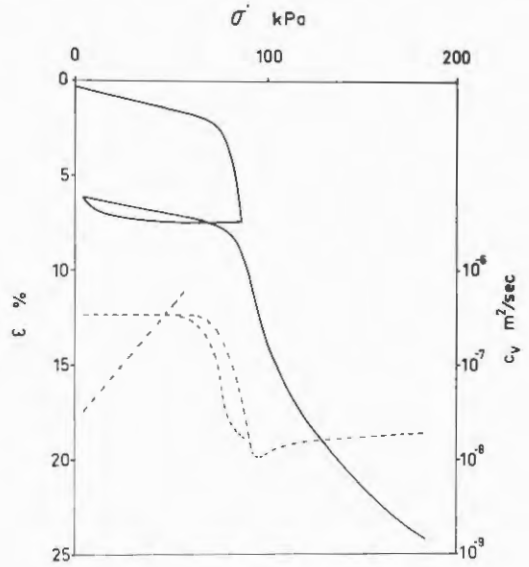

CRS test with loading, unloading and reloading.

APPENDIX 2

Effective stress paths in creep tests.

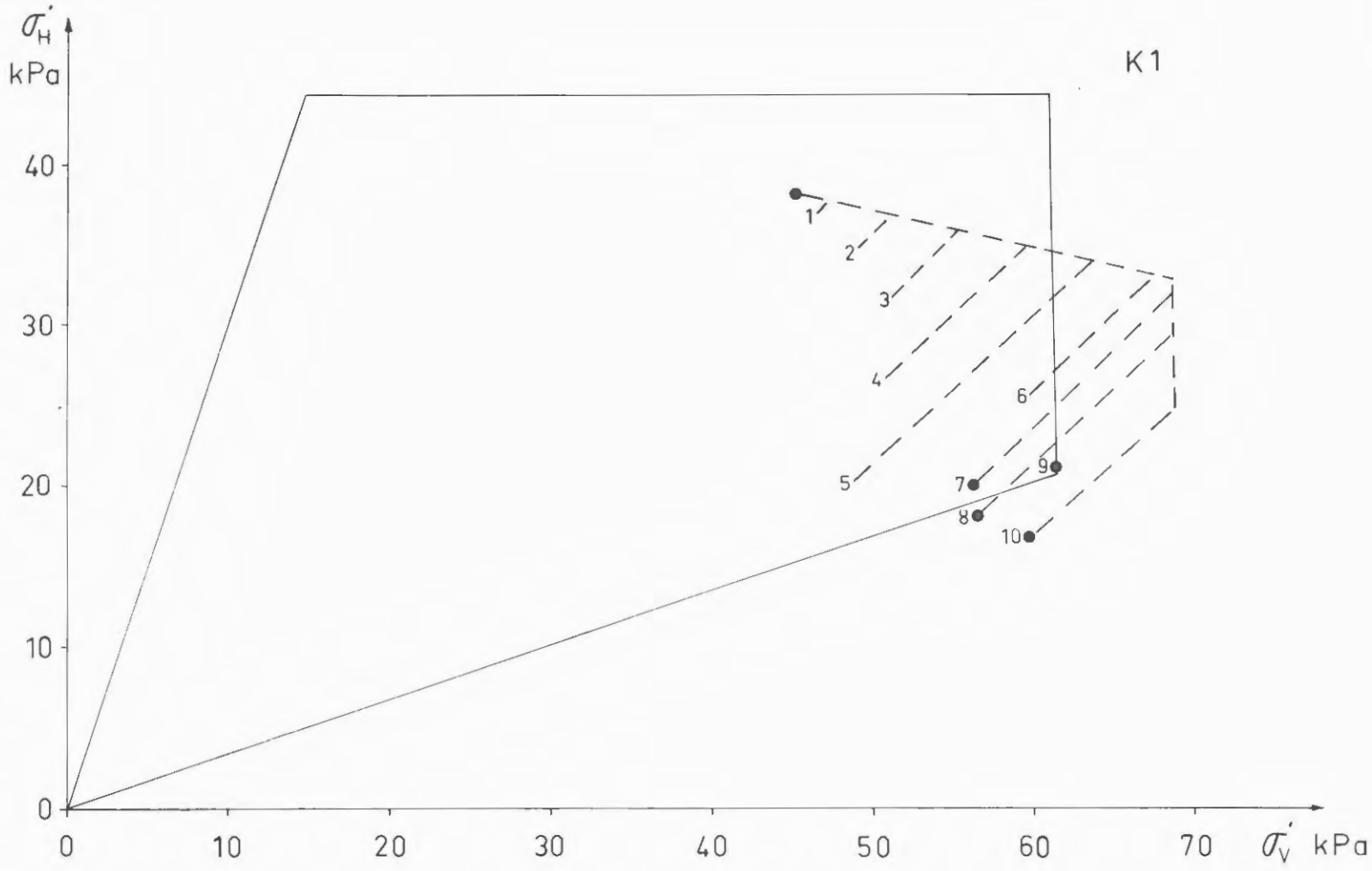
K1
σ_H' kPa
40
30
20
10
0
0
10
20
30
40
50
60
70
σ_V' kPa
1
2
3
4
5
6
7
8
9
10

2:1

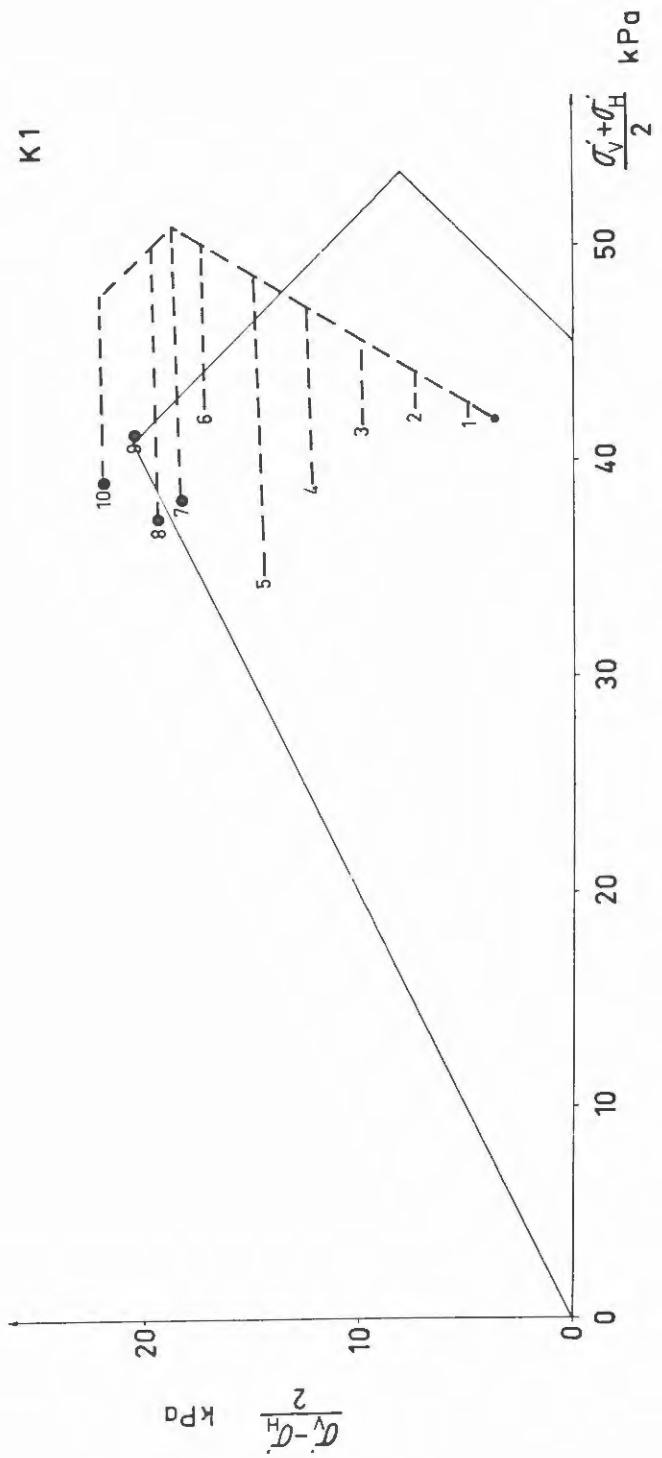
K1
$\frac{\sigma'_V - \sigma'_H}{2}$ kPa
$\frac{\sigma'_V + \sigma'_H}{2}$ kPa
0
10
20
0
10
20
30
40
50
1
2
3
4
5
6
7
8
9
10

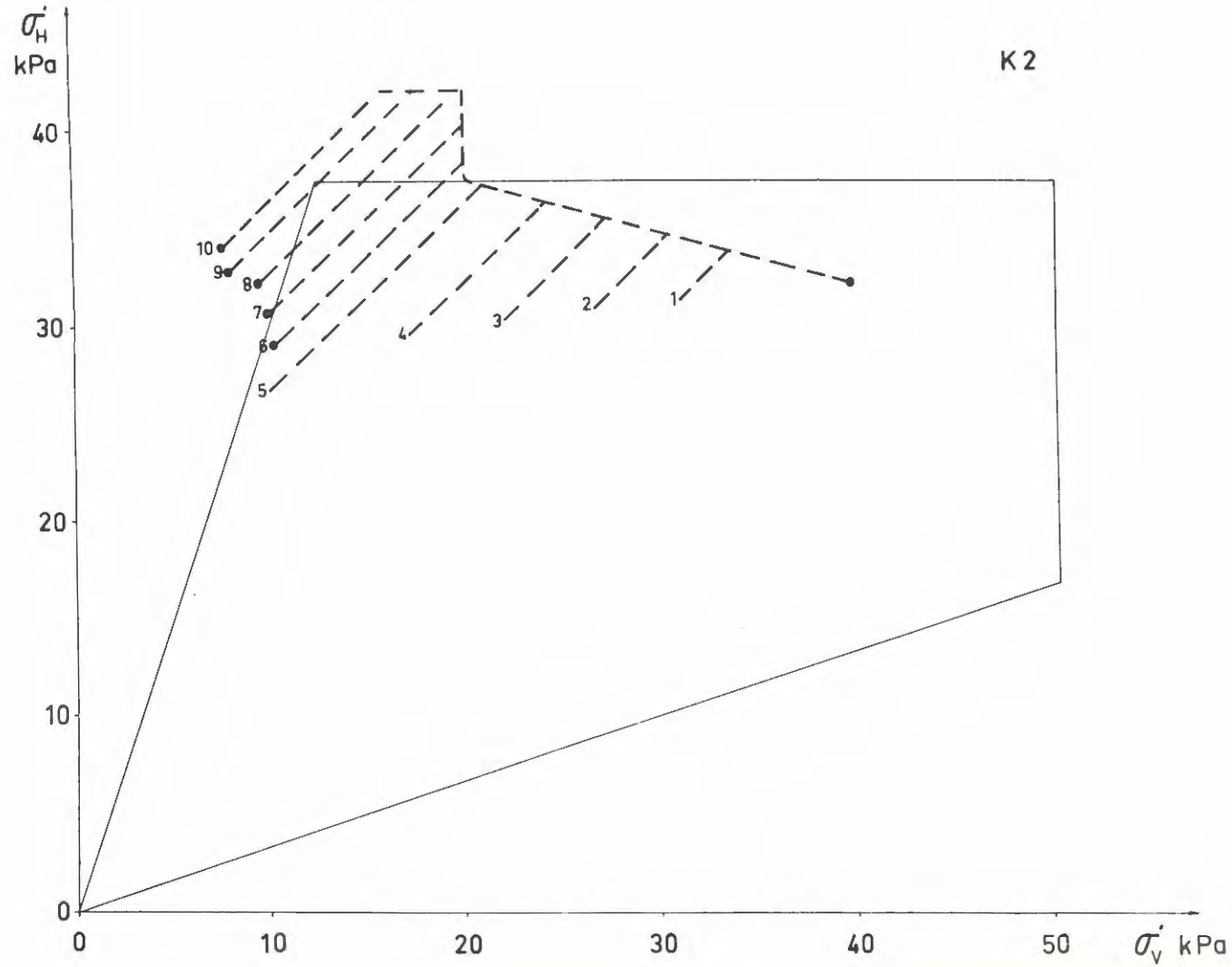
σ'_H
kPa
K 2
40
30
20
10
0
0
10
20
30
40
50
σ'_V kPa
10
9
8
7
6
5
4
3
2
1

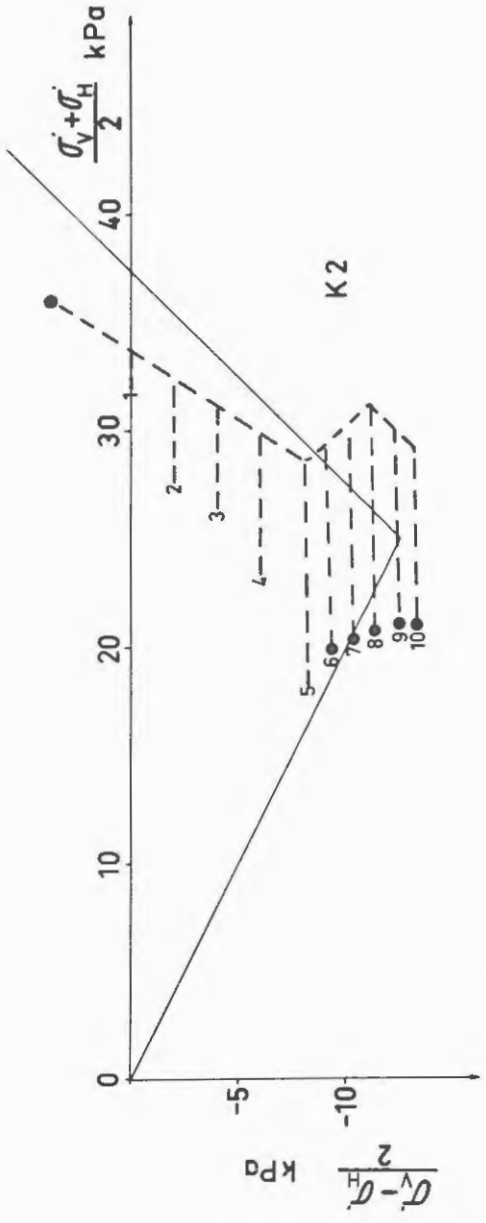
K2
$\frac{\sigma_v'+\sigma_H'}{2}$ kPa
$\frac{\sigma_v'-\sigma_H'}{2}$ kPa
0
10
20
30
40
-5
-10
1
2
3
4
5
6
7
8
9
10

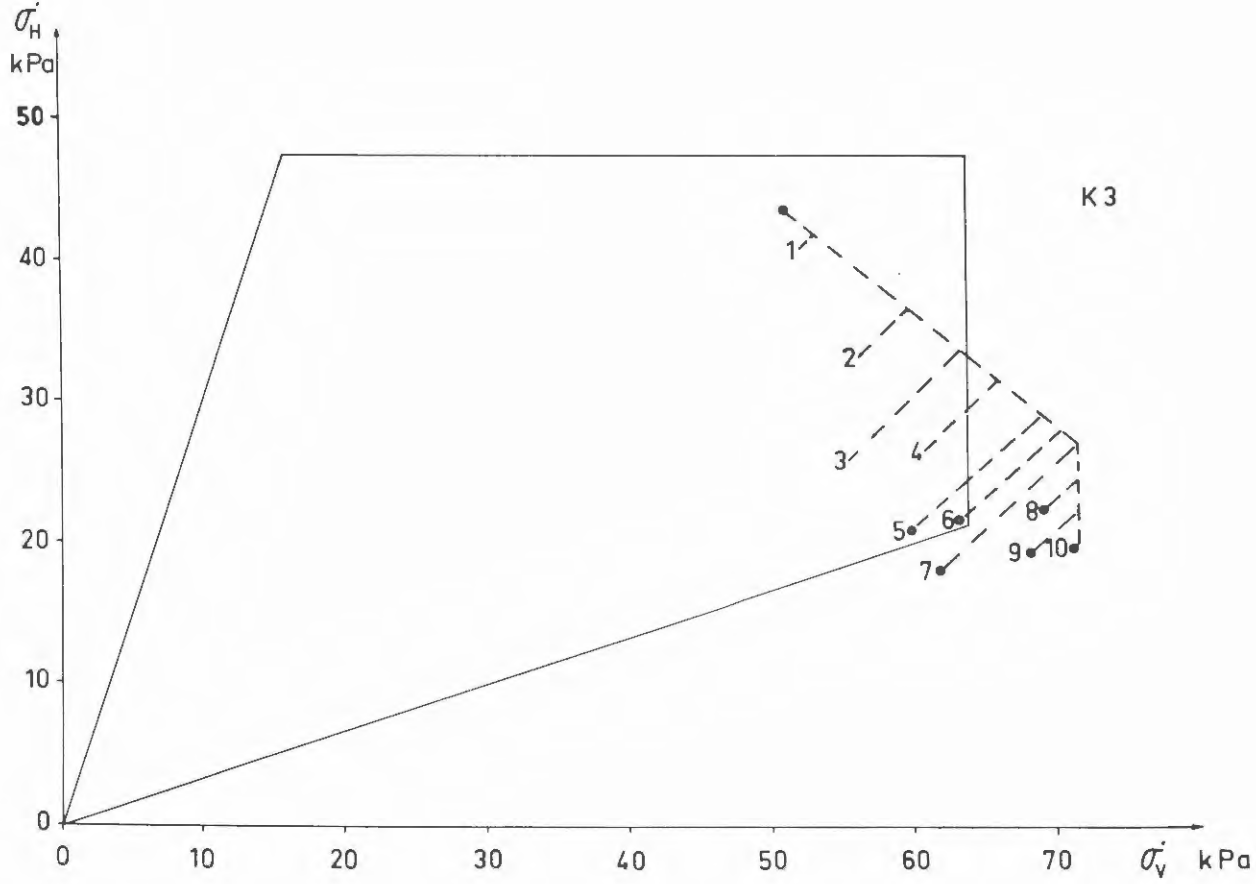
σ'_H
kPa
50
40
30
20
10
0
0
10
20
30
40
50
60
70
σ'_v kPa
K 3
1
2
3
4
5
6
7
8
9
10

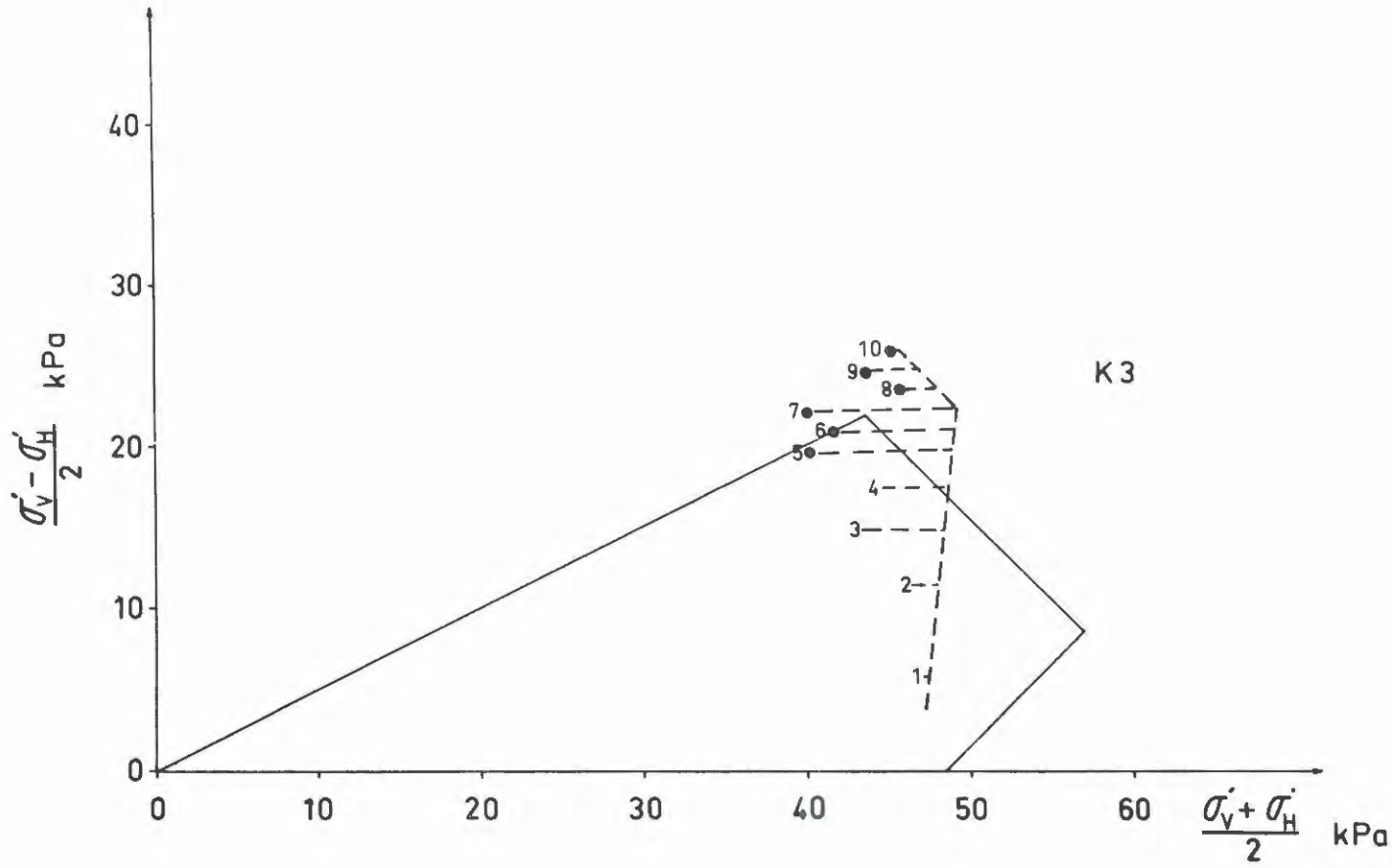
K 3
$\frac{\sigma_v' - \sigma_H'}{2}$ kPa
$\frac{\sigma_v' + \sigma_H'}{2}$ kPa
0
10
20
30
40
50
60
1
2
3
4
5
6
7
8
9
10

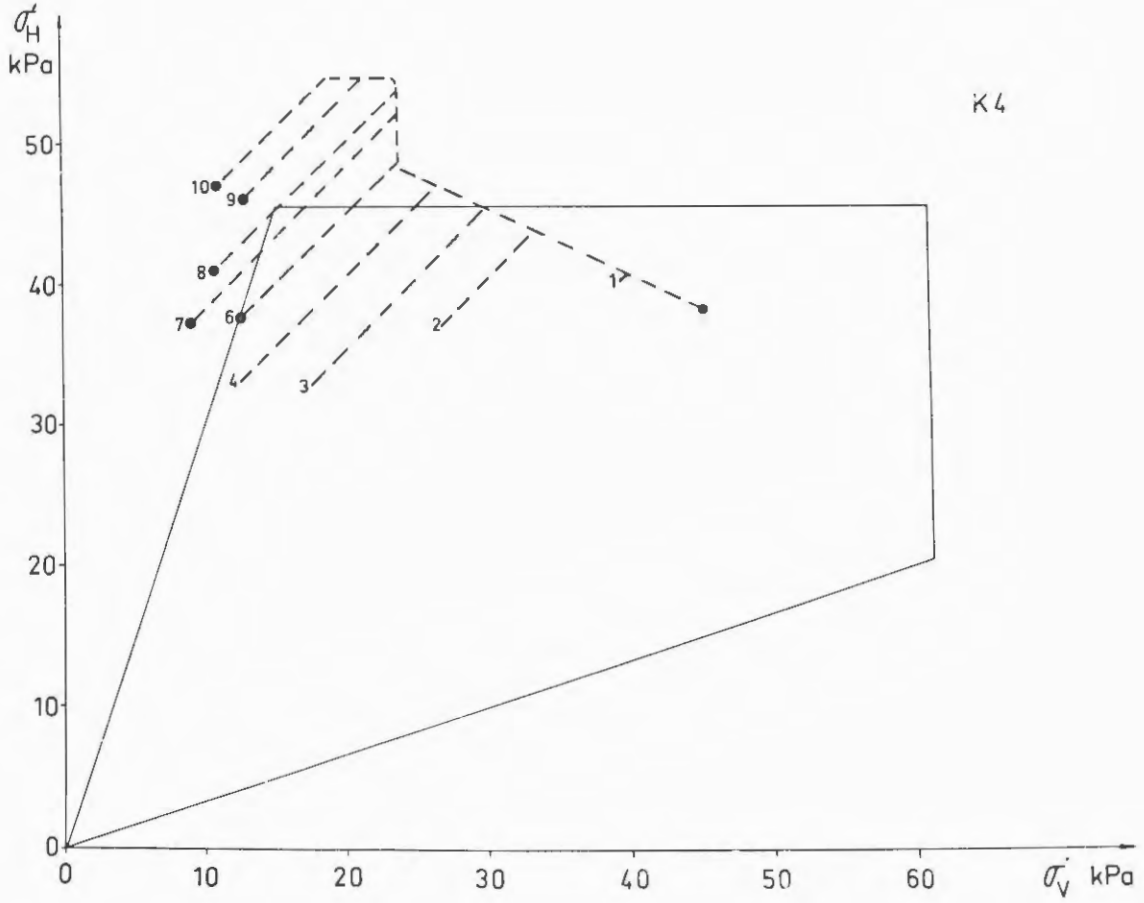
σ'_H kPa
K4
50
40
30
20
10
0
10
9
8
7
6
4
3
2
1
0
10
20
30
40
50
60
σ'_V kPa

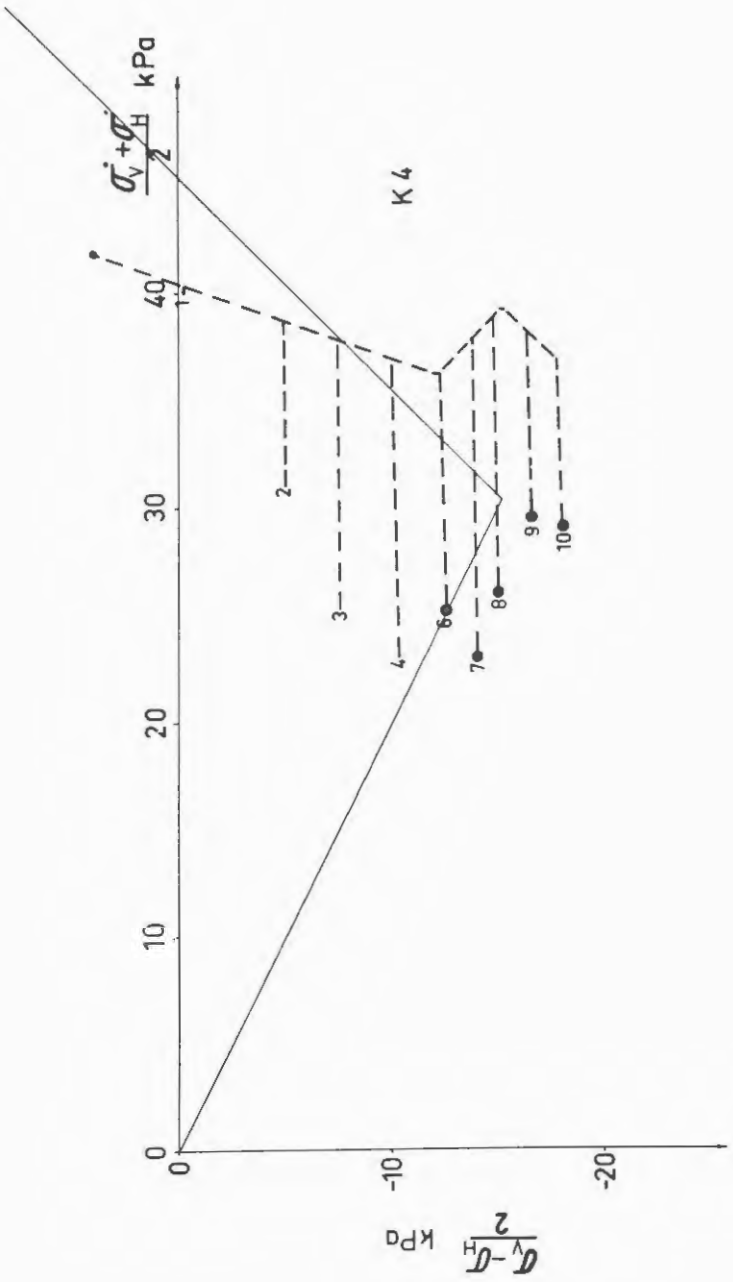
K 4
$\frac{\sigma'_v+\sigma'_H}{2}$ kPa
$\frac{\sigma_v-\sigma_H}{2}$ kPa
0
10
20
30
40
-10
-20
1
2
3
4
6
7
8
9
10

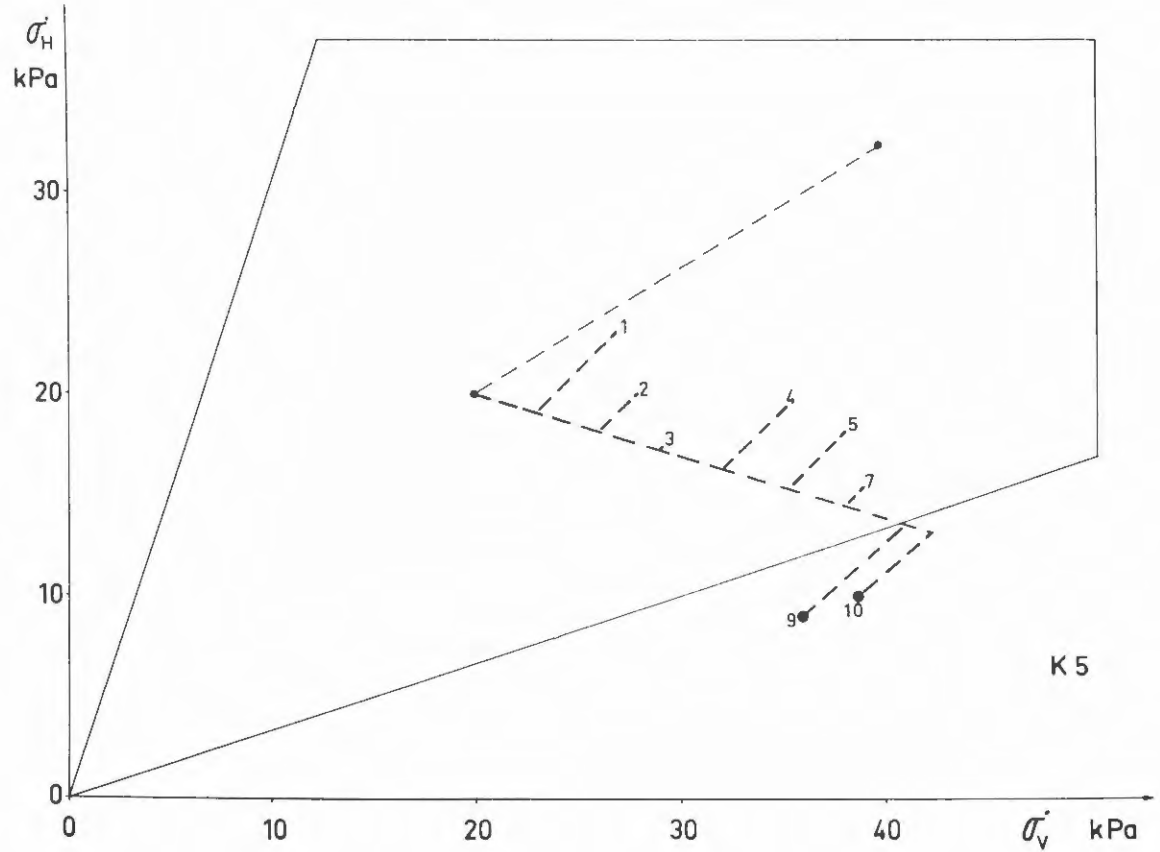
σ'_H
kPa
30
20
10
0
0
10
20
30
40
σ'_v kPa
1
2
3
4
5
7
9
10
K 5

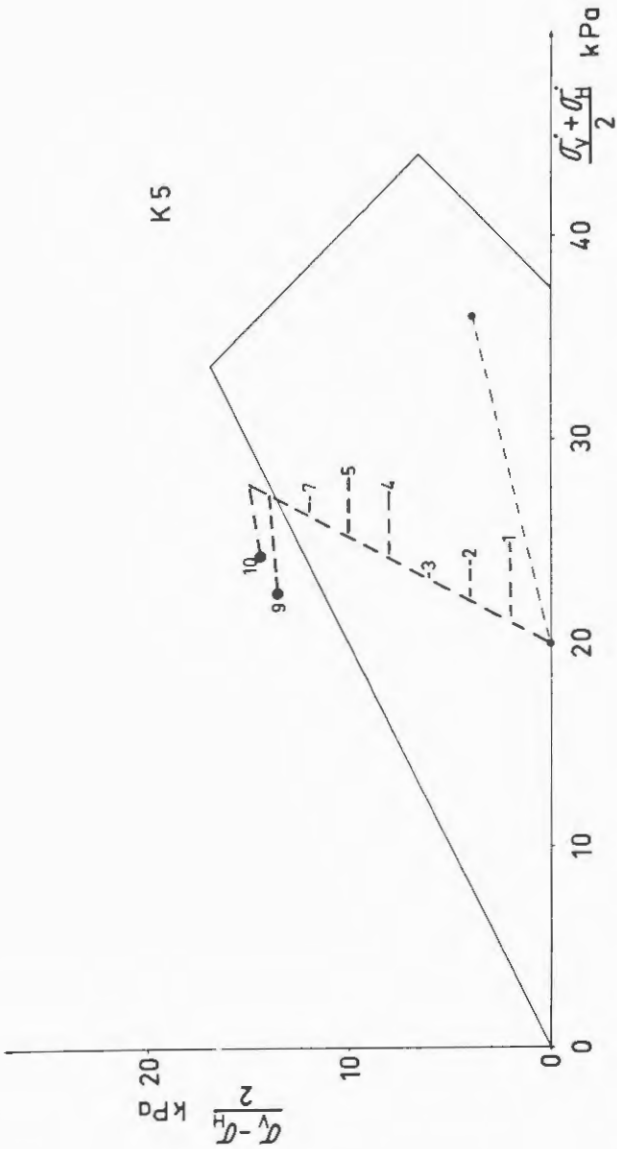
K 5
$\frac{\sigma_V' + \sigma_H'}{2}$ kPa
$\frac{\sigma_V - \sigma_H}{2}$ kPa
0
10
20
30
40
0
10
20
1
2
3
4
5
7
9
10

APPENDIX 3

Micrographs of inorganic clay from Lilla Mellösa and organic clay from Välen.

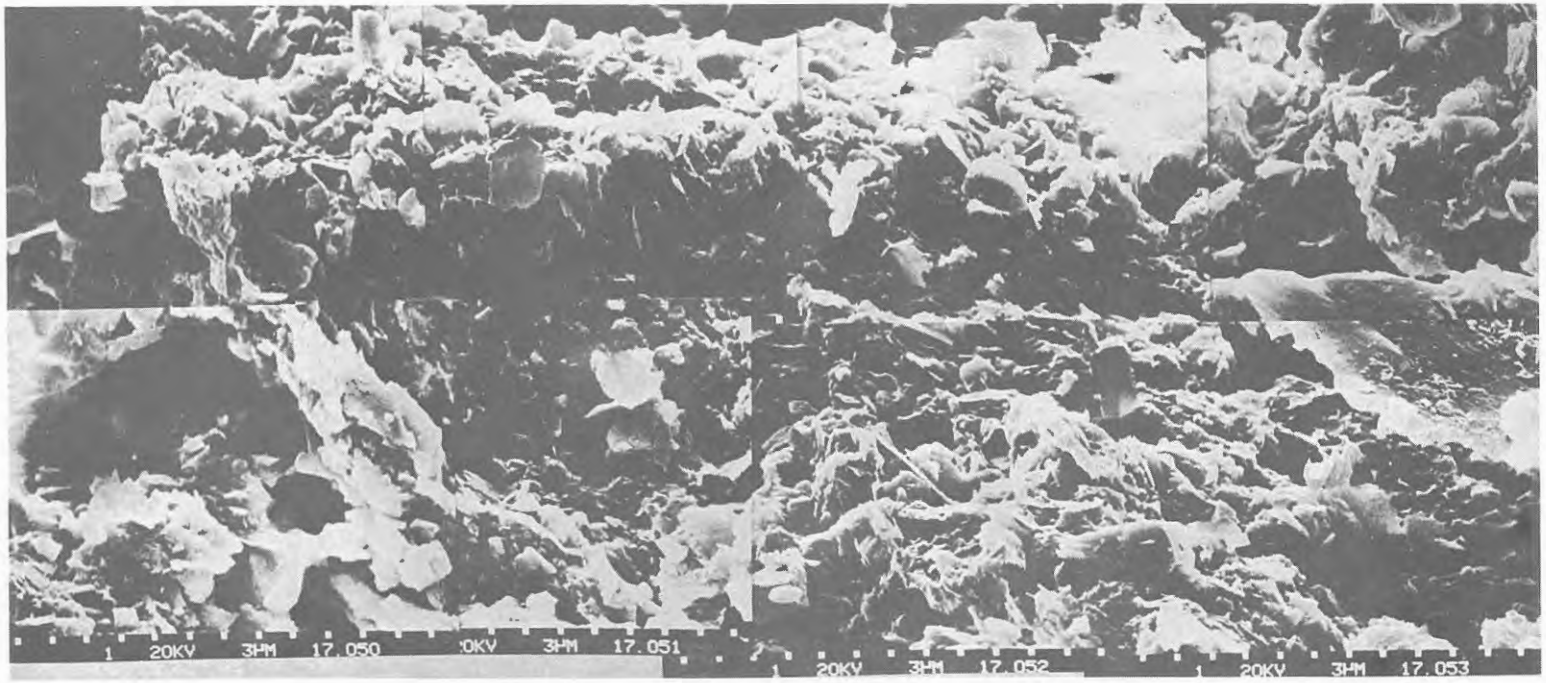

Serial micrograph of Lilla Mellösa clay.

3:1

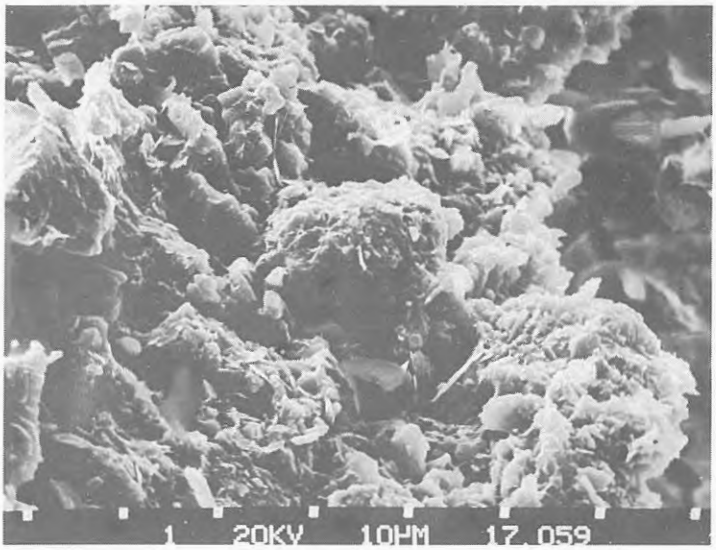

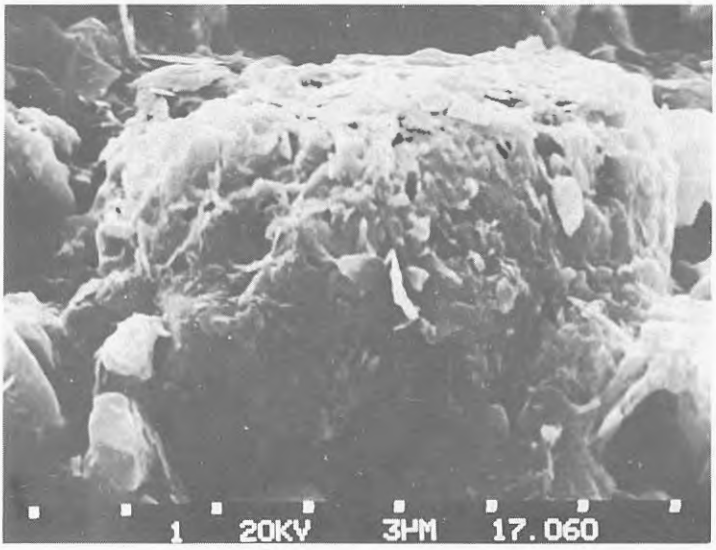

Pictures 17059-17060. Aggregate consisting of numerous small particles in Lilla Mellösa clay.

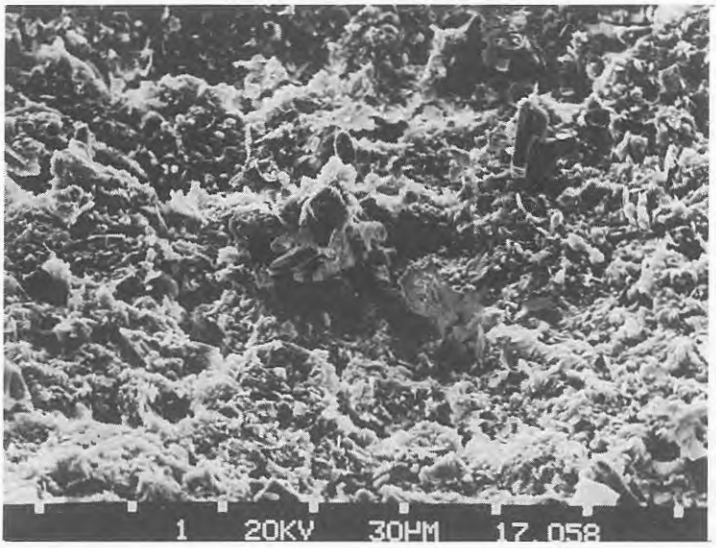
1 20KV 30UM 17.058

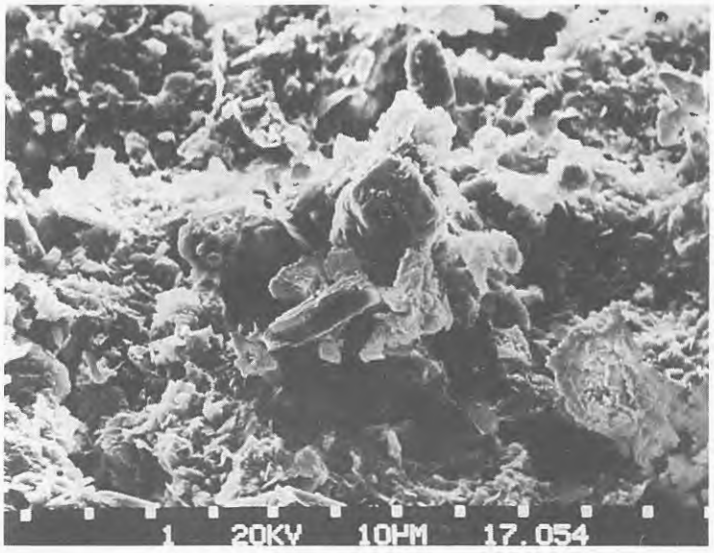
1 20KV 10UM 17.054

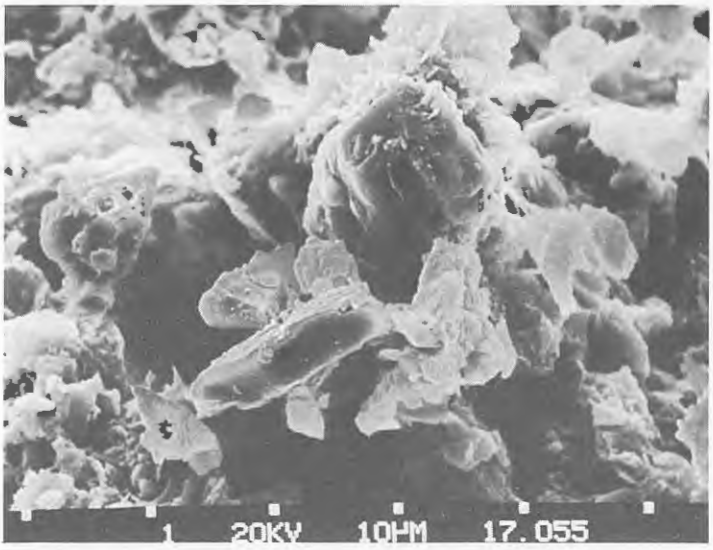
1 20KV 10UM 17.055

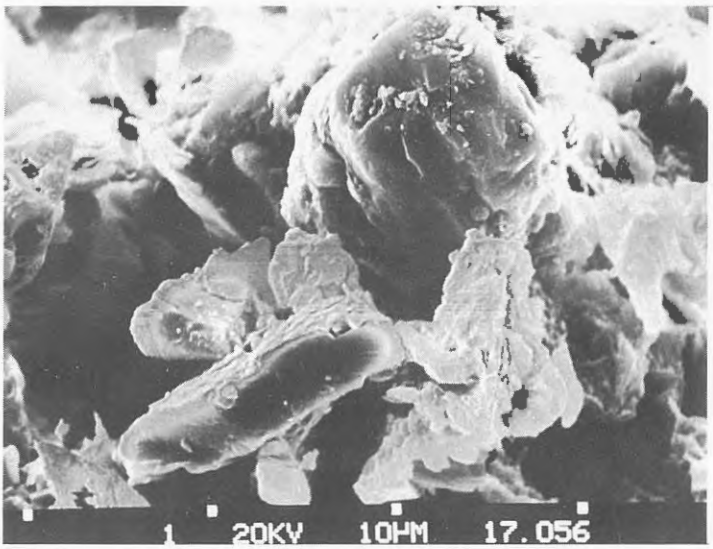

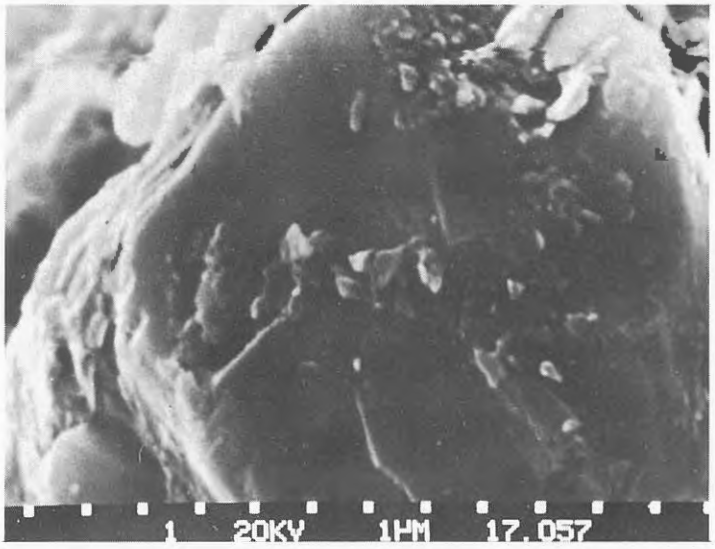

Pictures 17054-17058. Different enlargements of an area in Lilla Mellösa clay. Picture 17058 has the same enlargement as the serial picture of Välen clay and the absence of fibres can be noted. The pictures show that that some grains are solid particles while others are aggregates of numerous small particles.

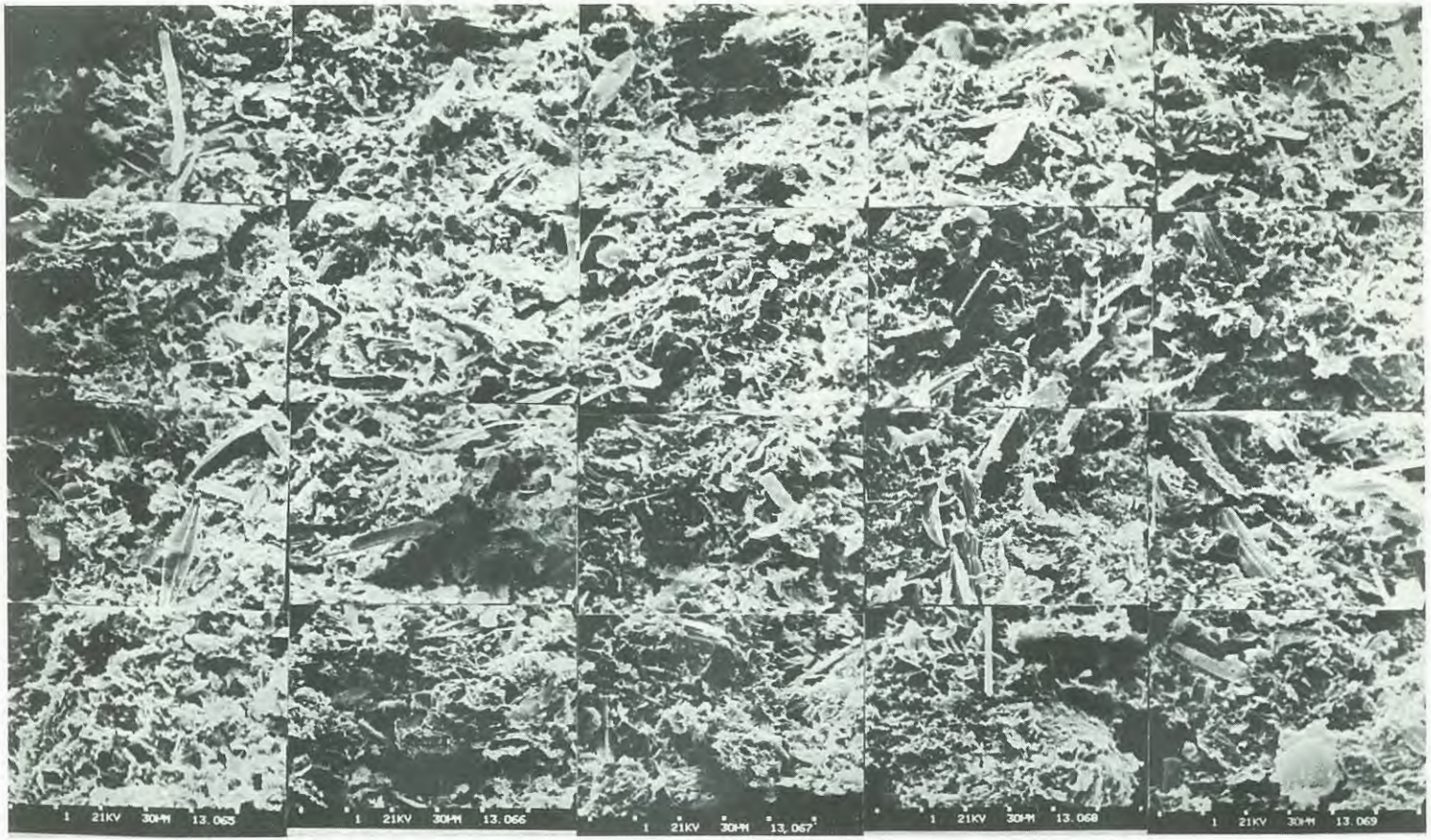

Serial micrograph of Välen clay showing a large amount of fibres in the clay.

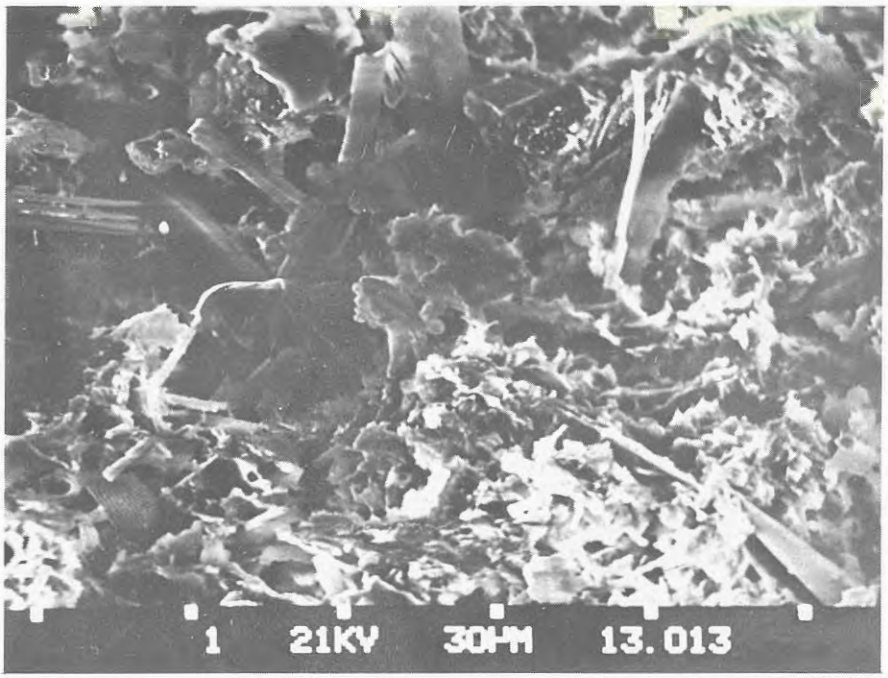

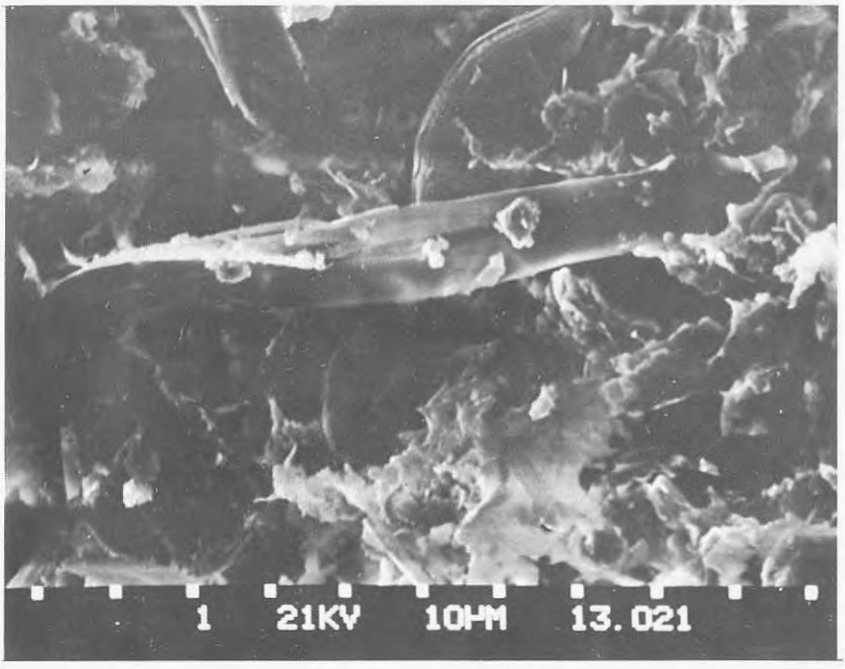

Pictures 13013 and 13021. Particles and fibres in Välen clay.

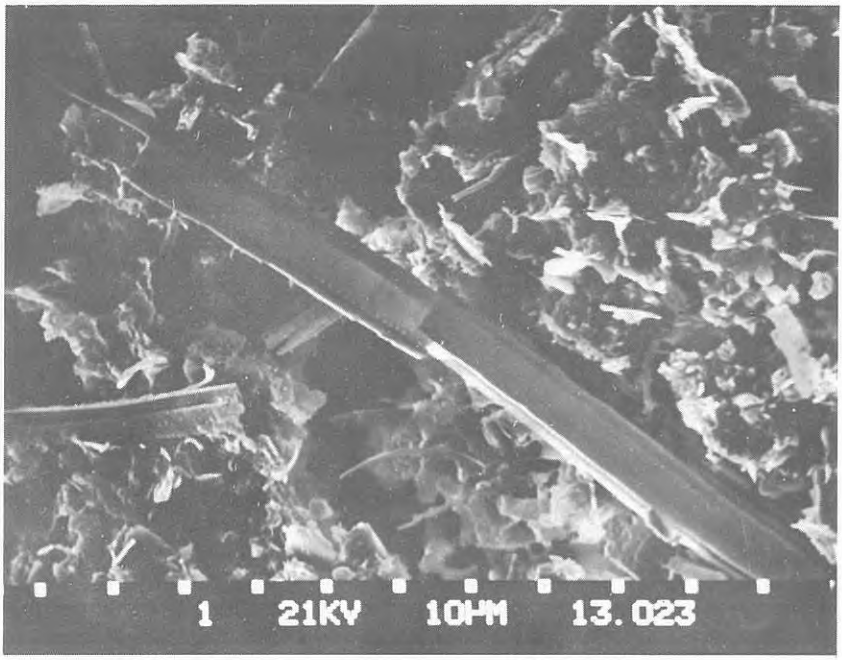

Picture 13023. Fibre in Välen clay.

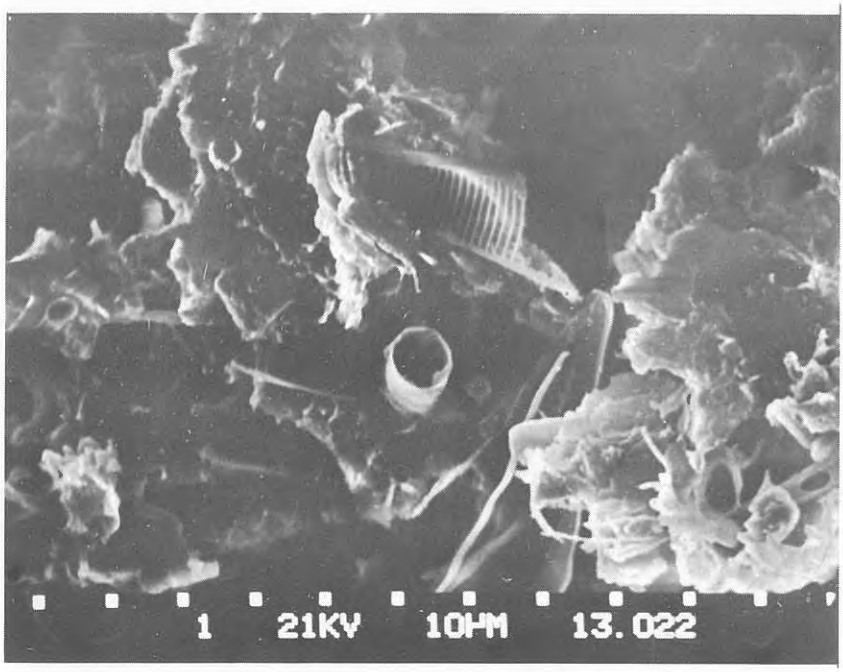

Picture 13022. Diatoms in Välen clay.

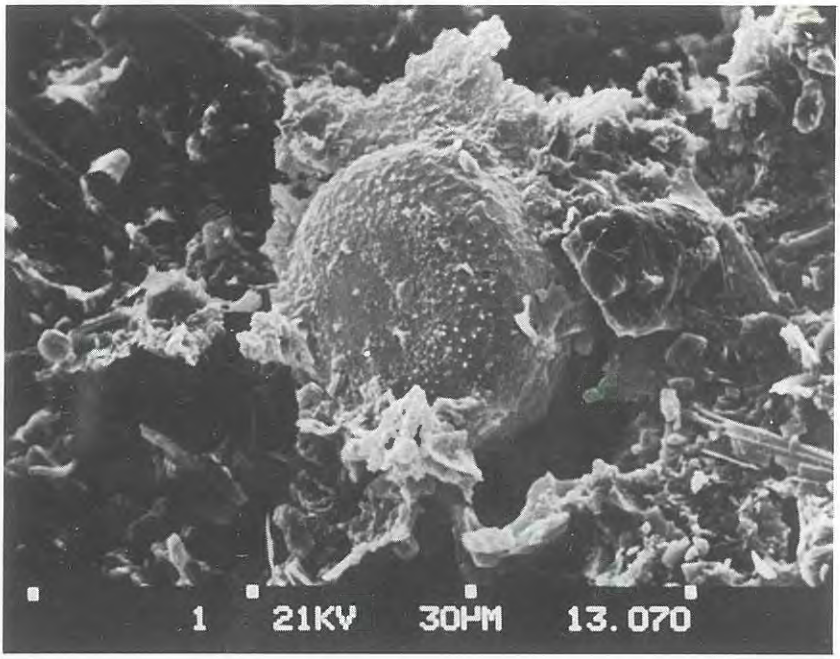

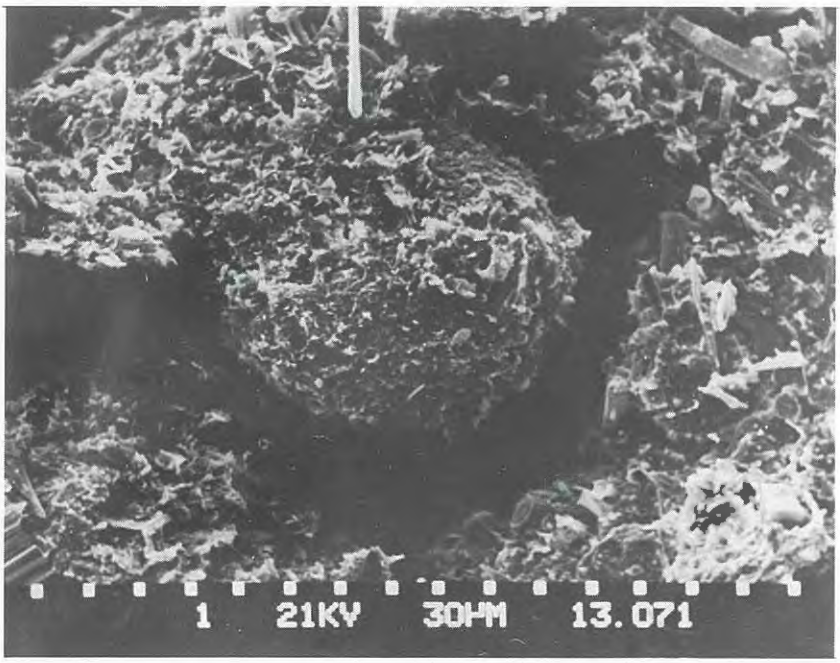

Pictures 13070-13071. Large particles in Välen clay.

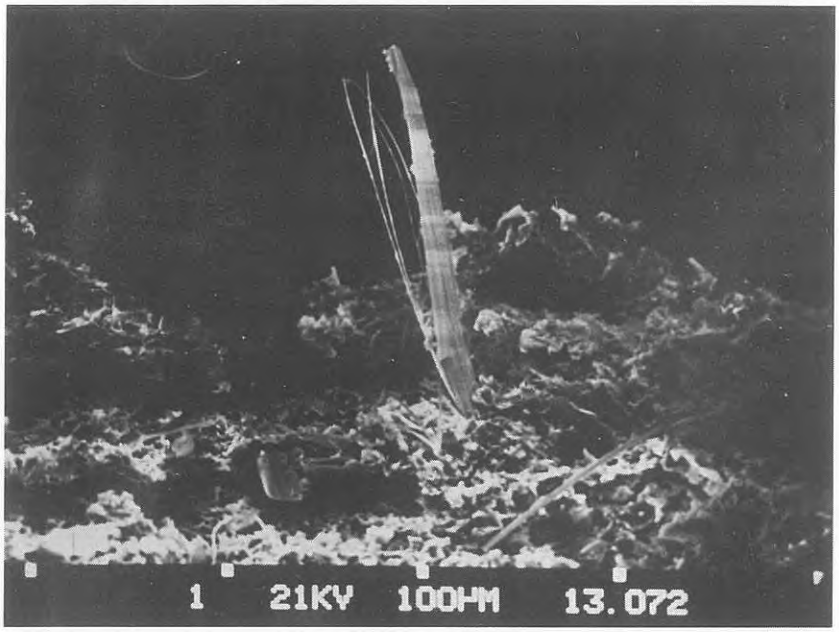

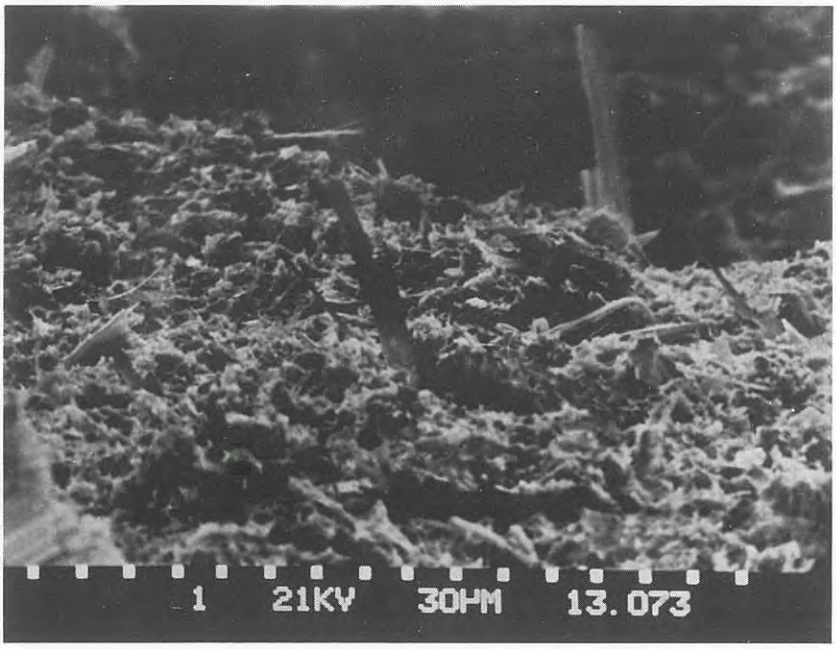

Pictures 13072-13073. Fibres protruding from fracture surfaces in Välen clay.

STATENS GEOTEKNISKA INSTITUT
Swedish Geotechnical Institute
Fack
S-581 01 Linköping
Tel: 013/11 51 00

No.	RAPPORT/REPORT	år	Pris kr (Sw.crs.)
1.	Grundvattensänkning till följd av tunnelsprängning. *P. Ahlberg, T. Lundgren*	1977	50:-
2.	Påhängskrafter på långa betongpålar. *L. Bjerin*	1977	50:-
3.	Methods for reducing undrained shear strength of soft clay. *K.V. Helenelund*	1977	30:-
4.	Basic behaviour of Scandinavian soft clays. *R. Larsson*	1977	40:-

STATENS GEOTEKNISKA INSTITUT
Swedish Geotechnical Institute
Fack
S-581 01 Linköping

Tel: 013/11 51 00